Characterising the role of LuxS during the biofilm formation of *Clostridioides difficile*

by

Ross Thomas Slater

Thesis submitted for the degree of Doctor of Philosophy

in

Medical Sciences

University of Warwick, Warwick Medical School

February 2018

Table of Contents

List of figures

List of tables

Acknowledgments

First and foremost, I would like to thank my supervisor, Dr Meera Unnikrishnan, for always guiding me with patience and moral support throughout my PhD journey. Her help and advice has been invaluable as I navigated my experiments and writing.

I would like to extend my gratitude to Dr Andrew Millard for his help with bioinformatics analysis. I would also like to thank Dr Chrystala Constantinidou for the help and advice in understanding my RNA-seq data, and Dr Emma Denham for her invaluable advice and expertise in the lab. Dr Gemma Kay, Dr Richard Brown and Dr Pavelas Sazinas for their help, advice and encouragement along the way. A special thanks goes to Dr Josie McKeown and Dr Emily Stoakes for helping me troubleshoot experiments, humouring my many questions and ensuring there was never a dull moment in the office. Dr Blessing Anonye for her insight and knowledge. Finally I wish to thank Jack Hassell and Thomas Brooker for helping to make the last 4 years enjoyable.

A special thank you goes to my husband Tom Goddard, his support and encouragement throughout my PhD has been invaluable, particularly during the writing of my thesis.

Author's Declaration

This thesis is submitted to the University of Warwick in support of my application for the degree of Doctor of Philosophy. It has been composed by myself and has not been submitted in any previous application for any Degree.

The work presented (including data generated and data analysis) was carried out by the author.

Signed: 

Date: 27-02-2018

Abstract

The Gram positive anaerobic bacterium, *Clostridioides difficile*, is one of the leading causes of hospital associated diarrhoea world-wide. An opportunistic pathogen, *C. difficile* colonises the gut during intestinal microbial dysbiosis, causing *Clostridioides difficile* infection (CDI). Treatment of CDI is complicated by the increasing numbers of recurrent infections.
C. difficile has demonstrated its ability to produce composite, adherent multicellular communities, or biofilms, *in vitro*. *In vitro* biofilms offer the bacteria within increased resistance to a range of environmental stresses including antibiotics and oxygen stress. However the mechanisms underlying *C. difficile* community formation are poorly understood. In other bacteria, quorum sensing, a process mediated by small signalling molecules that accumulate in the extracellular environment, coordinates biofilm formation. In several bacteria, the metabolic enzyme LuxS, produces the signalling molecule autoinducer-2 (AI-2), which plays a key role in quorum sensing. AI-2 is considered to be a cross-species signalling molecule and for many bacterial species AI-2 has been shown to have a signalling role during biofilm formation and development.

Here we show *C. difficile luxS* mutants (LuxS) are defective in biofilm formation and demonstrate the ability for chemically synthesised AI-2 to partially restore the biofilm defect of LuxS. Through RNA-seq analysis we show that LuxS/AI-2 quorum sensing likely influences *C. difficile* prophage expression, affecting levels of extracellular DNA present within the biofilm. Additionally we show that *Bacterioides fragilis* has an inhibitory effect on *C. difficile,* with increased levels of inhibition observed in WT compared to LuxS.

By utilising dual species RNA-sequencing we propose a number of possible mechanisms responsible for the observed inhibition.

List of abbreviations

ACP	acyl carrier protein
AHL	acyl homoserine lactone
AI	autoinducer
AI-2	autoinducer-2
AIP	autoinducing peptide
APD	autoprotease domain
BHI	brain-heart infusion
BHIS	brain-heart infusion supplemented with yeast and l-cysteine
BHIS-G	brain-heart infusion supplemented with yeast, l-cysteine and glucose
BLAST	basic local alignment search tool
CDAD	*Clostridioides difficile* associated disease
CDI	*Clostridioides difficile* infection
CDT	*Clostridioides difficile* transferase
cDNA	complementary DNA
CFU	colony forming unit
COGs	clusters of orthologous groups
CV	crystal violet
CWP	cell wall protein
DNA	deoxyribonucleic acid
DPD	4,5-dihydroxy-2,3-pentanedione
E	expected value
eDNA	extracellular DNA
FDA	food and drug administration
FMT	faecal microbiota transplantation

GBK	GenBank file
GFF	general feature format file
GFP	Green fluorescent protein
GTD	glycosyltransferase domain
HMW	high molecular weight
KEGG	Kyoto Encyclopedia of Genes and Genomes
LMW	low-molecular-weight
LuxS	*C. difficile* R20291::*luxS* mutant
MHF	5-methyl-4-hydroxy-3(2H)-furanone
mRNA	messenger RNA
NCBI	National Center for Biotechnology and Information
OD	optical density
PaLoc	Pathogenicity locus
PBS	phosphate-buffered saline
PCA	principle component analysis
PCR	polymerase chain reaction
PFA	paraformaldeyhyde
PMC	pseudomembranous colitis
PTS	phosphotransferase system
QS	quorum sensing
RefSeq	reference sequence database
RLO	relative light output
RNA	ribonucleic acid
RNA-seq	RNA-sequencing
RPKM	reads per kilobase per million reads
rRNA	ribosomal RNA
RT	room temperature

SAH	S-adenosylhomocysteine
SAM	sequence alignment map
SLPs	S-layer proteins
SRH	S-ribosylhomocysteine
T6SS	Type 6 Secretion System

Chapter 1 INTRODUCTION

Clostridioides difficile

Clostridium difficile is an anaerobic, Gram positive bacterium belonging to the phylum Firmicutes. It exists in two forms: the motile, rod-shaped, vegetative cell and the endospore (spore) (Hall and O'Toole, 1935). The vegetative bacteria are metabolically active and capable of reproduction whilst spores are metabolically dormant, allowing the bacteria to survive for long periods in unfavourable conditions such as: extreme temperatures, oxygen and harsh physical or chemical environments (Setlow, 2007). As proposed by Lawson and Rainey (2015) recently, *Clostridium difficile* was reclassified to the new genus of *Clostridioides* (Lawson *et al.,* 2016), in order to restrict the genus *Clostridium* to *Clostridium butyricum* and related species,

It is interesting to note that initial knowledge of *Clostridiodies difficile* and *C. difficile* Infection (CDI) stem from three separate lines of study spanning an 80-year period (Bartlett, 1994). The earliest known studies were on pseudomembranous colitis (PMC), a condition first described in 1893 by John Finney (Finney, 1893) and characterised by pseudomembranous lesions of the intestinal tract. However, relatively little was known about PMC until the 1950s, when it became a relatively common complication of antibiotic usage (Bartlett, 1994). At the time, *Staphylococcus aureus* was suspected to be the pathogen responsible, due to recovery of this organism from patient stools (Bartlett, 1994). Nonetheless, with the benefit of hindsight it is clear that *C. difficile* was the most likely cause (Bartlett, 1994).

Research on *C. difficile* itself, did not to begin until its isolation in 1935. Formerly named *Bacillus difficilis* from the Latin '*difficilis'*, which means difficult or obstinate, due to the "unusual difficulties" encountered in its isolation and study (Hall and O'Toole, 1935). *C. difficile* was originally described as a component of the normal intestinal microbiota of newborn infants (Hall and O'Toole, 1935). Whilst not harmful to neonates, it was shown that *C. difficile* produced a toxin that was highly lethal to guinea pigs (Hall and O'Toole, 1935).

A third line of study began during the Second World War with the creation of a rodent model to investigate the potential benefits of penicillin for treatment of gas gangrene (Hambre M, 1943). During the study, guinea pigs were inoculated with *Clostridium perfringens* and treated subcutaneously with penicillin. It was found that many of the guinea pigs developed typhlitis, which proved more lethal than *C. perfringens*-induced gas gangrene (Hambre M, 1943, Bartlett, 1994). The cause of this was to remain elusive until 1978, when these separate lines of study were finally linked and *C. difficile* was implicated as the causative agent of PMC and antibiotic-associated diarrhoea (Bartlett, 1994).

It is now known that *C. difficile* is an opportunistic pathogen of both humans and animals causing a toxin-mediated intestinal disease, more commonly known now as *C. difficile* infection (CDI) (Smits *et al.,* 2016) (also known as *C. difficile* associated disease or CDAD). The symptoms of this infection can

range from mild diarrhoea to severe conditions such as PMC and toxic megacolon.

Since the 1970s, *C. difficile* has been well studied, with a lot of emphasis placed on the role of two large toxins, toxin A and toxin B, which were quickly recognised as the main virulence factors (Voth and Ballard, 2005). In recent years recurrent infections have become a significant problem affecting 20-36% of patients (Aslam *et al.*, 2005, Zar *et al.*, 2007) leading to greater research focus on other processes important to pathogenesis such as colonization and sporulation.

1.1 *C. difficile* infection

C. difficile is transmitted by spores that can be readily isolated both in healthcare settings and at low levels in the environment and food supply, allowing for both nosocomial and community transmission (Dubberke *et al.*, 2007, Otter *et al.*, 2015, Lund and Peck, 2015). Whilst carriage of *C. difficile* is most commonly asymptomatic (as is the case for neonates [Hall and O'Toole, 1935]), in susceptible individuals colonisation by *C. difficile* can lead to disease formation, with symptoms ranging from mild self-limiting diarrhoea to severe, relapsing and potentially fatal pseudomembranous colitis (Smits *et al.,* 2016). CDI is recognised to be one of the leading causes of infectious diarrhoea in the healthcare setting (Rupnik *et al.,* 2009) with elderly patients undergoing treatment with broad-spectrum antibiotics at the highest risk of infection (Goorhuis *et al.*, 2008, Vardakas *et al.*, 2012).

Although the precise mechanisms for colonisation resistance are yet to be deduced, disruption to the intestinal microbiota, usually due to antibiotic use, increases the availability of nutrients and alters the production of secondary metabolites that are inhibitory to *C. difficile* germination and outgrowth (Theriot *et al.,* 2016). Once ingested, the *C. difficile* spores survive the gastric acid and digestive enzymes of the stomach passing through to the duodenum where they germinate and proliferate (Smits *et al.,* 2016). The vegetative cells associate in the caecum and colon, where they are thought to adhere and quickly establish itself as a dominant species within the gut of susceptible individuals (Rupnik *et al.,* 2009, Dubberke and Olsen, 2012).

The early 2000s marked the beginning of an epidemic, with hospitals around the world reporting dramatic increases in the number of severe instances of CDI over the next several years (Rupnik *et al.,* 2009), with about 450,000 cases and 29,000 deaths each year, in the United States alone (Lessa *et al.,* 2015). Isolates from this period were sequenced and subsequently known as BI/NAP1/027 (McDonald *et al.,* 2005). This strain is characterised by high-level fluoroquinolone resistance, efficient sporulation, and high toxin production. Although there is no clear explanation for the dramatic increase in instances of CDI, a number of theories have been proposed, including a growth advantage observed for *C. difficile*, in the presence of trehalose, a food supplement that became widely used at around the same time period (Collins *et al.*, 2018b).

The most important risk factor for CDI remains antibiotic use, with broad range antibiotics such ampicillin, amoxicillin, cephalosporins, clindamycin and

fluoroquinolones most frequently associated with CDI (Ananthakrishnan, 2011, Owens *et al.,* 2008, Pepin *et al.,* 2005). The risk and severity of CDI increases with age (Rupnik *et al.,* 2009). Whilst the majority of cases are thought to be hospital acquired, *C. difficile* is now recognised as a cause of community-associated diarrhoea. Furthermore, the PCR ribotypes of strains isolated from patients within the community have a significant overlap with strains isolated from patients with CDI in hospitals, suggesting a common source of *C. difficile* (Hensgens *et al.,* 2014, Eyre *et al.,* 2013). Interestingly, more than 30% of patients experiencing CDI within the community do not have the typical risk factors *i.e.* recent antibiotic treatment (Hensgens *et al.,* 2011, Wilcox *et al.,* 2008). Studies have also suggested that the use of proton pump inhibitors could be a risk factor, however the underlying rationale for this is unclear (Janarthanan *et al.,* 2012, Kim *et al.,* 2012).

Outbreaks of CDI are particularly disruptive, often resulting in patient isolation, ward closures and in some cases, hospital closures (Cartman *et al.,* 2010). Treatment for *C. difficile* is complicated by its intrinsic antibiotic resistance which is attributed to the large number of mobile elements containing antibiotic resistance genes, within the bacterium's genome (Sebaihia *et al.,* 2006). For mild, single occurrences of CDI associated with antibiotic-induced alterations to the gut microbiota, treatment can simply involve withdrawal of antibiotics, which allows the gut microbiota to recover (Rupnik *et al.,* 2009). In severe or recurrent infections however, treatment is more challenging. Patients experience high levels of recurrence ranging from 20% after an initial episode to 60% after multiple recurrences. Recurrent infections are often caused by re-exposure to or reactivation of *C. difficile*

spores in patients with an impaired immune system or weakened barrier function of the colonic microbiota (Marsh *et al.,* 2012). Patients with multiple recurrences respond to treatment with metronidazole or vancomycin initially, but symptoms return days or weeks after the treatment is stopped (Rupnik *et al.,* 2009).

Historically vancomycin and metronidazole were the only available antibiotics for *C. difficile*, with CDI patients being treated with pulse dosing of vancomycin every other or third day. The hope of this was to enable the normal gut biota to re-establish, whilst preventing *C. difficile* from re-growing (Leong and Zelenitsky, 2013). In 2011, fidaxomicin, a poorly absorbed antibiotic with activity against specific anaerobic gram-positive bacteria, was approved by the food and drug administration (FDA) for the treatment of CDI. Fidaxomixin has been shown to have a similar cure rate for acute infections as vancomycin, however, it substantially lowers the risk of recurrence compared to vancomycin (Cornely *et al.,* 2012, Louie *et al.,* 2011). Despite this, the high cost of fidaxomycin has curtailed its use (Vaishnavi, 2015).

In recent years, the most effective treatment for severe multiple occurrences of CDI has been the replenishment of the normal gut biota by means of a faecal transplantation, a procedure first reported in 1958 (Aas *et al.,* 2003). Although successful in 90% of patients experiencing recurrent infections (Rohlke and Stollman, 2012), this treatment has some risks associated with it. Not only have changes to the gut microbiota been associated with certain types of cancer (Zackular *et al.,* 2013), but there is also the risk of disease

transmission from the faecal donor to the recipient. The precise organisms responsible for providing resistance against *C. difficile*, and the mechanisms involved are not yet known, but multiple studies have indicated that both the *Bacteroidetes* and *Firmicutes* may play important roles (Seekatz and Young, 2014). As the *Bacteroides* have been shown to be nutritionally diverse, capable of utilising a wide variety of carbon sources, these organisms may simply be better adapted to surviving in the gastrointestinal tract. Additionally, these organisms have been shown to play an important role in the biotransformation of primary bile acids into secondary bile acids (Theriot and Young, 2015). Some secondary bile acids such as taurocholate, have been shown to promote *C. difficile* germination, whilst others such as deoxycholate have been shown to inhibit *C. difficile* outgrowth. This ability for secondary bile acids to both enhance and inhibit *C. difficile* germination and outgrowth is thought to play an important role in the restoration of colonisational resistance.

Finally if all treatments fail to stem the infection, the only life-saving alternative is for the removal of the colon (Lamontagne *et al.,* 2007).

1.2 Virulence Factors

The diarrhoeagenic phenotype of CDI is accredited to the toxins produced by *C. difficile* (Vedantam *et al.,* 2012). The main toxins produced by the organism are TcdA and TcdB, with an additional toxin, *Clostridioides difficile* transferase (CDT), found in some strains, most notably ribotypes 027 and 078. All naturally occurring diarrhoeagenic strains produce TcdB with most strains also producing TcdA (Vedantam *et al.,* 2012).

As the majority of *C. difficile* strains associated with CDI are toxigenic, the two large clostridial toxins TcdA and TcdB are the most well characterised *C. difficile* virulence factors (Borriello *et al.,* 1990, Voth and Ballard, 2005, Warny *et al.,* 2005). Nonetheless, a number of other factors are needed for the disease to take hold e.g. Colonisation of the host, adhesion to the gut mucosa, and dissemination (Vedantam *et al.,* 2012). However, the late development of molecular tools for *C. difficile* hindered the study of these other non-toxin virulence factors (Vedantam *et al.,* 2012). Whilst studies are now focusing on these gaps in our knowledge, little is known about the role these virulence factors play during infection.

1.2.1 Toxins

1.2.1.1 Toxin A and toxin B

The two large toxins TcdA and TcdB produced by *C. difficile* (Voth and Ballard, 2005), have long been shown to cause the symptoms of the disease, triggering intestinal damage and the release of nutrients from the damaged colonic epithelium (Voth and Ballard, 2005). Both toxins glucosylate Rho family GTPases, leading to the disruption of the actin cytoskeleton, cell death and a strong inflammatory response (Just *et al.,* 1995, Voth and Ballard, 2005, Carter *et al.,* 2012).

Both toxins are encoded in the 19.6 kb Pathogenicity Locus (PaLoc) (Figure 1). The PaLoc is very stable and conserved amongst toxigenic strains (Cohen *et al.,* 2000). Although nontoxigenic strains lack the PaLoc, they are still capable of colonising the gut (Cohen *et al.,* 2000, Curry *et al.,* 2007).

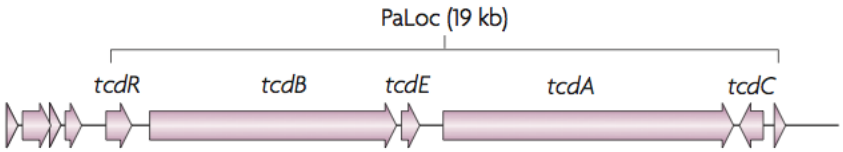

Figure 1: PaLoc locus encodes *C. difficile* Toxins

The 19 kb pathogenicity locus (PaLoc) encodes both toxin A and toxin B (TcdA and TcdB). In non-toxigenic strains PaLoc is replaced by a 115 bp sequence (Rupnik *et al.*, 2009). Reproduced with permission from Springer Nature.

The PaLoc encodes five genes: *tcdA, tcdB, tcdC, tcdE and tcdR*. Both genes encoding toxins *tcdA* and *tcdB* are separated by an intervening sequence, *tcdE* (Voth and Ballard, 2005). TcdE shares homology to phage holin, a protein with pore-forming activity used to release the phage from the host cell. It has been demonstrated that TcdE is important for the release of TcdA and TcdB from R20291 cells (Govind and Dupuy, 2012, Govind *et al.,* 2015). However its function is less clear in 630 (Olling *et al.*, 2012).

TcdR, an alternative sigma factor, directs transcription from both TcdA and TcdB promotors as well as its own promotor, while TcdC is an anti-sigma factor that negatively regulates TcdR. Genes within the PaLoc are expressed during stationary phase and it has been demonstrated that the expression of the toxin genes is regulated by the global gene regulator CodY (Dineen *et al.,* 2007). When nutrients are in abundance, CodY binds to the promoter region of *tcdR* thus repressing toxin gene expression. When environmental nutrients are lacking, CodY disassociates from *tcdR* thus enabling expression of both large toxins (Voth and Ballard, 2005, Dineen *et al.,* 2007, Carter *et al.,* 2012).

TcdA and TcdB are both glucosyltransferases and transfer glucose from UDP-glucose to small GTPases such as Rho, Rac and Cdc42 in the host cell. Glucosylation deforms these small proteins, disrupting the signalling pathways that they are involved in. This results in alterations to the actin cytoskeleton leading to disruption of tight junctions and loosening of the epithelial barrier, disruption of barrier function, and eventually, cell apoptosis (Figure 2a) (Abt *et al.,* 2016). The net effect of these alterations is rapid fluid loss into the intestinal lumen, manifesting as diarrhoea (Voth and Ballard, 2005, Carter *et al.,* 2012, Vedantam *et al.,* 2012).

In addition to the direct cytotoxic effects of TcdA and TcdB, both toxins have also been demonstrated to provoke inflammatory responses to which the additional tissue damage may lead to serious clinical conditions such as pseudomembranous colitis (Ng *et al.,* 2010).

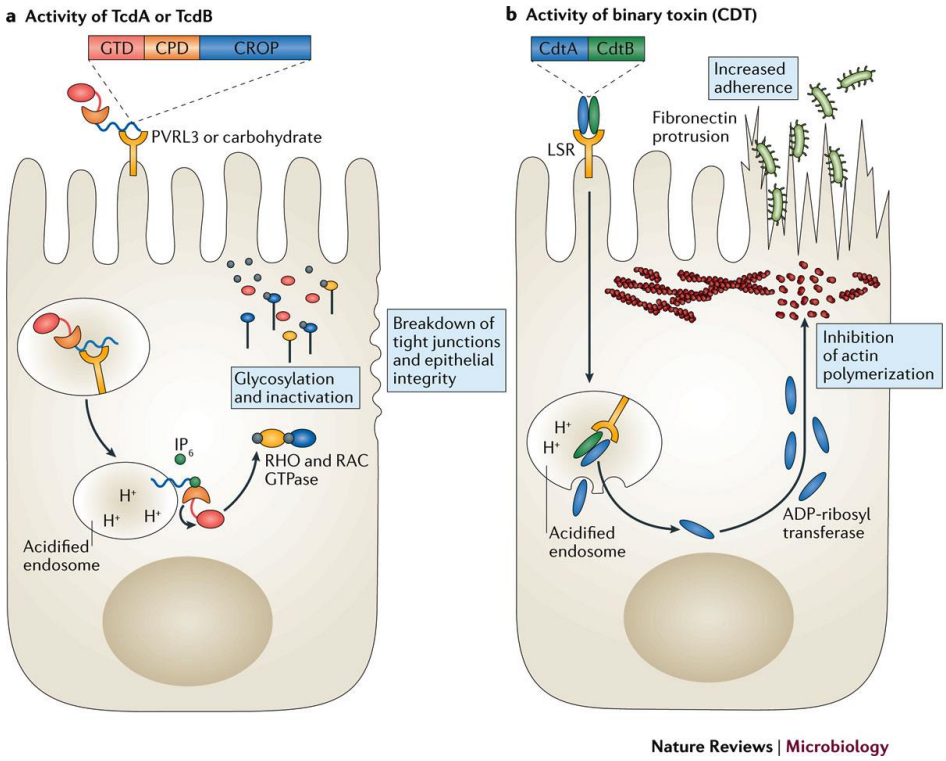

Figure 2: Mechanism of action of *C. difficile* toxins in epithelial cells.

(**A**) the repetitive oligopeptides (CROPS) domain of TcdA binds to carbohydates on the apical surface of epithelia cells, whereas TcdB binds to a poliovirus receptor-like 3 (PVRL3) expressed on colonic epithelial cells. Both toxins are internalised, where the acidification of the endosome enables the CROP domain to embed into the endosomal membrane. The cysteine protease domain (CPD) and the glucosyl transferase domain (GTD) are consequently transported into the cytosol. The cysteine protease is activated by inositol hexakisphosphate (IP_6) to release the toxin glucotransferase. RHO or RAC GTPases are inactivated by glucosylation, which results in the breakdown of tight junctions and epithelial integrity. (**B**) *C. difficile* transferase (CDT) is internalised by binding to the lipolysis-stimulated lipoprotein receptor (LSR). The CdtB subunit creates pores in the acidified endosome releasing the CdtA subunit into the cytosol. The ADP-ribosyl transferase activity of the CdtA subunit inhibits actin polymerisation near the cell membrane. This enables the fibronectin microtubules to elongate and protrude through microvilli enhancing *C.*

difficile adherence to the epithelium (Abt *et al.,* 2016). Reproduced with permission from Springer Nature.

Structural analyses of both TcdA and TcdB have shown both toxins to be single stranded proteins, each possessing four structural domains, including: (i) an amino-terminal glucosyltransferase domain (GTD), (ii) an autoprotease domain (APD), (iii) a pore-forming and delivery domain, (iv) the combined repetitive oligopeptides (CROPS) domain. Although receptor binding occurs at the CROPS domain located at the C termini of both toxins, a number of studies have demonstrated the ability for the toxin to bind to cells in the absence of the CROP domain (Olling *et al.*, 2011, Goy *et al.*, 2015, Manse and Baldwin, 2015). Activation of the APD by eukaryotic inositol hexakisphophate releases the GTD into the cytosol of the host cell resulting in toxin activity (Abt *et al.,* 2016).

Another important *C. difficile* toxin is CDT which is an actin-specific ADP-ribosylating toxin encoded by *cdtA-cdtB* (Figure 3) (Carter *et al.,* 2007, Rupnik *et al.,* 2009). The ADP-ribosyl transferase activity of the CdtA subunit inhibits actin polymerisation, inducing morphological changes in the host intestinal epithelial cells (Figure 2B) (Abt *et al.,* 2016). Thus facilitating increased adherence of the organisms possessing this toxin (Schwan *et al.,* 2014).

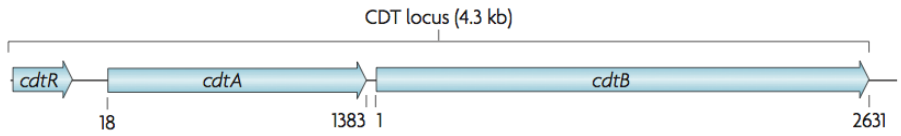

Figure 3: *Clostridioides difficile* transferase locus.

Clostridioides difficile transferase (CDT) is encoded on a separate region of the chromosome on the CDT locus which comprises three genes (Rupnik *et al.*, 2009)**.** Reproduced with permission from Springer Nature.

The contributions of both TcdA and TcdB to disease progression remains a matter of debate with two laboratories separately obtaining conflicting results with regard to the role of TcdA in the hamster model. One study showed that both toxins could individually cause severe disease, whilst the other found that TcdB alone was required for virulence (Lyras *et al.*, 2009, Kuehne *et al.*, 2010, Kuehne *et al.*, 2011).

1.2.2 Sporulation

When bacteria exist as spores they are highly resistant to a range of environmental factors including extremes of heat, pH and chemical stresses. *C. difficile* spores are no exception; additionally being resistant to mechanical forces and aerobic conditions (Borriello *et al.,* 1990). Due to their morphological and physiological features these spores can persist for large amounts of time on hospital surfaces as well as in the air, resisting conventional disinfection protocols (Lawley *et al.,* 2009). The ability of the

spore to endure in the environment is crucial to both acquisition and transmission of CDI (Deakin *et al.*, 2012).

Upon ingestion, the spore is able to tolerate the low pH environment of the stomach, passing through to the intestinal tract where it germinates. Patients with CDI excrete large numbers of spores into the environment leading to transmission of the disease (Deakin *et al.,* 2012). However, a small number of spores may remain in the intestinal tract. As the antibiotics used to treat CDI do not kill spores, they are able to germinate and recolonise the intestinal tract once treatments are stopped (Sarker and Paredes-Sabja, 2012).

During sporulation, external factors trigger the signal cascade of sigma factors causing the vegetative form of the bacterium to be transformed into a highly resistant spore. One of the most common signals to induce sporulation is starvation (Setlow, 2007). The initial stages of sporulation are evolutionarily conserved between *Bacillus subtilis* and *C. difficile* with sigma factors remaining the key regulators of the pathway. Although it should be noted that the sigma factors controlling sporulation behave quite differently in both species, activating at different times (Pereira *et al.,* 2013).

The master regulatory protein Spo0A, which is activated by phosphorylation, governs entry into sporulation (Molle *et al.,* 2003, Deakin *et al.,* 2012, Pereira *et al.,* 2013). As Spo0A regulates several other cell processes including biofilm formation, the concentration of phosphorylated Spo0A present within the bacterial cell is used to control which cell process becomes activated, with higher levels of phosphorylated Spo0A committing the cell to

sporulation and repressing other vegetative cell functions (Piggot and Hilbert, 2004).

1.2.3 Surface Virulence Factors

S-layer

Surface layer proteins (SLPs), also called the S-layer, are surface associated paracrystalline arrays, formed by identical subunits of glycoproteins or proteins. Present in most prokaryotes (Sara and Sleytr, 2000), the function of the SLPs are far reaching and includes: acting as molecular sieves, protective factors against parasitic attack, virulence factors, adhesion sites for extracellular proteins and, maintaining the cell envelope integrity. Roles for SLPs have even been observed in cell division, biofilm formation and swimming (Sara and Sleytr, 2000). In C. difficile the S-layer appears to be important for growth. As such, research into its function has been seriously hampered by a lack of *slpA* mutants (Dembek *et al.*, 2015).

The S-layer of *C. difficile* is mainly composed of two proteins, a high-molecular-weight (HMW) SLP of 40kDa and a low-molecular-weight (LMW) SLP of 35 kDa (Cerquetti *et al.,* 2000). Both the HMW and LMW SLPs are derived from the same precursor, SlpA. The SlpA pre-protein contains a signal peptide directing translocation of the protein across the cell membrane. Once across the membrane, SlpA is cleaved by the cysteine protease Cwp84, to form both the HMW and LMW SLPs (Calabi *et al.,* 2001, Fagan *et al.,* 2009). The SLPs are then tightly linked by a non-covalent complex, with the HMW SLP localised to the bacterial cell wall and the LMW SLP displayed as the external surface of the bacterium (Fagan *et al.,* 2009) (Figure 4). As the LMW SLP is immunologically variable (Cerquetti *et al.,* 2000,

Fagan *et al.,* 2009), it has been suggested that this may play a part in evasion of the immune system (Vedantam *et al.,* 2012). However, a recent study by Kirk *et al*. (2017) noted that the LMW SLP is the binding site for bacteriophages suggesting this antigenic variation could be a result of selective pressure to change the bacteriophage receptor (Kirk *et al*., 2017). In other studies it has been found that *C. difficile* chemically stripped of SLPs show a diminished adherence in both animal models and human HeLa cells, demonstrating a role of the SLP in adhesion to the host (Takeoka *et al.,* 1991).

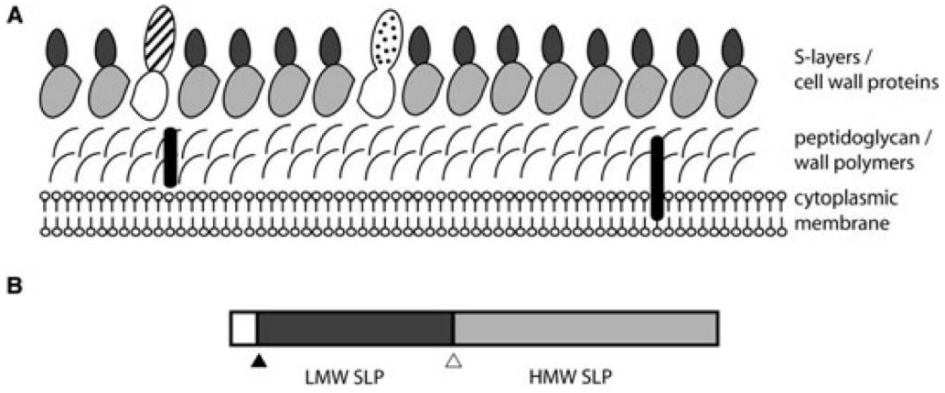

Figure 4: *C. difficile* cell wall model.

(**A**) Two types of surface layer proteins are presented. High MW SLP are shown as light grey molecules, and low-molecular-weight SLP shown as dark grey. Two-lobed structures (white) represent other minor cell wall proteins with thevertical black bars representing putative cell wall polymers. (**B**) The precursor protein SlpA, the cleavage sites producing the signal peptide is indicated by th dark arrow head and the mature HMW SLP and LMW SLP by thelight arrow head (Fagan *et al*., 2009) Reproduced with permission from John Wiley and Sons.

1.2.4 Cell wall proteins

Genetic studies have also demonstrated the presence of 28 paralogs of SlpA within the *C. difficile* 630 genome. Collectively known as cell wall proteins (CWP), these proteins were all found to contain three copies of the Pfam 04122 motif, a complex cell wall binding motif characteristic of the SLPs. It has been proposed (Karjalainen *et al.,* 2001) that this motif mediates the binding of these proteins to the underlying cell wall. Many of these proteins also carry a second variable motif.

The best characterised examples of CWPs are Cwp66, a putative adhesin (Waligora *et al.,* 2001), Cwp84 (Janoir *et al.,* 2007), a cysteine protease that mediates the cleavage of the SlpA precursor (Kirby *et al.,* 2009, Dang *et al.,* 2010) and the degradation of a variety of host cell extracellular matrix proteins (Janoir *et al.,* 2007), and CwpV, a phase-variable protein that provides anti-phage protection to *C. difficile* (Emerson *et al.,* 2009, Sekulovic *et al.,* 2015).

1.2.5 Flagella

For many species, the flagella not only provides force-driven motility, but have also been implicated in promoting adherence to host cells, facilitating the translocation of virulence factors across cell membranes, and in promoting biofilm formation (Harshey, 2003, Duan *et al.,* 2013). Naturally occurring nonflagellated strains were reported to demonstrate a 10-fold reduction in adherence to tissue in the mouse cecum (Tasteyre *et al.,* 2001). Recent studies have investigated specific genes in the flagellar operon,

although the role of flagella during infection remained undefined. (Stevenson *et al.,* 2015).

Inactivation of either the flagellin (*fliC*) or flagellar cap (*fliD*) results in complete loss of flagella and motility of *C. difficile* (Dingle *et al.,* 2011). Recent studies in strain R20291 have also implicated a role for the flagella in the later stages of *C. difficile* biofilm formation with a *fliC* mutants displaying decreased biofilm formation at 5 days (Đapa *et al.*, 2013). Contradictions within the literature, regarding the role of the flagella in colonisation likely stem from difference between strain 630 and R20291.

1.4 Biofilm

Biofilms are communities of surface-associated microorganisms, encased in a self-produced extracellular matrix. First appearing in the fossil record, between 3.2-3.4 billion years ago (Rasmussen, 2000, Westall *et al.,* 2001), formation of a biofilm is a common feature amongst bacteria and can be found to occur on practically any natural or artificial surface. In the past few decades it has become established that biofilms are ubiquitous in nature, likely being the prevalent form of bacteria living in the natural setting (Hall-Stoodley *et al.,* 2004). Biofilms are known to play an important role in disease, as biofilm formation greatly influences the ability of several pathogens to colonise and establish an infection (Nobbs *et al.,* 2009, Allsopp *et al.,* 2010), Biofilms provide an enclosed environment for bacteria within to escape immune responses as well as providing increased resistance to antibiotics (Mah and O'Toole, 2001, Beloin *et al.,* 2008).

1.4.2 Structure

Bacterial cells within a biofilm are morphologically and physiologically different from planktonically cultured cells (Vlamakis *et al.*, 2008). The three-dimensional structure of the biofilm provides variations in the concentration of nutrients within the biofilm, this in turn enables genetically identical bacteria within the monoculture biofilm to simultaneously express different genes, resulting in the production of subpopulations containing functionally different cell types (motile cells, matrix producing cells and spores) (Vlamakis *et al.,* 2008).

One of the best studied organisms for biofilm formation is *Bacillus subtilis*. For this organism to form a biofilm, planktonic cells must first adhere to a surface to produce a microcolony. The bacteria within the microcolony use a form of cell-cell communication, known as quorum sensing (QS), to co-ordinate responses to external stimuli in a cell density-dependent manner (Hall-Stoodley *et al.,* 2004). The microcolony then starts to expand through both the recruitment of additional planktonic cells and cell division (Figure 5) (Vlamakis *et al.,* 2013). The bacteria then start to produce an extracellular matrix composed of proteins, nucleic acid and polysaccharides (Vlamakis *et al.,* 2013) with the biofilm architecture maturing as a result of interactions between the microbial colonies and extracellular substances (Davies *et al.,* 1998). The 3D structure of the mature biofilm often forms pores, and in some cases channels to help with the distribution of nutrient and signalling molecules (Costerton *et al.,* 1999, Fux *et al.,* 2004, Hall-Stoodley *et al.,* 2004, Hall-Stoodley and Stoodley, 2005). The final step in biofilm development is dispersion of the biofilm (Figure 5). Numerous environmental conditions

such as the availability and perfusion limitation of nutrients and waste, determine when the biofilm has reached its critical mass and when the dispersion of the biofilm starts (Vlamakis *et al.,* 2008). Through the dispersion of motile cells from a mature biofilm the bacteria can colonise new surfaces. This disassembly of the biofilm causes the continuous release of single cells, spores, or small clusters, or even large portions of the biofilm, over an extended period of time and results in rapid bacterial spreading (Vlamakis *et al.,* 2008).

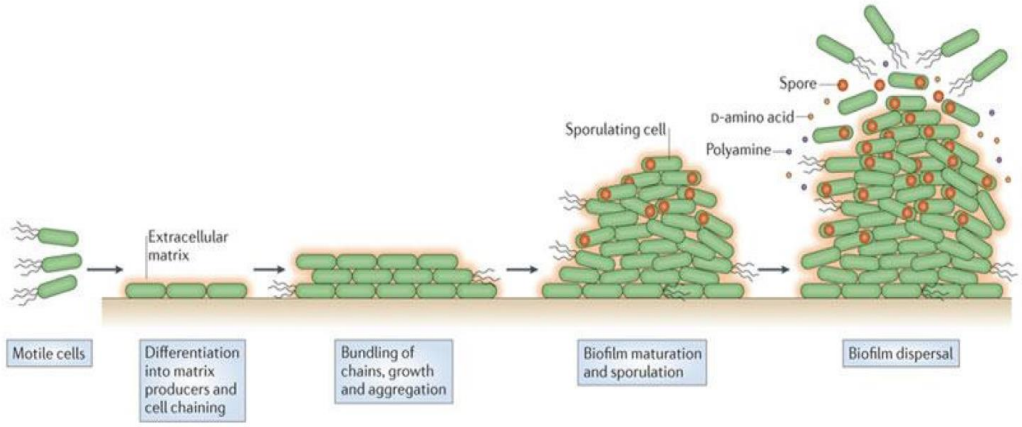

Figure 5: Different stages of biofilm formation by *Bacillus subtilis.*

The main stages are: development, maturation and disassembly. After initial attachment to a surface, motile cells differentiate into either non-motile or matrix-producing cells. During this stage the cells form chains, surrounded by self-produced extracellular matrix. Next comes the maturation of the biofilm, here *B. subtilis* cells begin to sporulate. The final step is biofilm disassembly. In biofilms, genetically identical cells differentiate into a specific cell type, although this is not terminal and can be altered when environmental conditions change (Vlamakis *et al.*, 2013). Reproduced with permission from Springer Nature

1.4.3 Role of biofilms in infection

Biofilms offer bacteria increased protection from their environment in a myriad of different ways, such as increased resistance to antibiotics, protection from phagocytosis, increased adherence to the epithelial tissues, and through the exclusion of host defence molecules like antibodies and anti-microbial peptides (Hall-Stoodley and Stoodley, 2009). Resistance to antibiotics can be up to 1000 times higher for bacteria within a biofilm compared to those existing planktonically (Olsen, 2015).

Not only has biofilm formation been associated with several persistent tissue infections such as chronic otitis media, chronic rhinosinositis, recurrent urinary tract infections, endocarditis and cystic fibrosis-associated lung infection (Costerton *et al.,* 1999), it also represents a significant problem when formed on artificial devices used in medicine such as: catheters, stents, orthopaedic implants, contact lenses and implantable electronic devices (Costerton *et al.,* 1999).

1.4.3 *C. difficile* biofilms

Bacterial populations located within the human gastrointestinal tract exist in two forms: free-floating planktonic communities within the lumen, and sessile bacteria within mucosal-associated biofilm communities (van der Waaij *et al.,* 2005). These sessile communities often contain a multitude of bacterial species (Edmiston *et al.,* 1982, Zoetendal *et al.,* 2002) and, are likely to play a more important role in disease pathogenesis than planktonic forms. However, the physical inaccessibility of the gut of healthy individuals has restricted the study of these mucosal communities (Crowther *et al.,* 2014).

Several *in vitro* studies have shown an ability of *C. difficile* to form single species biofilms (Dawson *et al.,* 2012, Dapa *et al.,* 2013, Crowther *et al.,* 2014, Semenyuk *et al.,* 2014). *In vitro* biofilms are composite structured communities likely to be encased in extracellular DNA, proteins and polysaccharides (Figure 6) (Dapa *et al.,* 2013, Crowther *et al.,* 2014, Semenyuk *et al.,* 2014). The bacterium's ability to form sessile communities *in vitro* have been shown to alter the effectiveness of vancomycin and metronidazole (Dapa *et al.,* 2013) suggesting *C. difficile* biofilms may have a role in recurrent infections. Dapa *et al.* additionally reported that surface protein Cwp84, which is required for the biogenesis of the S-layer, is required for biofilm formation *in vitro.* Mutants in the *C. difficile* flagellar proteins also showed defective biofilms, but only in the later stages, indicating a role in biofilm maturation. A subsequent study by Maldarelli *et al.* (2016) demonstrated that type IV pili of *C. difficile* also play an important role in biofilm formation.

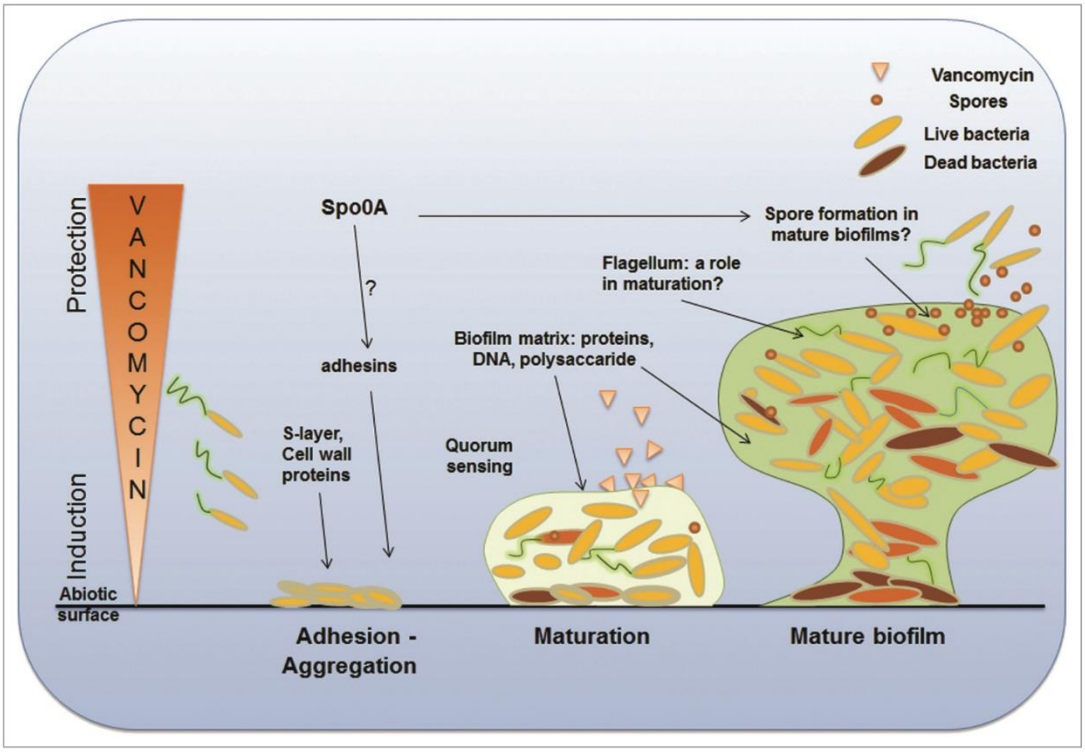

Figure 6: A hypothetical model for *C. difficile* biofilm formation

The S-layer and adhesins initiate biofilm formation, with quorum sensing important for maturation of the biofilm. Proteins DNA and polysaccharide are the key components of the biofilm matrix, which offers the bacteria within increased resistance to vancoycin (Dapa and Unnikrishnan, 2013). Reproduced with permission from Landes Bioscience.

More recently *in vivo* studies have demonstrated that *C. difficile* is a minority member of mixed species communities in a mouse model (Semenyuk *et al.*, 2015). Whilst a germ-free mouse model demonstrated the ability of strain R20291 to organise itself in a glycan-rich biofilm architecture, which sustainably maintains the bacteria outside the mucus layer (Soavelomandroso *et al.*, 2017).

Studies from our lab and others have also shown a very interesting link between sporulation and biofilm formation. Spo0A negative mutants were unable to form biofilms (Dapa *et al.,* 2013). Spo0A is known to modulate other cellular pathways in addition to sporulation (Molle *et al*., 2003) and likely regulates adhesins and other proteins important for adhesion. As mature biofilms contain microenvironments that are nutritionally deprived, it is plausible that the biofilm acts as a niche for spore formation during infection. More work is needed to identify the exact role Spo0A during infection.

Another interesting finding of Dapa *et al.* (2013) was the role of the quorum sensing regulator LuxS. Mutants lacking a functional form of the gene were unable to initiate biofilm formation *in vitro,* with genetic complementation providing partial restoration of the phenotype. This suggests that a LuxS-mediated quorum sensing system is important for biofilm formation and development. The precise mechanisms involved in LuxS-mediated regulation remain unclear (Dapa and Unnikrishnan, 2013, Dapa *et al.,* 2013).

Current knowledge of *C. difficile* biofilm formation and regulation is extremely limited compared to that of other bacterial species (Kolter, 2010). Therefore there is a clear need for global studies to be conducted to determine the requirements for *C. difficile* biofilm formation and regulation. Bacterial communities of *C. difficile* are likely to be crucial in recurrent CDI. Additionally, given that *C. difficile* has been isolated from various marine environments (Pasquale *et al.,* 2011, Hargreaves *et al.,* 2013), biofilm formation may be important for bacterial survival in such environments.

1.3 Quorum Sensing

QS was first described in the regulation of bioluminescence of *Vibrio fischeri* and *Vibrio harveyi* (Nealson *et al.,* 1970, Nealson and Hastings, 1979). QS is a form of cell-cell communication amongst bacteria (Antunes *et al.,* 2010). Through the detection of signalling molecules, autoinducers (AIs) released from individual bacterial cells, bacteria can get an indirect measure of their population density in a particular environment, and adjust gene expression accordingly (Antunes *et al.,* 2010). These AIs are released during growth, accumulating in the environment. Once the concentration of these molecules reaches a threshold, or 'quorum', they can bind to and activate receptors on the cell (Antunes *et al.,* 2010). This generally leads to a cascade of events, which ultimately ends in a change to gene regulation (Bassler and Losick, 2006). Genes regulated by QS include those involved in cell migration, biofilm production, virulence, sporulation and the production of toxins (Hammer and Bassler, 2003, Carter, 2005, Antunes *et al.,* 2010). Three main QS signalling pathways have been characterised, which included the peptide based system in Gram-positives, the LuxSI/LuxR system in Gram-negatives and the LuxS/AI-2 of *Vibrio spp*.

1.3.1 Bacterial quorum sensing systems

Many gram-positive bacteria utilise peptide quorum sensing systems to control gene expression. *Staphylococcus aureus* has served as the model organism for studying bacterial peptide signalling (Novick and Geisinger, 2008). The peptide-based QS system of *S. aureus* is encoded by the accessory gene regulator (*agr*) locus (Novick and Geisinger, 2008). *agrD* encodes an autoinducing peptide (AIP) which is an oligopeptide that is

trimmed and secreted by the membrane bound protein AgrB (Ji *et al.,* 1995, Saenz *et al.,* 2000, Zhang and Dong, 2004). The secreted AIP is 7-9 aa in length and contains a 5- membered thiolactone ring (Roux *et al.,* 2009). The extracellular AIP binds to AgrC, a membrane-bound sensor kinase, leading to AgrC autophosphorylation and activation of AgrA. The *agr* system activates two promoters, P2 and P3, which produce RNAII and RNAIII respectively (Morfeldt *et al.,* 1995, Novick and Geisinger, 2008). Activation of P2 initiates the transcription of the agr operon from the RNAII transcript. Transcription from P3 produces the effector molecule of the agr system, RNAIII (Roux *et al.,* 2009). It is thought that over 70 genes are regulated by the *agr* system in *S. aureus* (George and Muir, 2007).

Gram-negative bacteria typically use LuxI/LuxR- type QS systems (Rutherford and Bassler, 2012). In these systems an AI synthase (homologous to LuxI in *Vibrio fischeri*) catalyses a reaction between Adenosylmethionine (SAM) and an acyl carrier protein (ACP) thus producing a freely diffusible acyl homoserine lactone (AHL) AI (Engebrecht and Silverman, 1984, More *et al.,* 1996, Schaefer *et al.,* 1996, Ng and Bassler, 2009). At high concentration, AHL AIs bind to cytoplasmic LuxR-like transcription factors enabling them to bind DNA and activate transcription of target genes (Rutherford and Bassler, 2012). Interestingly, the AHLs produced by different bacteria possess different length Acyl side-chains (Fuqua *et al.,* 2001, Ng and Bassler, 2009). As the interactions between the AHL AI and LuxR are highly specific, this chemical diversity promotes intraspecies-specific bacterial cell-cell communication.

1.3.3 *luxS* / Autoinducer-2

The other main QS system is that of LuxS/AI-2 which is perhaps best studied in the marine bacterium *Vibrio harveyi,* being used to regulate the organism's bioluminescence (Nealson and Hastings, 1979, Bassler and Losick, 2006). The signalling molecule AI-2 is synthesised through reactions involving the enzymes Pfs and LuxS (Figure 7A). During the activated methyl cycle in bacteria, S-Adenosylmethionine (SAM) acts as a methyl donor, creating the toxic metabolite S-adenosylhomocysteine (SAH). Bacteria detoxify SAH in a two-step reaction, first converting it to S-ribosylhomocysteine (SRH) through the action of the enzyme Pfs. Finally LuxS converts SRH into homocysteine, producing the potent QS signalling molecule, AI-2 as a by-product from this reaction (Schauder *et al.,* 2001).

There are currently two characterised signalling pathways for AI-2, the Lsr internalisation pathway exemplified by *Salmonella*, and the LuxPQ receptor pathway of *Vibrio spp* (Figure 7B). During the Lsr signalling pathway, AI-2 is internalised by Lsr ABC transport-type transporter where it is phosphorylated by LsrK. Phosphorylated AI-2 inhibits the *lsr* operon repressor LsrR and induces transcriptional changes to QS controlled genes. For LuxPQ, AI-2 binds to the LuxP membrane bound receptor, which interacts with the inner membrane bound protein LuxQ, causing a conformational change. This process removes a phosphate from LuxU, a two-component phosphorelay protein, which in turn dephosphorylates the response regulator, LuxO (Vendeville *et al.*, 2005).

In recent years, BLAST (NCBI) searches have shown that LuxS homologues are present in most of the bacteria for which complete genome sequences are available (Hilgers and Ludwig, 2001, Xavier and Bassler, 2003). This revelation has led to the speculation that the LuxS system could serve as a 'universal signal' for interspecies cross-talk whereby the LuxS homologue of one species could regulate the gene expression of a different species. However, this is yet to be proven in species other than *Vibrio.*

A

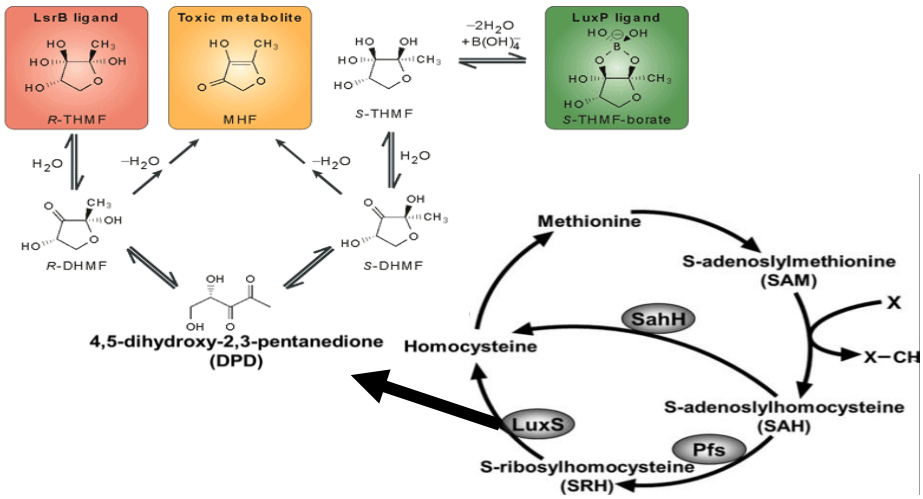

B

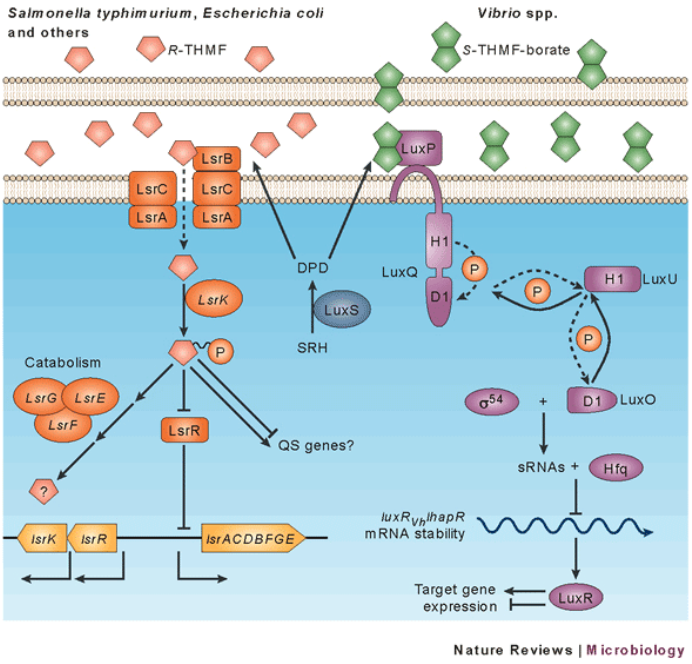

Figure 7: Production and response of AI-2

(**A**) The enzyme, LuxS, is responsible for the conversion of S-ribosylhomocysteine (SRH) to Homocysteine producing the bi-product 4,5,dihydroxy-2,3-pentanedione (DPD). DPD undergos spontaneous cyclisation to produces several ligands collectively known as AI-2. (**B**) Currently there are two characterised schemes for AI-2 signalling. In one group of bacteria AI-2 binds to the periplasmic binding protein LsrB which forms part of the Lsr ABC transport system. After internalisation, AI-2 is

phosphorylated by LsrK ebalibing it to repress the action of LsrR, the *lsr* operon repressor and induced changes to gene expression. A protein complex consisting of LsrG, LsrE and LsrF then binds to the phospho-AI-2, forming products no longer capable of inducing a signalling response. In Vibrio spp. AI-2 binds to the membrane bound receptor LuxP which induces a conformational change to LuxQ that confers phosphatase activity. This process extracts a phosphate from LuxU that inter dephosphorylates the response regulator LuxO (Vendeville *et al.*, 2005). Reproduced with permission from Springer Nature.

Despite the proposed role in QS, others have speculated that LuxS is in fact a metabolic side product produced during the activated methyl cycle (a recycling pathway involved in the metabolism of methionine) (Winzer *et al.,* 2003). Evidence to support this comes from a study on *S. aureus.* Here Doherty *et al.* (2006) demonstrated that the inactivation of *luxS* in *S. aureus* had no effect on virulence-associated traits. Whilst it is possible that the phenotypic changes observed in some bacteria following inactivation of *luxS*, may be due to the absence of the AI-2 signal molecule, they could also be attributed to the disruption of the activated methyl cycle (Winzer *et al.,* 2003).

1.3.2 Quorum Sensing in *C. difficile*

Whole genome sequencing of *C. difficile* strain R20291 by Martin *et al.* (2013), revealed the presence of the *C. difficile agr* locus (*agrACDB*) which showed similarity to the *agr* genes of *S. aureus*. Furthermore it was shown that the *agr* locus modulates known *C. difficile* virulence factors (including flagellar biosynthesis and TcdA) *in vitro* and has a contributory role in colonisation and relapse *in vivo* (Martin *et al.,* 2013).

1.3.4 LuxS in *C. difficile*

A study by Lee and Song (2005) revealed that *C. difficile* possesses the LuxS/AI-2 homolog. The authors demonstrated that exposing early–log phase cells to cell free supernatants containing high levels of AI-2 obtained from mid-log phase culture, resulted in an increase in mRNA transcripts for TcdA and TcdB, suggesting a signaling role for LuxS (Lee and Song, 2005). Conversely, Carter *et al.* (2005) failed to demonstrate a role for LuxS as neither exogenous AI-2 nor chemically synthesized AI-2 (MHF) was found to have any discernible effect on toxin production. Nevertheless, it has been demonstrated by both groups that the AI-2, or AI-2-like molecules produced by *C. difficile,* are capable of inducing bioluminescence in a *Vibrio harveyi* AI-2 reporter strain (Carter *et al.,* 2005, Lee and Song, 2005). The specific role of LuxS in *C. difficile* remains unclear from these studies.

At present, it is not known how *C. difficile* biofilms are regulated. During studies by Dapa *et al.* (2013) it was found that biofilms formation was significantly impacted in LuxS deficient mutants. Thus LuxS somehow plays a role in biofilm development, though the precise mechanism of action is unclear. As described above, LuxS may mediate quorum sensing through production of AI-2, and/or bacterial metabolism through S-adenosyl methionine synthesis (Hardie and Heurlier, 2008). Although it is likely that LuxS has a quorum sensing role, we cannot rule out a role in metabolism: clearly further work is needed to establish the exact role of LuxS.

With contradictions within the literature, surrounding the role of LuxS in *C. difficile* (Lee and Song, 2005, Carter *et al.*, 2005) combined with its apparent

role in *C. difficile* biofilm formation (Dapa and Unnikrishnan, 2013), this project aimed to utilise next generation sequencing technologies in order to characterise the role of LuxS during *C. difficile* biofilm formation. Since LuxS/AI-2 is hypothesised to be a cross-species QS signalling molecule (Bassler *et al.*, 1997), we additionally set out to investigate its role in mediating interations with another member of the gut microbiota, *Bacteroides fragilis*.

Chapter 2 Materials and Methods

2.1 Bacterial Strains and Culture Conditions

Two bacterial species were primarily used in this study – *C. difficile* 630 and B1/NAP1/027 R20291 (isolated from the Stoke Mandeville outbreak in 2004 and 2005), and *Bacteroides fragilis* (kindly provided by Dr Gianfranco Donelli, Rome). Unless otherwise stated, these were cultured under anaerobic conditions (80% N_2, 10% CO_2, 10% H_2) at 37°C in an anaerobic workstation (Don Whitley, United Kingdom).

Bacteria were streaked from glycerol stocks and grown overnight on Brain Heart Infusion (BHI) agar plates, supplemented with L-Cysteine [1 g/l; Sigma, UK] and yeast extract [5 g/l; Oxoid]. 5 ml supplemented BHI (BHIS) to which 0.1 M glucose was added was inoculated with a streak of colonies and grown overnight to stationary phase.

Bacterial growth curves were performed in BHIS containing 0.1 M glucose (BHIS-G). Overnight cultures of *C. difficile* R20291 were diluted to OD_{600} 0.05 and regrown to mid-exponential phase (0.4-0.8). Cultures were then diluted to a starting OD_{600} of 0.01 and OD_{600} was taken at 1 hr intervals for 12 hrs.

The medium was additionally supplemented as appropriate with either thiamphenicol [15 µg/ml in agar or 7.5 µg/ml in broth], lincomycin [20 µg/ml], or *Clostridium difficile* Selective Supplement [D-cycloserine 250 µg/ml Cefoxitin 8 µg/ml] (Oxoid, UK).

For genetic manipulation, *Escherichia coli* strain DH5α (Invitrogen) and the conjugative donor strain CA434, were grown in Luria-Bertani (LB, Bacto, USA) at 37°C, supplemented with 20 µg/ml chloramphenicol when required.

Vibrio harveyi was grown at 30°C in LB supplemented with 50 µg/ml kanamycin.

2.2 Biofilm Assay

Biofilms were grown as per a previously published protocol (Dapa *et al.*, 2013). Overnight cultures of *C. difficile* were diluted 1:100 in fresh BHIS-G. 1 ml aliquots were pipetted into 24-well tissue culture treated polystyrene plates (Costar), and incubated under anaerobic conditions at 37°C, for 6 – 120 hr. Tissue culture plates were pre-reduced for 48 hr in the anaerobic workstation prior to use. The plates were wrapped with parafilm to prevent liquid evaporation. Biofilm biomass was measured using crystal violet (CV) as previously described (Dapa *et al.*, 2013, Varga *et al.*, 2008). After the required incubation, each well of the 24-well plate was washed once with sterile phosphate buffer saline (PBS) and allowed to dry for a minimum of 10 min. The biofilm was stained using 1 ml CV. Following a 30 min incubation period the CV was removed, and wells were subsequently washed twice with sterile PBS. The dye was extracted by incubation with 1 ml methanol for 30 min at room temperature (RT) in aerobic conditions. The methanol-extracted dye was diluted 1:1, 1:10 or 1:100 and OD_{570} was measured with a spectrophotometer.

For bacterial cell counts from the biofilm, the planktonic phase was removed and wells were washed once using sterile PBS. The adherent biofilms were then detached by scrapping with a sterile pipette tip and re-suspended into 1 ml PBS. Serial dilutions were prepared and plated onto BHIS plates to determine the CFU present in the biofilm.

2.3 Co-culture Biofilm Assay

For co-culture biofilm assays, both *C. difficile* and *B. fragilis* were diluted to a matching OD_{600} and diluted 1:100 into fresh BHIS-G. Biofilms were set up as before and measured by a combination of CV staining and CFU. To distinguish between *C. difficile* and *B. fragilis*, serial dilutions used for determining CFU were plated on BHIS plates additionally supplemented with *C. difficile* Selective Supplement (Oxoid, UK).

2.4 Confocal Microscopy

C. difficile strains were grown in 4-well glass chamber slides (BD Falcon, USA) in BHIS-G. Chamber slides were incubated at 37°C in anaerobic conditions for 24 hrs – 72 hrs and stained with BacLight live/dead stain mixture (Molecular Probes, Invitrogen), which contains the nucleic acid stains Syto 9 and propidium iodide (staining live bacteria green and dead bacteria red respectively). Following incubation, wells were gently washed twice with PBS 0.1% w/v saponin to remove unattached cells and permeabilise the biofilm. Biofilm samples were incubated with the dye for 15 minutes at 37°C after which the samples were washed twice with PBS. Cells were fixed with 4% paraformaldeyhyde (PFA) for 15 min.

All samples were visualised with a Zeiss Observer LSM 880 confocal scanning microscope at 60x – 100x magnification.

2.5 Transmission Electron Microscopy

For phage visualisation, *C. difficile* strains were grown in 24 well tissue culture plates (Costar, USA), 12 wells per strain, in BHIS-G. At either 24, 48 or 72 hrs samples were pooled. Bacterial cells were removed by centrifugation at 6000 x g for 30 mins. Phage were pelleted via ultra-centrifugation (Beckman Optima L-80 XP, Warwick) at 35,000 x g overnight.

10 µl of concentrated phage was placed on an electron microscopy grid and incubated at RT for 2 mins. Whatman filter paper was used to draw and blot the suspension across the grid. Grids were air dried for 2 mins before being coated in 10 µl of concentrated uranyl acetate. Grids were incubated at RT for 2 mins before excess stain was removed by blotting. Phage were visualised with a transmission electron microscope (JEOL 2100 TEM/STEM, Warwick) and images were captured digitally at a magnification of 10,000x and 50,000x.

2.6 AI-2 assay

Vibrio harveyi BB170 was grown from frozen stocks on LB plates supplemented with 50 µg/ml kanamycin at 30°C. Single colonies were isolated and inoculated into 2 ml medium and grown O/N. 400 µl 50% glycerol, 500 µl 1M HEPES, 200 µl of 1M K_2HPO_4 and 200 µl 0.1 M arginine were added to 18.7 ml autoinducer bioassay medium [sodium chloride (17.52 g/l), $MgSO_4$ (12.33 g/l) and casamino acids (2.0 g/l), pH adjusted to 7.5 with

KOH] and inoculated with 4 µl O/N BB170 culture. 180 µl aliquots were placed in 96-well optical plates (Costar, USA). 20 µl of supernatant was added and the plate was measured on a combined luminometer/spectrometer, recording OD_{600} and light output every 30 minutes for 12 hrs. For each supernatant sample, the fold bioluminescence induction was calculated at the point that the blank samples gave the minimal relative light output (RLO).

2.7 Quantitation of DNA in biofilms

To study the presence of extracellular DNA (eDNA) within preformed *C. difficile* biofilms, biofilms were grown in a 24-well plate as described above. At 24 hrs the medium was removed and replaced with pre-incubated BHIS-G containing DNase I at either 1 U/ml or 2 U/ml. Biofilms were incubated for an additional 24 hrs before being stained with 0.2% CV as described above.

2.8 Exogenous addition of DPD

Biofilm assays were setup as described above in BHIS-G containing 1 nM, 10 nM, 100 nM, or 1 µM of chemically synthesised, exogenous DPD (OMM scientific, USA). BHIS-G was used as a control. Samples were washed and stained with 0.2% CV at either 24 or 72 hrs.

2.9 Liquid Chromatography Mass Spectrometry

To analyse the biological molecules produced and utilised by both *C. difficile* and *B. fragilis*, biofilm supernatants were filter-sterilised (0.2 µm) to remove bacterial cells. Biological molecules were extracted by combining the cell-free supernatants with an equal volume of ethyl acetate. Ethyl acetate

supernatant mix was centrifuged at 15,000 g for 5 minutes and the ethyl acetate phase containing the biological molecules was removed.

2.10 DNA Extraction

DNA was extracted using phenol:chloroform:isoamyl alcohol (25:24:1) (pH 8) (Sigma-Aldrich, UK). 1- 10 ml of bacterial cultures were centrifuged at 5000 g for 10 min and the cell pellet was re-suspended in 180 µl lysis buffer (PBS with 10 mg/ml lysozyme). Samples were incubated at 37°C for 30 min. 4 µl RNase was added and samples were incubated for 15 min. After incubation 25 µl proteinase K solution (Qiagen, Germany), 85 µl ddH2O and 110 µl 10% w/v SDS solution were added and samples were incubated at 65°C for 30 min. An equal volume of phenol:chloroform:isoamyl alcohol (25:24:1) (pH 8) (Sigma-Aldrich, UK) was added and samples were mixed thoroughly by inversion. Samples were centrifuged at 15,000 x g for 3 min. The top layer was transferred into a fresh phase-lock tube and phenol/chloroform extraction was repeated a further 2 times. DNA was precipitated through the addition of 40 µl 3M sodium acetate and 800 µl ice-cold 100% ethanol. Samples were mixed and incubated at -80°C for 30 min. DNA was pelleted by centrifugation at 15,000 x g for 15 min. Supernatants were removed and samples were washed with 1 ml 70% ethanol followed by centrifugation at 15,000 x g for 3 min. Supernatants were removed and samples were allowed to air dry for 45 min at RT. Finally the DNA pellets were re-dissolved in 50 µl ddH2O. DNA concentrations were determined by use of Nano-drop or Qubit 2.0 Fluorometer (Life Technologies, UK) following the manufacturers protocol.

2.11 RNA Extraction

RNA was extracted from both planktonic cells and adherent biofilms. For planktonic RNA extraction, 1-2 ml of bacterial culture was centrifuged at 5000 x g for 10 min. The supernatant was removed and the cells were re-suspended in 1 ml Trizol (Ambion, USA).

For biofilm extractions, the biofilms were grown in 24-well tissue culture plates. At the desired time-point, wells were washed once with PBS before adherent cells were disrupted and re-suspended in 1 ml Trizol (Ambion, USA).

For both conditions, the re-suspended bacteria were transferred to lysing matrix tubes (MP Biomedicals, USA) containing 0.1 mm silica beads. Tubes were processed in a FastPrep-24 instrument (MP biosciences) for 6 x 20 second cycles at 6.5 m/s. Following disruption, samples were centrifuged at 16,000 x g for 5 min at 4°C. Approximately 700 µl of liquid was transferred to fresh RNase-free tubes and incubated at RT for 5 min, before 300 µl chloroform was added. Samples were vortexed for 10 sec and centrifuged at 16,000 x g for 15 min at 4°C. The aqueous phase was transferred to a fresh RNase-free tube containing 200 µl 95% ice-cold ethanol and incubated on ice for 10 min.

The mixture was transferred to a spin column assembly (SV Total RNA isolation system; Promega, USA) and centrifuged at 16,000 x g for 1 min. Columns were washed twice with 600 µl and 250 µl RNA washing solution. RNA was eluted in 45 µl RNase free water. DNase treatment was carried out

using Turbo DNase kit (Ambion, USA) according to the manufacturer's instruction for rigorous clean-up.

RNA was cleaned up using RNeasy mini kit (Qiagen, Germany). The volume of each sample was adjusted to 100 µl with RNase free water and 350 µl of RLT buffer was added. RNA was diluted with 250 µl 100% ethanol. Samples were transferred to RNeasy Mini Spin column and centrifuged at 8000 x g for 15 sec. The flow-through was discarded. Samples were washed twice with 500 µl RPE buffer at 8000 x g for 15 seconds and 2 minutes respectively. Samples were eluted in 45 µl RNase-free water.

RNA integrity was confirmed on a RNA 6000 pico lab-chip using a bioanalyzer 2100 instrument (Agilent, UK) following the manufacturer's instruction. Samples were stored at -80°C until further analysis.

2.12 Qubit® 2.0 Fluorometer assay

The Qubit® 2.0 fluorometer assay kit (Life Technologies, UK) was routinely used for the quantification of both DNA and RNA in studies samples, as per the manufacturer's instructions. The Qubit® reagent was diluted 1:200 in Qubit® buffer and mixed briefly by vortexing. 1-10 µl of DNA or RNA sample was combined with 190-199 µl of the prepared reagent, mixed briefly and incubated for 2 minutes. Samples were measured using the Qubit® fluorometer. The DNA BR (broad range; 1-1000 ng/µl) assay kit was used for measuring DNA concentration. For sequencing experiments the DNA HS (high sensitivity; 0.02-100 ng/µl) assay kit was used. The RNA BR (1-1000

ng/µl) assay kit was used to quantify all RNA samples. The fluorometer was calibrated using the appropriate standards.

2.13 Genomic DNA Sequencing

Extracted genomic DNA was diluted to 0.2 ng/µl and 5 µl (1 ng) was used to prepare DNA sequencing libraries as per the manufacturer's instruction (Nexteria® XT DNA Library Preparation Kit, illumina). Each sample was uniquely indexed using 2 index primers, index 1 (i7/N7XX) and index 2 (i5/S5XX), as described by the manufacturer. The Agilent 2100 Bioanalyzer (Agilent, UK) was used to determine both the quality and size of the DNA fragments following the manufacturer's instruction (DNA High Sensitivity kit, Agilent).

The molar concentration for the DNA libraries was calculated using the formula:

Molar concentration = concentration (g/l) / (DNA fragment size (bp) x 650)

The DNA libraries were diluted to a concentration of 4 nM, combined and denatured using 0.2 M sodium hydroxide. The final DNA library was prepared to a concentration of 10 -12 pM and sequenced using paired end technology using a version-2 500-cycle kit on an illumina MiSeq™ (illumina, UK).

2.14 RNA sequencing

Following RNA extraction and clean-up, rRNA was depleted from a total of 5 µg of extracted RNA using RiboZERO™ (illumina, UK) according to the

manufacturer's protocol, purifying the RNA with ethanol precipitation for optimal RNA recovery. RiboZERO rRNA depletion resulted in 7 µl rRNA-depleted RNA. The Agilent 2100 Bioanalyzer (Agilent, UK) was used to assess both the quality and to confirm rRNA depletion as described above. cDNA libraries were prepared using 5 µl rRNA depleted RNA following the manufacturer's instruction (TruSEQ LT, illumina), Unique RNA adapter indices were used to identify individual samples (Table 1). The DNA High Sensitivity kit (Agilent, UK) was used to determine both the fragment sizes and quality of the cDNA libraries using the 2100 Bioanalyzer (Agilent, UK) instrument, with the cDNA concentration determined by a fluorometer assay (as described previously). Each sample was diluted to a concentration of 4 nM, before being combined and denatured using 0.2 M sodium hydroxide. The final cDNA library was prepared to a concentration of 10 -12 pM and sequenced using paired end technology using a version-3 150-cycle kit on an illumina MiSeq^{TM} (illumina, UK).

Table 1: Indices used for RNA sequencing

Sample	Replicates	Indices
WT (Planktonic)	Planktonic: 1/2/3	1.AR002 2:AR004 3:AR005
	Biofilm: 1/2/3	1.AR013 2:AR008 3:AR006
	Co-culture: 1/2/3	1.AR018 2:AR004 3:AR015
LuxS (Planktonic)	Planktonic: 1/2/3	1.AR013 2:AR016 3:AR012
	Biofilm: 1/2/3	1.AR008 2:AR002 3:AR005
	Co-culture: 1/2/3	1.AR015 2:AR013 3:AR016
	DPD: 1/2/3	1.AR002 2:AR003 3:AR005
B. fragilis	Biofilm: 1/2/3	1.AR006 2:AR007 3:AR008

2.15 Quantitative-PCR

To confirm phage differences between *C. difficile* WT and LuxS, PCR primers were designed for each phage gene identified by RNA-sequencing (Table 2). Blast searches were conducted on each primer to confirm specificity within the *C. difficile* genome.

Table 2: PCR primers for Phage genes identified by RNA-seq

Gene	Name	Sequence
CDR20291_1212	CDR20291_1212_FW	atatatTCAGCAGGACAGGATGAACC
	CDR20291_1212_REV	cgcgcgGCTGTAAACTCTTTTCCTCCTGC
CDR20291_1208	CDR20291_1208_FW	atatatAGGCTCCAACACCAAAAGAA
	CDR20291_1208_REV	cgcgcgACCATAACCCATAACATCTTGAAGT
CDR20291_1215	CDR20291_1215_FW	atatatTGGGCTTTGGAAGTAGATGGAG
	CDR20291_1215_REV	cgcgcgGACCTTAACTGTTCCTGGACCA
CDR20291_1436	CDR20291_1436_FW	atatatACAAAAGTTTCCAGAGATGGATGC
	CDR20291_1436_REV	cgcgcgTGCTGTGTTACCTAATGCGGT
CDR20291_1444	CDR20291_1444_FW	atatatTCATCTGAAGAAGACGAAGCACT
	CDR20291_1444_REV	cgcgcgTGTCCAGTATGCTTACCATTGT
CDR20291_1449	CDR20291_1449_FW	atatatGAGGGGTTTTGCTAGCGACT
	CDR20291_1449_REV	cgcgcgTGAAGAGGAAGCAGCGTGAG

Supernatants were collected from biofilm samples at 24 or 72 hrs. Bacterial cells were removed by centrifugation at 5000 g for 10 min and the resulting supernatant was treated with Turbo DNase (Invitrogen) following the manufacturer's protocol to removed biofilm extracellular DNA. Phage DNA was extracted by combining samples with an equal volume of phenol/chloroform as described previously (section 2.10).

Phage DNA was quantified using a fluorometer assay (section 2.12). 16S PCR was used to confirm the removal of bacterial genomic DNA. A standard qualitative PCR with prophage primers (Table 2) was used to determine the presence of the prophage.

2.16 Generation of chemically competent *E. coli*

Chemically competent *E. coli* cells were created using Mix and Go *E. coli* Transformation kit (Zymo Research, USA) following the manufacturer's instruction. *E. coli* strain DH5α or CA434 was plated on LB agar and single colonies were picked for overnight growth in 5 ml LB broth at 37°C. 0.5 ml of fresh overnight culture was inoculated into 50 ml ZymoBroth™ and bacteria were incubated at 26°C shaking at 150-250 rpm, until OD_{600} 0.4-0.6. Cultures were incubated on ice for 10 min before being pelleted by centrifugation (1,600-2500 x g) at 4°C for 10 min. The supernatant was removed and the cells were re-suspended in 5 ml of ice-cold 1x Wash buffer before a second centrifuge at 1,600-2,500 x g for 10 min at 4°C. The supernatant was completely removed and the cells were gently re-suspended in 5 ml ice-cold competent buffer. 200 µl aliquots were prepared on ice and stored at -80°C until needed.

2.17 Sanger Sequencing

Plasmids and amplicons were Sanger sequenced by GATC- Biotech. The single primer reaction required a 2.5 pmol final primer concentration. 20-80 ng DNA was required with a final volume 10 µl. A combination of A Plasmid Editor (ApE) and SnapGene Viewer software was used to analyse the sequence data.

2.18 Generation of a $SNAP^{CD}$ tag fluorescent *luxS* promotor fusion

The *luxS* promoter sequence was cloned into the pFT47 vector (Figure 8).

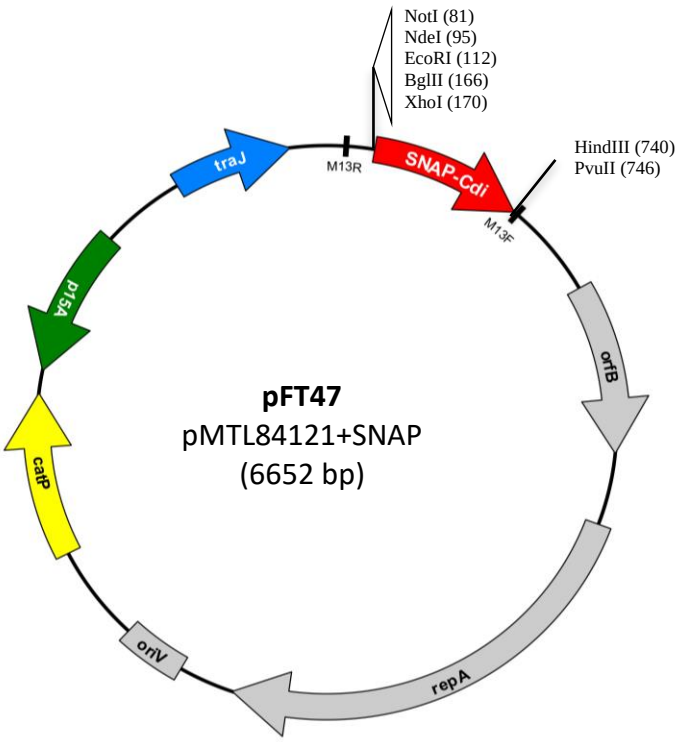

Figure 8: Schematic for pFT47

The 281 bp promoter region, immediately upstream of the *luxS* gene was amplified by PCR from R20291 genomic DNA (isolated using 2.10). The amplification reaction was carried out using Phusion High-Fidelity DNA polymerase (New England Biolabs, USA) (Table 3) with primers F1_*luxS*promoter and R1_*luxS*promoter, both of which contained the appropriate restriction site (Table 4):

Table 3: PCR conditions for Phusion High-Fidelity DNA polymerase

Reaction volume		**PCR Program**
10 µl	5X Phusion HF	95°C for 5 minutes
1 µl	10 mM dNTPs	Then 35 cycles of:
2.5 µl	10 µM Forward Primer	95°C for 30 seconds
2.5 µl	10 µM Reverse Primer	60°C for 30 seconds
2 µl	Genomic DNA < 250 ng	72°C for 30 seconds
0.5 µl	Phusion DNA Polymerase	72°C for 10 minutes
31.5 µl	H_2O	4°C hold
50 µl	Total Volume	

Table 4: Sequences for primers used for cloning the *luxS* promotor region into pFT47. Restriction sites shown in blue.

Name	**Sequence**
F1_*luxS*promoter	atatatatGCGGCCGCACAACTGCCAATAATACAATCAGC
R1_*luxS*promoter	cgcgcgCTCGAGCTTTTTCCATTATTTAATCCTCCA

The PCR fragment was checked using agarose gel electrophoresis, and cleaned up using Wizard® SV Gel and PCR Clean-Up System (Promega, USA), following the manufacturer's instruction.

Two double restriction enzyme digestion reactions were carried out for the vector and PCR product respectively using restriction enzymes NotI-HF (New England Biolabs, USA) and XhoI (New England Biolabs, USA). 1 µg of DNA was combined with 5 µl 10X CutSmart® NEB Buffer, 1 µl NotI-HF restriction

enzyme, and 1 µl XhoI restriction enzyme. The final volume was adjusted to 50 µl with Nuclease-free water and incubated at 37°C for 15 min.

Following a second clean-up with wizard® SV Total Gel and PCR Clean-Up System (Promega, USA) the *luxS* promoter region was cloned into the pFT47 vector by one-step ligation with T4 DNA ligase (New England Biolabs). 2 µl T4 DNA Ligase Buffer was combined with 50 ng vector DNA, 10 ng PCR product, 5 µl H_2O and 1 µl T4 DNA Ligase. The reaction was incubated at RT for 10 min and then transformed into chemically competent *E. coli* DH5α (Section 2.16). LB agar supplemented with 25 µg/ml chloramphenicol was used to select for transformants. Several colonies were picked and inoculated into LB liquid broth supplemented with 12.5 µg/ml chloramphenicol. Plasmid was purified from overnight cultures using a MiniPrep kit (Qiagen, Germany) following the manufacturer's protocol. The DNA sequence was checked by Sanger sequencing using primers F1_*luxS*Promotor and R1_*luxS*promotor.

The reporter SNAP-tag was transferred into the *C. difficile* recipient by conjugation. A sequence verified plasmid, was re-transformed into chemically competent *E. coli* conjugative donor strain CA434, using LB plates supplemented with 25 µg/ml chloramphenicol to select for transformants. *C. difficile* R20291 and *E.coli* CA434/pFT47-*luxS*promoter were inoculated for overnight culture in BHIS and LB supplemented with 12.5 µg/ml Chloramphenicol respectively. 1 ml stationary overnight culture of *E. coli* was pelleted by centrifugation at 5000 x g for 10 min and washed with 0.5 ml PBS. The *E. coli* donor pellet was then re-suspended in 200 µl stationary overnight culture of *C. difficile* R20291 and the conjugation mixture was

pipetted onto a BHIS non-selective plate in discrete drops and incubated for 24 hrs under anaerobic conditions to allow conjugal transfer of the SNAP-tag promotor fusion from the *E. coli* donor to the *C. difficile* recipient. Following incubation, all cells were harvested and re-streaked on *C. difficile* selective BHIS plates (supplemented with D-cycloserine 250 µg/ml, Cefoxitin 8 µg/ml and thiamphenicol 15 µg/ml. The plates were incubated under anaerobic conditions at 37°C for 24 - 72 hrs. Single colonies were isolated and re-streaked and cultured for storage in 30% glycerol at -80°C. The plasmid was extracted and checked by Sanger sequencing as described above, to confirm uptake of pFT-47 containing the *luxS* promotor fusion.

2.19 SNAP^{CD} tag promotor fusion assay

Overnight cultures of *C. difficile* R20291 WT, R20291::*luxS,* R20291::*luxS*/pFT47, and R20291::*luxS*/pFT47-*luxS*promoter were inoculated 1-100 into fresh BHIS with 0.1 M glucose. 1 ml aliquots were taken when culture had reached OD_{600} 0.5, 1, 1.5, and 2. Samples were stained with 250 nM SNAP-cell TMR-Star (New England Biolabs, USA) and incubated for 30 min at RT. Cells were collected by centrifugation at 4000 x g for 5 min and washed with 1 ml PBS. Washing was repeated a further 3 times before the cells were re-suspended in 1 ml PBS and 50 µl of sample was transferred into a 96 well plate (Costar, USA) in triplicate. Plates were measure on a plate reader measuring florescence.

2.20 Bioinformatics methods

2.20.1 Genomes used for analysis

Whole-genome reference sequences of *C. difficile* R20291 and 630, and *B. fragilis* NCTC 9343 were downloaded from the online archive of the National Centre for Biotechnology Information (NCBI). The accession numbers were NC_013316 (R20291), NC_009089 (630) and CR626927 (NCTC 9343).

2.20.2 Whole genome assembly and annotation

RNA SPAdes3.6 was employed for the *de novo* assembly of *B. fragilis* (Bankevich *et al.*, 2012). The recommended "careful" mode was selected to minimise mismatches. The contigs generated were then reordered using the Mauve Contig Mover (Rissman *et al.*, 2009) based on the CR626927 reference genome. Finally Prokka (version 1.11) (Seemann, 2014) was used to annotate the draft genome ready for use in subsequent RNA-seq analysis. Whole genome and RNA-seq data were visualised in Artimus (Rutherford *et al.*, 2000)

2.20.4 Genome variant calling

To confirm *C. difficile* mutant integrity and ensure that there were no second-site mutations, the computational pipeline breseq (Deatherage and Barrick, 2014) was used with default parameters, to compare both R20291 WT and R20291::*luxS* to the reference genome (2.20.1) identifying single nucleotide polymorphisms (SNP).

2.20.5 RNA-seq analysis

The paired-end sequencing reads from RNA-seq experiments were mapped against the appropriate reference genome (NC_013316 for R20291 and the de novo assembled sequenced [2.20.2] for *B. fragilis*). To account for the first and second read being in the opposite orientation (an artefact from the cDNA stranded preparation), the first read was flipped into the correct orientation using the seqtk command-line tool. The reference genome was indexed using BWA index (Li and Durbin, 2009) after which BWA mem was used to map the sequencing reads. The outputted "SAM" file containing the aligned reads was converted to a binary "BAM" file before being sorted and indexed using SAMtools (Li *et al.*, 2009).

2.20.6 Differential gene expression analysis

Sorted BAM (2.20.5) and GFF (general feature format) files were input into the coverageBed tool (Quinlan and Hall, 2010), producing a text file (one for each biological replicate), with the number of reads mapping to each feature of the genome. These text files were input into the R package DESeq2 which calculated the differential gene expression using a negative binomial distribution model (Love *et al.*, 2014). The data was filtered by applying a cut-off of 1.6 for the fold change and 0.05 for the adjusted P-value.

2.21 Statistical Analysis and figure generation

Microsoft Excel was used to create bar graphs and line graphs from numeric data. Paired student's t-test was used to determine if differences between two groups were significant. Fishers exact t-test was used to confirm RNA-seq data. Heat maps were generated using the "heatmap.2" function of the

"gplots" package in R or microscope bioinformatics (http://microscopebioinformatics.org/). Both figures and tables were generated using Microsoft PowerPoint. Image analysis was performed with the Fiji image processing package (Schindelin *et al.*, 2012).

Chapter 3

The role of *LuxS* in *C. difficile* – *C. difficile* interactions within biofilms

3.1 Introduction

With the discovery of the cross-species signalling role for the LuxS/AI-2 QS system (Bassler *et al.*, 1997), it was quickly assumed that many species of bacteria possessing a functional LuxS homolog, utilise AI-2 QS. However, given the absence of a clear receptor for AI-2, and conflicting studies for the role of LuxS during toxin production (Carter, 2005, Lee and Song, 2005), the precise function of LuxS in *C. difficile* remains shrouded.

Currently bacteria are known to respond to AI-2 through two major pathways. One mechanism is triggered by the interaction of AI-2 with LuxPQ, a two-component signal regulator found in *Vibrio* species. The other mechanism uses an ATP-binding-cassette transporter to import AI-2. The lack of genomic evidence of these AI-2 receptors in many bacteria, coupled with the potentially important role of LuxS in central metabolism, has led some to suggest a non-QS role of LuxS in many bacteria (Rezzonico and Duffy, 2008). However, as a number of these species are capable of responding to AI-2, it is possible that there are other uncharacterised AI-2 receptors/ pathways (Yoshida *et al.*, 2005, Huang *et al.*, 2009, Sztajer *et al.*, 2008, Shao *et al.*, 2007, Li *et al.*, 2015).

Quorum sensing plays an important role in the biofilm formation, development and dispersal of many species (Davies *et al.*, 1998, Hammer and Bassler, 2003, Solano *et al.*, 2014, Abee *et al.*, 2011, De Araujo *et al.*, 2010, Hardie and Heurlier, 2008, Sakuragi and Kolter, 2007). The LuxS/AI-2 QS system in particular has been implicated for a role in biofilm formation, development and dispersal in a number of different species (Huang *et al.*, 2009, Karim *et al.*, 2013, Li *et al.*, 2015, Sztajer *et al.*, 2008, Wilson *et al.*, 2012, Yoshida *et al.*, 2005, Auger *et al.*, 2006, De Araujo *et al.*, 2010, Hardie and Heurlier, 2008).

Recently mutants of *luxS* were reported to be defective for biofilm formation of *C. difficile* (Dapa *et al.*, 2013), but the mechanisms responsible have yet to be elucidated. Utilising a number of molecular biology techniques, this study aimed to determine the function of LuxS during *C. difficile – C. difficile* interactions and in biofilm formation.

3.2 Results

3.2.1 Genomic Sequencing for mutant confirmation

To confirm the identity of both WT and *luxS mutant* (*LuxS*) strains, and to ensure that no additional SNPs were introduced during the handling of either strain, single colonies of both strains were sequenced in triplicate as described in chapter 2. Whole genome sequences for each replicate were compared to the published reference genome of *C. difficile* R20291 (accession number: NC_013316).

As genomic sequencing confirmed that with the exception of *luxS,* both WT and *LuxS* possessed the same SNPs, the observed defect in biofilm formation for *LuxS* was caused by the insertional mutation to this gene (Table 5).

Table 5: Observed mutations present in both WT and *LuxS* compared to published genome (NC_013316)

Position	Mutation	Annotation	Gene
9,694	G→T	G82V (GGA→GTA)	rsbW
32,998	+AAT	noncoding (75/76 nt)	CDR20291_t27
132,959	T→C	noncoding (25/77 nt)	CDR20291_t40
206,398	+A	intergenic (+957/-214)	CDR20291_0157 / CDR20291_0158
358,260	Δ1 bp	coding (165/891 nt)	rbsK →
581,480	+A	intergenic (+314/-264)	CDR20291_0482 / glsA
581,487	+A	intergenic (+321/-257)	CDR20291_0482 / glsA
581,494	+A	intergenic (+328/-250)	CDR20291_0482 / glsA
593,845	68 bp x 2	duplication	CDR20291_0492 / CDR20291_0493
1,564,432	Δ1 bp	intergenic (-190/-104)	CDR20291_1320 / CDR20291_1321
1,568,676	C→A	Q138K (CAA→AAA)	CDR20291_1323
1,578,167	Δ1 bp	intergenic (-88/-158)	CDR20291_1334 / CDR20291_1335
1,578,202	+A	intergenic (-123/-123)	CDR20291_1334 / CDR20291_1335
1,592,813	A→T	intergenic (-173/-67)	CDR20291_1346 / CDR20291_1347
1,864,416	+T	intergenic (-357/+171)	CDR20291_1575 / CDR20291_1577
1,899,596	Δ1 bp	intergenic (+263/-537)	CDR20291_1614 / CDR20291_1615
2,077,305	Δ1 bp	intergenic (+47/-70)	CDR20291_1777 / CDR20291_1778
2,120,669	A→G	D202G (GAC→GGC)	vncR
2,235,738	Δ1 bp	coding (246/270 nt)	CDR20291_1913
2,262,059	+A	intergenic (-203/-163)	CDR20291_1935 / CDR20291_1936
2,264,190	Δ1 bp	intergenic (+96/-398)	CDR20291_1938 / CDR20291_1939
2,298,110	+T	intergenic (-120/+216)	CDR20291_1968 / CDR20291_1969
2,361,948	C→A	intergenic (+54/+234)	CDR20291_2018 / CDR20291_2019
2,361,956	+A	intergenic (+62/+226)	CDR20291_2018 / CDR20291_2019
2,367,941	+T	intergenic (-547/-536)	CDR20291_2022 / bipA
2,578,157	Δ1 bp	intergenic (-716/-91)	CDR20291_2190 / CDR20291_2191
2,674,744	Δ1 bp	intergenic (-96/+547)	CDR20291_2280 / CDR20291_2281
2,680,786	+T	intergenic (-267/+103)	CDR20291_2286 / CDR20291_2287
2,772,179	Δ1 bp	intergenic (-803/+619)	CDR20291_2367 / CDR20291_2369
2,881,464	Δ1 bp	coding (1308/2337 nt)	CDR20291_2456
3,077,986	Δ1 bp	intergenic (-232/-97)	glyA / CDR20291_2616
3,162,098	Δ1 bp	intergenic (-163/+74)	secA2 / slpA
3,361,915	Δ1 bp	intergenic (-151/-432)	CDR20291_2840 / CDR20291_2841

3.2.3 *LuxS* is required for biofilm formation

The WT and *LuxS* strains were studied for biofilm formation at different times using a previously described biofilm formation assay (in 24 well dishes). Biofilms were quantitated by crystal violet and colony counting as described in Chapter 2. As observed by Dapa *et al.* (2013), the *C. difficile LuxS* produces a dramatic defect during biofilm formation, observed with both crystal violet staining (Figure 9A) and by fluorescent microscopy (Figure 9B & C) at both 24 and 72 hrs in BHIS supplemented with 0.1 M glucose (BHIS-G). Interestingly, the CFU/ml for both WT and *LuxS* remained at similar levels during both timepoints, despite the observed defect in biofilm formation (Figure 9D). Since both strains display similar planktonic growth (Figure 10), these data suggest that the biofilm defect is caused by differences in the amount of extracellular matrix produced by WT and *LuxS*, rather than a growth defect.

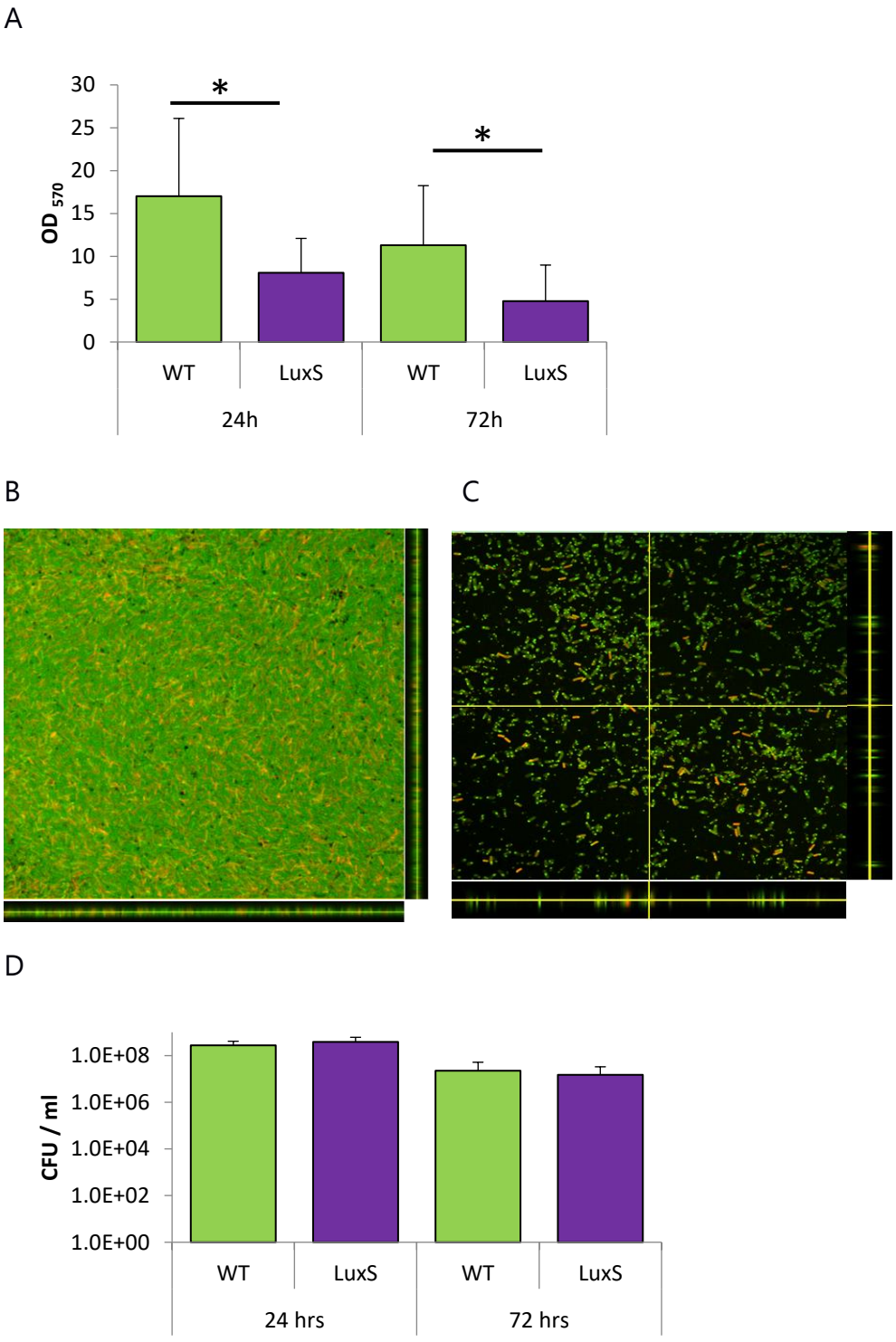

Figure 9: Analysis of *LuxS* biofilm formation *in vitro*

(**A**) WT and *LuxS* biofilms were grown for 24 and 72 hrs and stained with 0.2% CV. (**B + C**) Biofilms were visualised by microscopy at 48 hrs using live/dead staining, WT (**B**) and *LuxS* (**C**). Live bacteria stained green whilst

dead bacteria stained red using syto 9 and propidium iodide dye respectively. (**D**) CFU was calculated from biofilms. N=7, error bars = standard deviation.

3.2.5 AI-2 production by *C. difficile*

To investigate *luxS* expression and to confirm production of the signalling molecule, AI-2, cell-free supernatants were collects at various timepoints and assayed with the AI-2 reporter, *Vibrio harveyi.* The amount of fluorescents induced by *C. difficile* produced AI-2 was compared to stationary-phase *V. harveyi* cell-free supernatants which were assumed to be inducing 100% fluorescents. As BHIS-G had an inhibitory effect on the growth of *V. harveyi* (data not shown), *C. difficile* was grown in BHI, in stationary planktonic conditions. At each time point the OD_{600} was measured and 1 ml of culture was filter-sterilised and the cell-free supernatants were frozen at -20°C before being assayed with *V. harveyi*. We found that AI-2 is maximally produced at the transition to stationary phase (Figure 10). As expected the *LuxS* did not produce AI-2 (Figure 10).

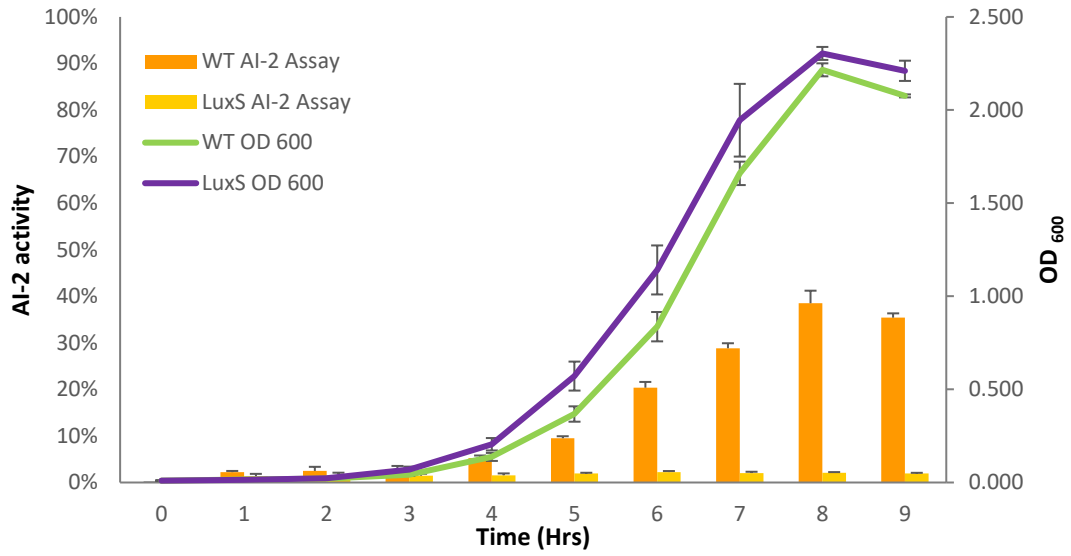

Figure 10: Growth and AI-2 production by WT and *LuxS*.

Strains were grown anaerobically in BHI medium. Aliquots were removed for OD_{600} readings (line) and cell-free supernatants from each time point were tested for AI-2 activity using *V. harveyi* BB170 reporter assay (bars). Bioluminescence is shown as a percentage of wildtype *V. harveyi* BB120 bioluminescence, which was assumed to be 100 %

3.2.4 Visualisation of *luxS* expression (SNAP)

In order to study the expression profile of *luxS* during biofilm formation, and to visualise the localisation of *luxS* expression within a biofilm, a florescent promoter fusion was generated. Since Green fluorescent protein (GFP) chromophores strictly require molecular oxygen for maturation of fluorescence (Cubitt *et al.*, 1995, Perez-Arellano and Perez-Martinez, 2003, Landete *et al.*, 2015) we utilised O-6-methylguanine-DNA methyltransferase based tags (SNAP-tags) which can function in anaerobic environments. As *luxS* is expressed as part of an operon, we cloned the 281 bp region directly upstream of *luxS* as described in Chapter 2 (2.18). While the PCR and Sanger

sequencing showed fusion was generated successfully (data not shown) we were unable to detect fluorescence at multiple timepoints during growth in BHIS-G and BHI.

3.2.6 Exogenous addition of AI-2 (MHF and DPD)

As *LuxS* has roles in the activated methyl cycle and in the LuxS/AI-2 QS system, it is unclear whether species that contain *LuxS*, but do not possess a clear AI-2 receptor use AI-2 for QS, or if AI-2 production is simply a metabolic by-product of the reaction of SRH to homocysteine catalysed by *LuxS* (Rezzonico and Duffy, 2008).

To determine whether *LuxS* possesses a QS role in *C. difficile*, we tested if the exogenous addition of two forms of AI-2, 5-methyl-4-hydroxy-3(2H)-furanone (MHF) and 4,5-dihydroxy-2,3-pentanedione (DPD), could restore biofilm formation in *LuxS*. No clear effect was observed with the addition of different concentrations of MHF (Figure 11a). We were able to partially complement *LuxS* with 100 nM DPD (Figure 11B&C). Whilst we were unable to observe full complementation with the selected concentrations of DPD, we observe that increased concentrations had an inhibitory effect. Such inhibitory effects of AI-2 /DPD have been reported previously (Rickard *et al.*, 2006).

A

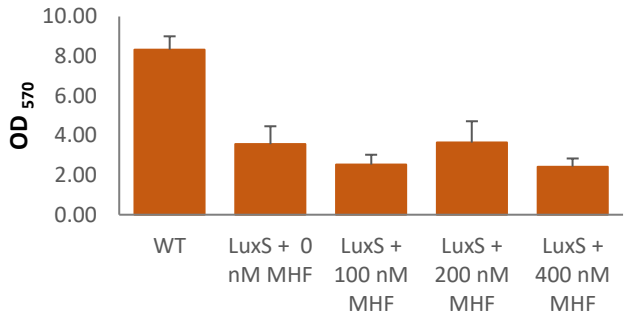

B

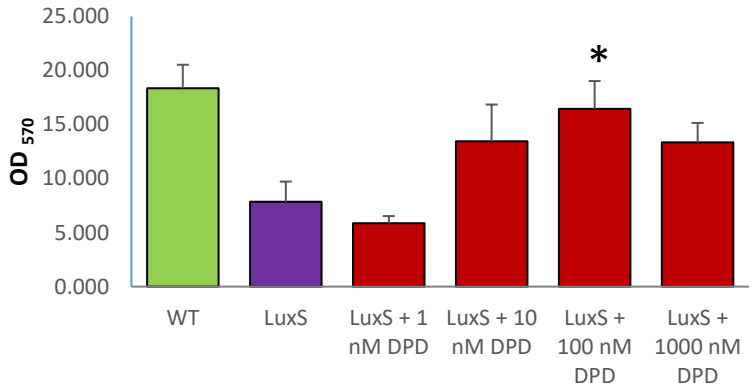

C

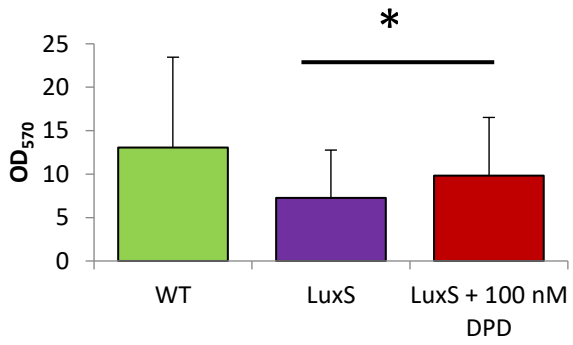

Figure 11: *LuxS* response to Exogenous AI-2

(**A**) No response was observed with various concentrations of 5-methyl-4-hydroxy-3(2H)-furanone (MHF) n=9 error bars show standard deviation. (**B**) Dosage response observed for *LuxS* with the addition of exogenous 4,5-dihydroxy-2,3-pentanedione (DPD), with high concentrations having an inhibitory effect. N=3 error bars show

standard deviation. (**C**) 100 nM DPD can partially compensate the biofilm defect of *LuxS*. N= 21 error bars show the standard deviation.

3.2.7 Planktonic RNA-sequencing (RNA-seq) analysis

AI-2 has been shown to affect expression of several virulence related genes in many bacteria (Cao *et al.*, 2011, Stroeher *et al.*, 2003, Sircili *et al.*, 2004, Coulthurst *et al.*, 2004). To probe the precise role of LuxS/AI-2 in *C. difficile* further, we analysed the global transcriptome of *LuxS* with the view that transcriptional pathways altered in *LuxS* would provide clues to LuxS/AI-2 function. We employed RNA-seq to take a "snap-shot" of the gene expression during planktonic growth. Logarithmic phase growth, where AI-2 was produced at a reasonable level (Figure 10) was selected to ensure reproducibility for replicates. Both strains were cultured in 50 ml falcon tubes in 25 ml BHI and incubated at 37°C in anaerobic conditions. Total RNA was extracted when the OD_{600} for each sample reached 0.8 (6 hrs). RNA replicates were prepared from cultures on different days to ensure reproducibility.

Following RNA isolation, samples were tested by PCR to ensure no contamination with genomic DNA. As bacterial RNA consists mainly of ribosomal RNA (most notably 16S and 23S), RiboZero (Illumina) was used for the depletion of rRNA substantially increasing the number of reads available for sequencing from mRNA. The Illumina TruSeq Stranded total RNA kit was used to generate cDNA libraries which were then sequenced on the Illumina MiSeq at 12 pM.

The sequencing reads for each replicate of both WT and *LuxS* were processed (2.14) and both strains were mapped to the published genome for R20291 (GenBank accession no. NC_013316). CoverageBed was used to count the reads that mapped to each gene of the reference sequence (Quinlan, 2014). The mapped reads were then normalised and analysed using DESeq2, to calculate the differential expression of genes and the log2-fold change between conditions (Love *et al.*, 2014). To account for false positives, DESeq2 uses P and Q-values to determine whether changes in gene expression are statistically significant, whereby the Q-value is a false discovery rate adjustment to the P-value *i.e.* a Q-value (P-adjusted value) of 0.05 indicates 5% of the statistically significant tests (by P-value) were false positives. The variation between samples was analysed using heat maps and principle component analysis (PCA) plots generated from the DESeq2 dataset. Significant changes to gene expression were based upon a P-adjusted value of ≤ 0.05 and log-fold change of ≥ 1.6.

Surprisingly, no differentially expressed genes passed these cut off values, with the log-2 fold change for a majority of genes being between 1 and -1 (Figure 12A). As the replicates for each condition do not cluster amongst themselves (Figure 12B & C), we hypothesise that *LuxS* is not influencing *C. difficile* at this timepoint.

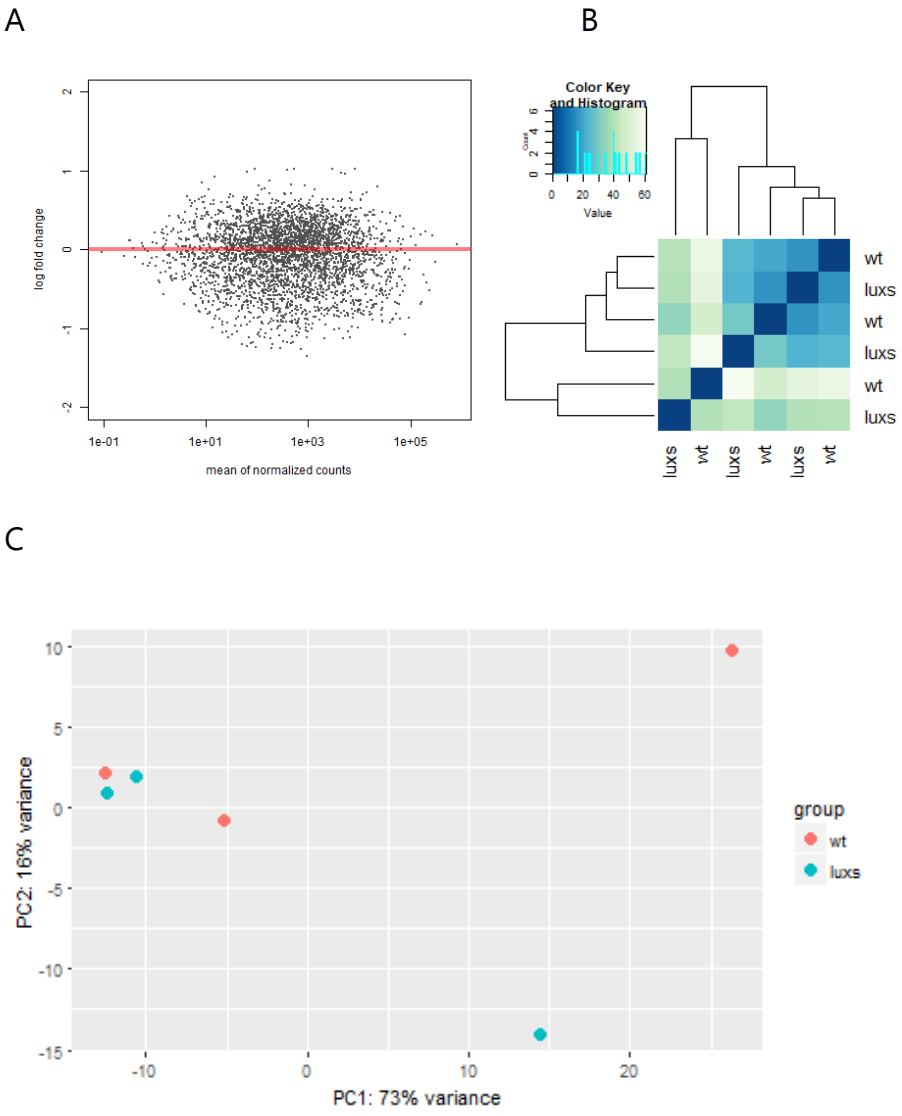

Figure 12: Planktonic RNA-seq quality control.

Mean normalised counts plotted against $\log_2$ fold change (**A**), a heat map (**B**) of Euclidian distances between samples and a PCA plot (**C**) showing sample-sample distances for replicates of WT and *LuxS*. These were calculated using R and DESeq2

3.2.8 Biofilm RNA-seq analysis

As we failed to detect changes in gene expression during planktonic growth, we focused our attention to analysing the gene expression of WT and *LuxS*

within biofilms. Given the clear phenotype for *LuxS* during biofilm formation and development, we would expect differences in the gene expression profiles between the two strains. Additionally, with the ability for DPD to partially complement *LuxS,* we also sought to analyse the gene expression for *LuxS* complimented with exogenous DPD.

RNA was extracted from 24 and 48h biofilms, however the quality of RNA obtained was poor, and contamination with genomic DNA was a major problem (data not shown). Good quality RNA was extracted from early biofilms (18 hrs) (Figure 13a and b). The cells were washed and lysed (as described in Chapter 2), the RNA was processed and sequenced as described above, and the DeSeq2 variance analysis package (Love *et al.*, 2014) was used to identify genes that were differentially expressed by ≥ 1.6-fold with a p-adjusted value ≤ 0.05, (N=3), in both *LuxS* and *LuxS* with DPD relative to the wildtype.

(A) WT *LuxS*

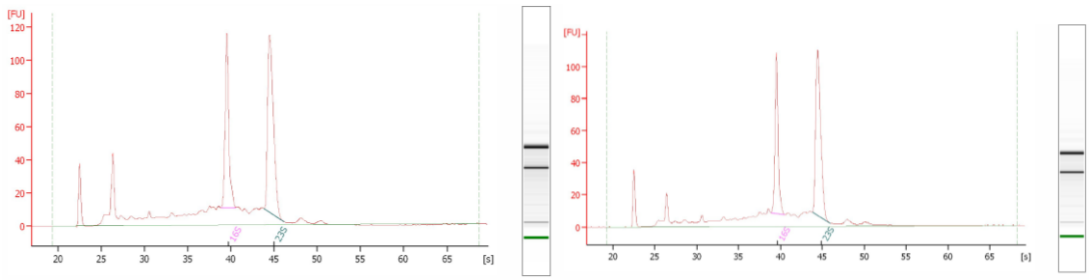

(B)

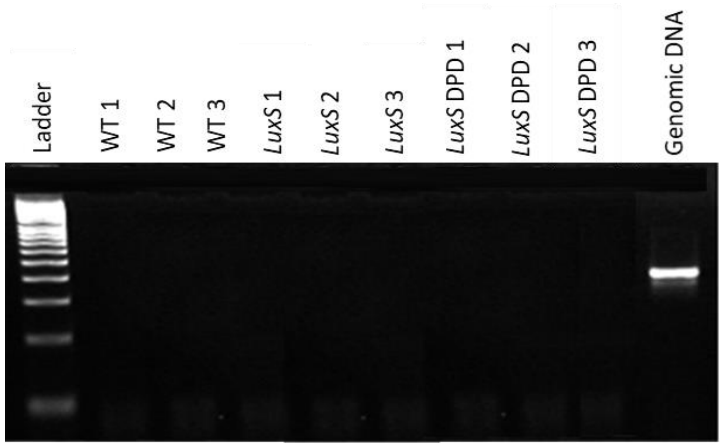

Figure 13: Bioanalyser and 16S PCR of RNA isolated form biofilms at 18 hrs. (**A**) shows the RNA isolated from biofilms 18 hrs post inoculation for the first biological replicate for WT and *LuxS*. (**B**) A 16S PCR was performed on all replicates to ensure all replicates were free of genomic DNA contamination.

Although statistical analysis using DESeq2 showed individual replicates for each condition did not cluster (Figure 14a), 21 genes were found to be consistently differentially expressed across all replicates of *LuxS* (Table 6) with 26 genes identified in *LuxS* supplemented with DPD (Table 7). We therefore hypothesise that similarities between both WT, *LuxS*, and *LuxS* with DPD were responsible for the lack in clustering, rather than variance between replicates.

A

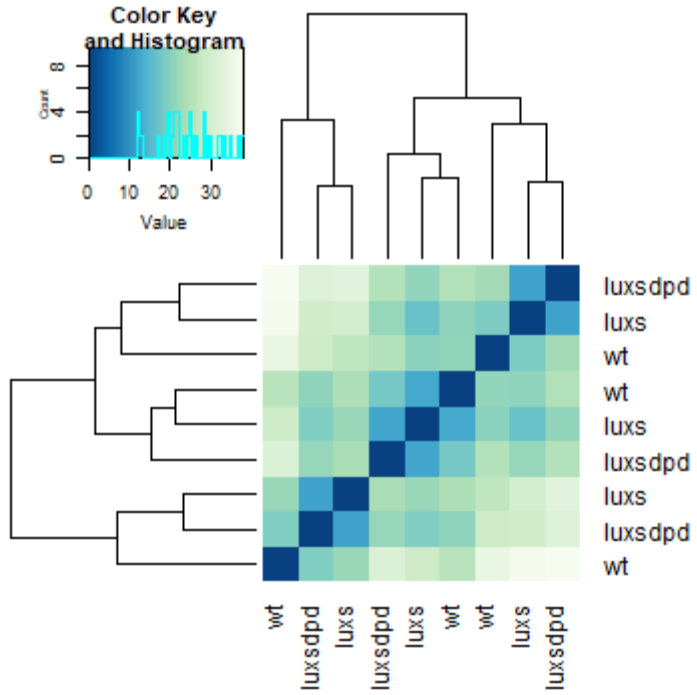

B

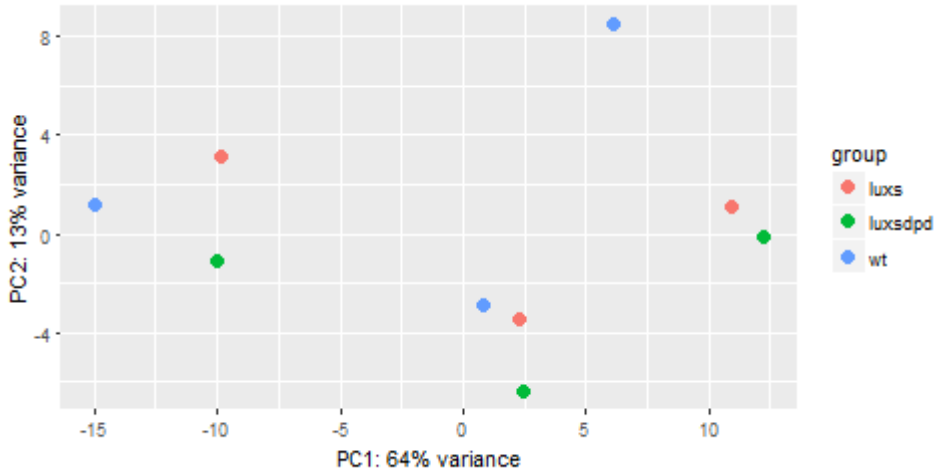

Figure 14: PCA plots and heat map of WT, *LuxS* and *LuxS* + DPD biofilm samples.

The heat map (A) shows the Euclidian distance between samples whilst the PCA plot (B) shows the sample-to-sample distances for replicates of WT, *LuxS* and *LuxS* + DPD. Both the heat map and PCA plot were calculated using R and DESeq2.

Transcriptional analysis of *LuxS* during biofilm formation

Interestingly, all 18 down-regulated genes correspond to two prophage regions (CDR20291_1197 - CDR20291_1226 and CDR20291_1415 – CDR20291_1464) located within the *C. difficile* R20291 genome (Figure. 15A, B & C), as identified using the online phage search tool: Phaster (Arndt *et al.*, 2016, Zhou *et al.*, 2011). Fishers exact T-test was used to validate the RNA-seq data with a calculated p-value < 0.001 for both prophage regions.

It is interesting to note that both trehalose-6-phosphate hydrolase (TreA, CDR20291_2930) and a PTS system transporter (CDR20291_2554) are up-regulated in *LuxS.* Trehalose is an osmoprotectant that can be hydrolysed to glucose and glucose 6-phosphate by the enzyme trehalose-6-phosphate hydrolase, where it can be utilised as a carbon source (Rimmele and Boos, 1994). Recent studies have demonstrated the ability for upregulation of the trehalose operon to enhance *C. difficile* growth in the presence of trehalose (Collins *et al.*, 2018a).

A

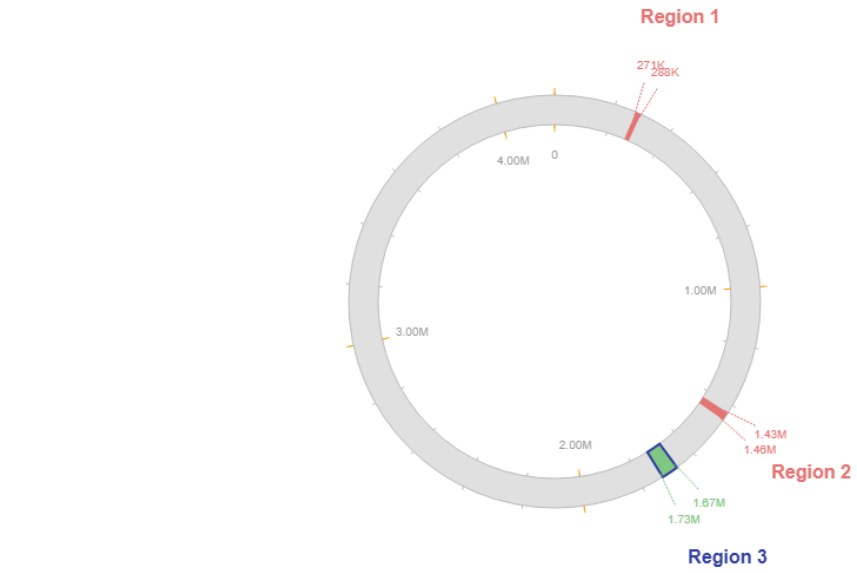

B

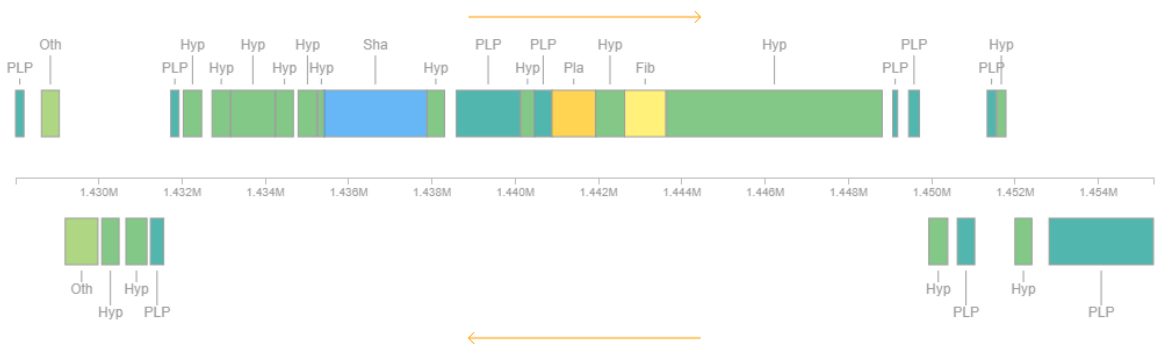

C

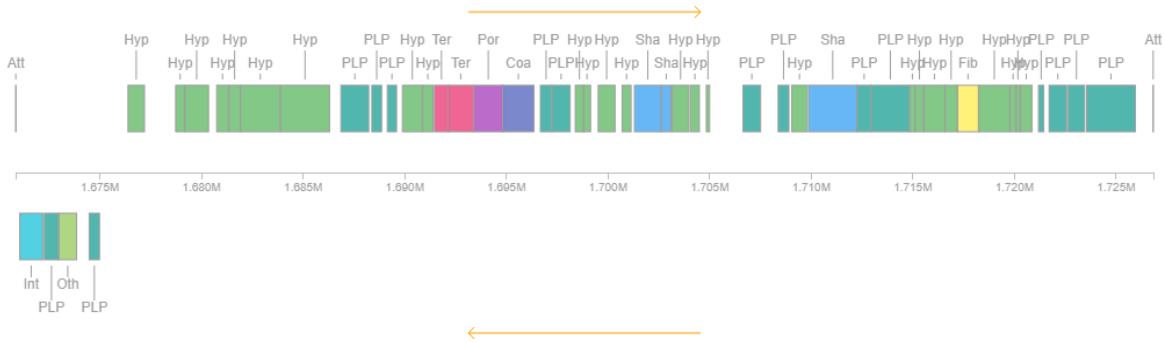

Figure 15: Phage genes present in *C. difficile.*

(**A**) Three Prophage regions are identified in C. difficile using Phaster. Regions 2 and 3 were detected as down regulated in *LuxS*. (**B**) shows locus of region 2. (**C**) shows locus of region 3.

Table 6: Genes up- and down-regulated in the ***LuxS*** relative to the WT *C. difficile*. Genes specific to *LuxS* (red), genes differentially expressed in both *LuxS and* LuxS *DPD (black).*

No.	Gene ID	log2FoldChange	Gene annotation
1	CDR20291_1206	-0.994213972	hypothetical protein
2	CDR20291_1207	-1.059645046	hypothetical protein
3	CDR20291_1208	-1.227114763	hypothetical protein
4	CDR20291_1210	-1.08584066	hypothetical protein
5	CDR20291_1211	-1.0763802	hypothetical protein
6	CDR20291_1212	-1.009946545	phage cell wall hydrolase
7	CDR20291_1214	-1.09972952	phage protein
8	CDR20291_1215	-1.038498251	phage protein
9	CDR20291_1216	-1.047731727	phage protein
10	CDR20291_1217	-0.999294901	phage tail fiber protein
11	CDR20291_1218	-0.898724949	hypothetical protein
12	CDR20291_1425	-0.928686375	virulence-associated protein e
13	CDR20291_1432	-1.243533992	phage terminase large subunit
14	CDR20291_1433	-1.154529376	phage portal protein
15	CDR20291_1436	-1.156306053	phage major capsid protein
16	CDR20291_1442	-1.085573967	phage protein
17	CDR20291_1444	-1.257181603	phage protein
18	CDR20291_1449	-1.008627768	phage tail tape measure protein
19	CDR20291_2554	0.895993497	PTS system glucose-specific transporter subunit IIA
20	CDR20291_2927	1.587075038	cellobiose-phosphate degrading protein
21	CDR20291_2930	1.444846424	trehalose-6-phosphate hydrolase

Note: P-adjusted value ≤ 0.05

Transcriptional analysis of *LuxS* + DPD during biofilm formation

A total of 26 genes were found to be differentially expressed in *LuxS* + DPD compared to wildtype. Of these, 22 were down-regulated with only 4 up-regulated genes detected. 20 of the differently expressed genes were found to match the differential expression of *LuxS.* 1 additional gene was found to be up-regulated (CDR20291_1523, encoding a two-component sensor

histidine kinase), whilst 5 additional genes were found to be down-regulated (CDR20291_0782, CDR20291_1219, CDR20291_1220, CDR20291_1450 and CDR20291_3144). The other two down-regulated genes correspond to a MarR family transcriptional regulator (CDR20291_0782) and pyruvate formate-lyase 3 activating enzyme (CDR20291_3144).

Table 7: Genes up- and down-regulated in the ***LuxS* DPD** relative to the WT *C. difficile*. Genes specific to *LuxS* DPD (red), genes differentially expressed in both *LuxS* and *LuxS* DPD (black)

No.	Gene ID	log2FoldChange	Gene annotation
1	CDR20291_0782	-1.1341491	MarR family transcriptional regulator
2	CDR20291_1206	-1.0880825	hypothetical protein
3	CDR20291_1207	-1.247361	hypothetical protein
4	CDR20291_1208	-1.171661	hypothetical protein
5	CDR20291_1210	-1.0380968	hypothetical protein
6	CDR20291_1211	-0.9248567	hypothetical protein
7	CDR20291_1212	-0.9178215	phage cell wall hydrolase
8	CDR20291_1215	-1.0082721	phage protein
9	CDR20291_1216	-0.9809553	phage protein
10	CDR20291_1217	-0.9891455	phage tail fiber protein
11	CDR20291_1218	-0.8462165	hypothetical protein
12	CDR20291_1219	-1.0438119	hypothetical protein
13	CDR20291_1220	-1.112373	hypothetical protein
14	CDR20291_1425	-1.0024545	virulence-associated protein e
15	CDR20291_1432	-1.3464056	phage terminase large subunit
16	CDR20291_1433	-1.1120734	phage portal protein
17	CDR20291_1436	-1.1073332	phage major capsid protein
18	CDR20291_1442	-1.1314477	phage protein
19	CDR20291_1444	-1.3252432	phage protein
20	CDR20291_1449	-1.0659773	phage tail tape measure protein
21	CDR20291_1450	-1.0110874	phage cell wall hydrolase
22	CDR20291_3144	-0.8819971	pyruvate formate-lyase 3 activating enzyme
23	CDR20291_1523	0.95295327	two-component sensor histidine kinase
24	CDR20291_2554	0.90467383	PTS system glucose-specific transporter subunit IIA

25	CDR20291_2927	1.81490679	cellobiose-phosphate degrading protein
26	CDR20291_2930	1.59849263	trehalose-6-phosphate hydrolase

Note: P-adjusted value ≤ 0.05

Transmission electron microscopy (JEOL 2100 TEM/STEM, Warwick) was utilised to visualise any phage particles produced within *C. difficile* biofilms or biofilm supernatants. Samples were taken from both disrupted biofilms and the supernatant at 48 hrs and phages were isolated via ultracentrifugation (Beckman Optima L-80 XP, Warwick) at 35,000 rpm for 12 hrs. Whilst phage-like particles could be observed in WT biofilm supernatants (Figure 16 A&B), these were very few in number, and not consistently detected.

A B

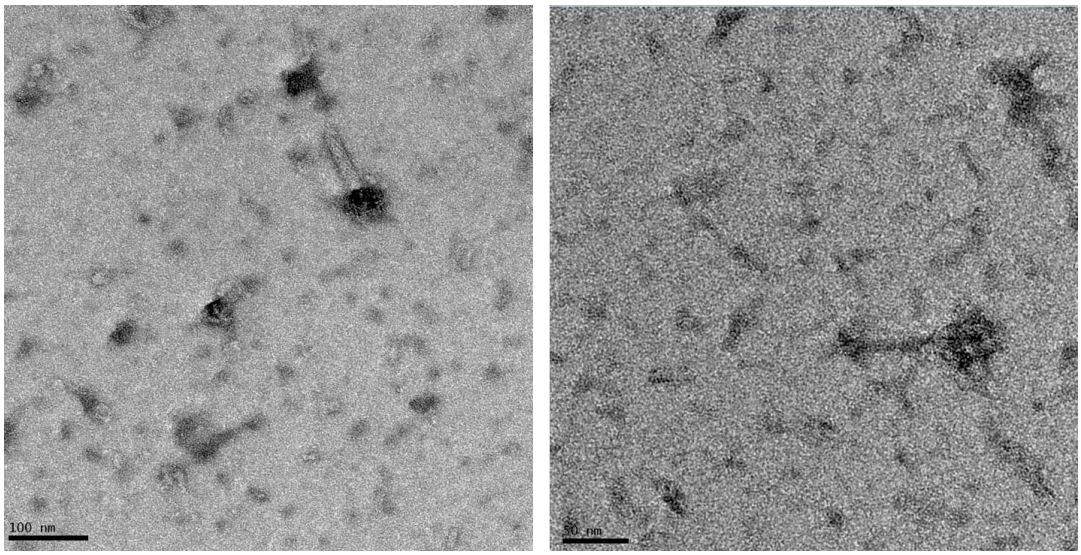

Figure 16: Transmission electron microscopy (TEM) image of phage like particles present in WT biofilm supernatants.

Samples prepared from biofilms at 24 hrs and were stained with concentrated uranyl acetate

To demonstrate the presence of phage within the biofilm we instead disrupted biofilms at 24 hrs and 48 hrs. Cells were removed via centrifugation at 10,000 x g for 10 minutes. Samples were then treated with DNase to remove extracellular DNA, a key component of biofilms. With the cells removed, and eDNA degraded, the only DNA present in each sample would be DNA that was protected from the DNase treatment *i.e.* within a phage. This DNA was isolated by phenol chloroform extraction as described in chapter 2 and PCR was performed with primers for the RNA-seq identified phage genes (Figure 17). 16S primers, which would detect any DNA from whole bacteria were used as a control. As no DNA band was present for the 16S control, we can conclude that bands present in phage primer samples, were as a result of the presence of intact phage within the *C. difficile* biofilms.

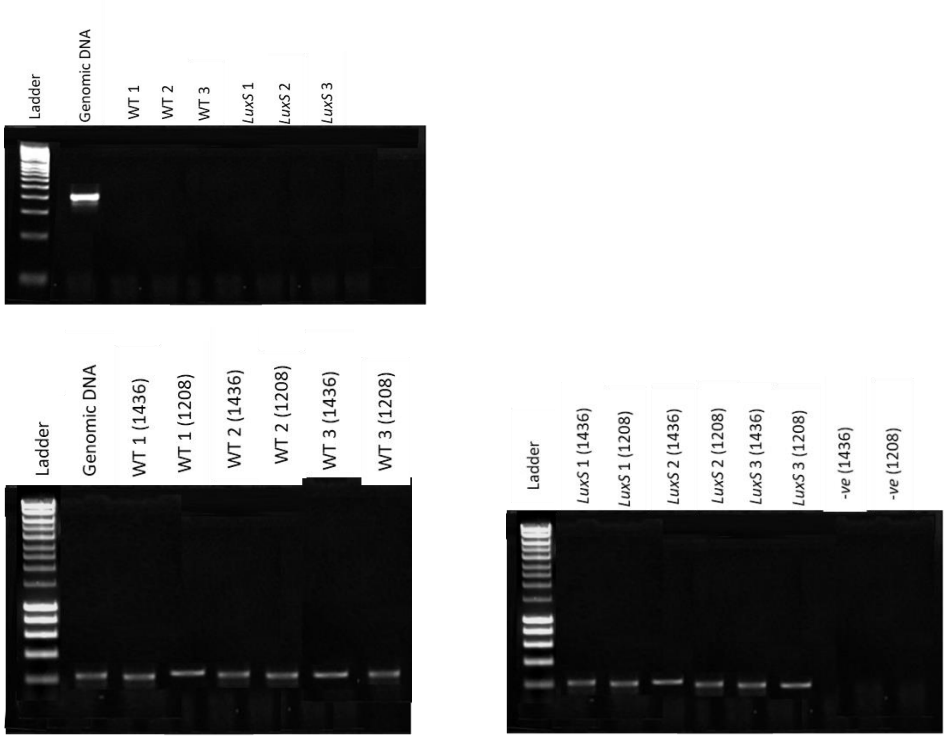

Figure 17: Phage present in *C. difficile* biofilms.

(a) 16S PCR of DNA isolated from biofilms of WT and *LuxS* post DNase treatment. (b) PCR of phage CDR20291_1436 (1436) and CDR20291_1208 (1208).

Discussion

Biofilms are an important mode of growth offering increased resistance to environmental stresses, resistance to antibiotics, and a means for persistence for pathogenic bacteria (Costerton *et al.*, 1999, Mah and O'Toole, 2001, Keren *et al.*, 2004b, Keren *et al.*, 2004a, Hall-Stoodley *et al.*, 2004, Lewis, 2005, Ahmed *et al.*, 2009). Many bacteria utilise QS to regulate the genes required for biofilm formation (Zhu and Mekalanos, 2003, Hammer and Bassler, 2003, Yoshida *et al.*, 2005, Sakuragi and Kolter, 2007, Hardie and Heurlier, 2008, Huang *et al.*, 2009, Ahmed *et al.*, 2009, De Araujo *et al.*, 2010, Li and Tian, 2012, Karim *et al.*, 2013, Li *et al.*, 2015, Dixit *et al.*, 2017). Interestingly many of

these studies have implicated AI-2 as being involved in biofilm formation and development (Gonzalez Barrios *et al.*, 2006, Shao *et al.*, 2007, Ahmed *et al.*, 2009, Li *et al.*, 2015).

Given the ability of *C. difficile* to produce *in vitro* biofilms (Dawson *et al.*, 2012, Đapa *et al.*, 2013, Crowther *et al.*, 2014, Walter *et al.*, 2015, Pantaleon *et al.*, 2015, Maldarelli *et al.*, 2016) and a notable defect in biofilm formation for mutants of *luxS* (Dapa *et al.*, 2013), we sought to investigate the mechanisms responsible for this defect.

Although *luxS* is responsible for the production of AI-2, the lack of a characterised receptor in many species (including *C. difficile*), has led some to question whether phenotypes associated with the inactivation of this enzyme are due to QS or due to its metabolic role in the activated methyl cycle (Rezzonico and Duffy, 2008, Wilson *et al.*, 2012). However, since we were able to achieve partial restoration of the biofilm within *LuxS* through the addition of exogenous DPD, our data suggests that *C. difficile* is not only capable of producing AI-2, but could also be responding via a currently uncharacterised receptor pathway. As specific concentrations of DPD are required to complement the biofilm defects in other bacteria (Rickard *et al.*, 2006), it is possible that a narrower range of concentrations would need to be tested in order to achieve complete restoration of the biofilm in *C. difficile.* Additionally the commercial DPD is known to be unstable, and this could also explain the reduced activity (Chen *et al.*, 2002, Federle and Bassler, 2003).

RNA-seq was used to identify genes responsible for the observed phenotype in *LuxS*. During the early stages of biofilm formation we identified 18 genes down-regulated in the *LuxS*. Interestingly all 18 of these genes correspond to two prophage regions present within the *C. difficile* genome. Upon further investigation, we were able to detect the presence on intact prophage within *C. difficile* biofilm samples. Bacteriophage have been associated with both biofilm formation (Secor, 2016) and biofilm dispersal (Rossmann *et al.*, 2015) in other bacteria. In *Pseudomonas aeruginosa* a filamentous phage has been shown to help bind bacteria, providing structure to the biofilm (Secor, 2016). Whereas in *Enterococcus faecalis,* an AI-2 induced phage release has been demonstrated to be playing an active role in biofilm dispersal (Rossmann *et al.*, 2015). Since the phage are down-regulated in *LuxS* we hypothesise that the prophage found in *C. difficile* are facilitating biofilm formation under the control of AI-2 which likely happens through cell lysis and the release of e-DNA, DNA has previously been shown to be a key component of the *C. difficile* biofilm with DNase activity impacting biofilm formation and preformed biofilms (Dapa *et al.*, 2013). Furthermore, our observation that *LuxS* biofilms relatively have more live bacteria than the WT supports the idea that bacterial lysis occurs in the presence of LuxS/AI-2.

With the gene expression profile for *LuxS* and *LuxS* with DPD being largely the same, with three additional prophage genes being down-regulated in *LuxS* with DPD, we can surmise that the DPD is having little affect at 18 hrs or 100 nM. Since previous studies have demonstrated a role for cysteine in the down regulation of pyruvate formate-lyase 3 activating enzyme (CDR20291_3144) (Dubois *et al.*, 2016). It is likely that the other differentially

expressed genes specific to this condition, are artefacts from the loss of metabolic function for LuxS in the activated methyl cycle.

During infection we suspect that as *C. difficile* cell numbers increase, so too does the extracellular concentration of AI-2. Once a critical concentration is detected, biofilm formation is induced together with the transcription of prophage genes within a subset of the population. Cells expressing these genes then lyse, releasing e-DNA and increasing the overall biomass of the biofilm. With the ability of biofilms to provide increased resistance to antibiotics (Lewis, 2008, Dapa *et al.*, 2013), we hypothesise that the production of biofilms during infection, could offer a reservoir for recurrent disease (Figure 18).

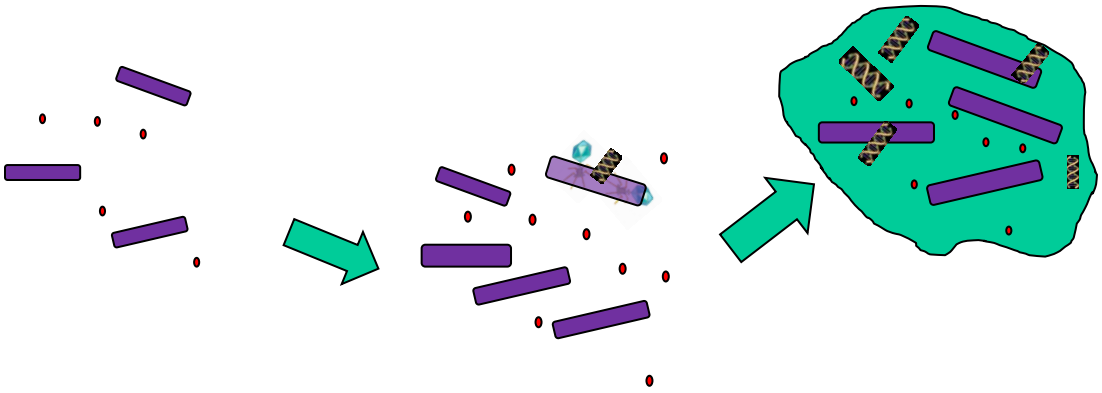

Figure 18: A hypothetical model for the role of phage in *C. difficile* biofilm formation.

Extracellular concentration of AI-2 increases as cells grow. When a threshold concentration is reached, phage expression is induced in a subset of the population. These cells lyse releasing eDNA, a key component of the biofilm.

Chapter 4

C. difficile interactions with *B. fragilis*

4.1 Introduction

It has long been proposed that a healthy gut microbiota offers colonisation resistance against *C. difficile,* and that only when the gut microbiota is in a state of dysbiosis, can the disease take hold (Vollaard and Clasener, 1994, Seekatz and Young, 2014). Whilst the precise mechanisms responsible for this innate resistance to *C. difficile* colonisation are yet to be understood, a number of factors have been proposed. These include competition for nutrients, ecological competition, niche exclusion, and more recently, the production of inhibitory secondary bile salts (Theriot and Young, 2015, Winston and Theriot, 2016, Theriot *et al.*, 2016, Robinson *et al.*, 2014, Britton and Young, 2012). The recent expansion in the use of FMT for the most severe cases of CDI, highlights the urgency in understanding how the different members of the microbiota interact with *C. difficile* (Adamu and Lawley, 2013). In the past decade, a number of studies have aimed at identifying the microbial taxa associated with either: disease development or *C. difficile* inhibition. However, due to the limited number of co-culture studies in this field, the exact microbes within these taxa and mechanisms of their interactions with *C. difficile* remain elusive (Seekatz and Young, 2014).

Multiple studies investigating the elderly, adults and FMT patients, have consistently identified *Bacteroides spp*. amongst others, as being negatively correlated to *C. difficile* colonisation (Weingarden *et al.*, 2014, Hopkins and Macfarlane, 2002, Manges *et al.*, 2010, Schubert *et al.*, 2014, Tvede and Rask-

Madsen, 1989, Khoruts *et al.*, 2010, van Nood *et al.*, 2013, Hamilton *et al.*, 2013, Fuentes *et al.*, 2014, Petrof *et al.*, 2013, Khanna *et al.*, 2016). As many of these studies have not resolved species level, the mechanisms of action remain unclear. *Bacteroides* have been shown to be nutritionally diverse, capable of utilising a wide variety of carbon sources. As such these bacteria are thought to be responsible for the majority of polysaccharide digestion that occurs in the large intestine (Franks *et al.*, 1998, Salyers, 1984). Additionally *B. fragilis* has been shown to influence the development of the immune response (Hopkins and Macfarlane, 2003).

The high microbial density within the gut means that *C. difficile* likely needs to interact with other members of the gut microbiota, to establish itself within this niche. Previously, a role for the LuxS/AI-2 QS system in inter-species signalling has been proposed (Bassler *et al.*, 1997, Hammer and Bassler, 2003). Given the potential signalling role for the LuxS/AI-2 within the *C. difficile* population we hypothesised that *C. difficile* LuxS/AI-2 QS may influence interactions of *C. difficile* with the other bacteria present in the gut. With the ability of several members of *Bacteroides* to produce AI-2, it would be interesting to investigate the mechanisms involved in *C. difficile* – *Bacteroides* interactions.

4.2 Results

4.2.1 Development of a mixed biofilm assay

In order to investigate the role of LuxS in influencing inter-species interactions of *C. difficile*, we first examined the interactions between the gut associated *Bacteroides spp*. *Bacteroides fragilis* and *C. difficile*.

To ensure that *B. fragilis* and *C. difficile* grow well in a common medium, growth curves were performed in BHIS-G (Figure 19), a medium previously shown to promote maximal *C. difficile* biofilm production (Dapa *et al.* 2013). Although growth dynamics were different, both *C. difficile* and *B. fragilis* grew to comparable OD_{600} (2.216 and 1.704 respectively). BHIS-G was used throughout the co-culture experimentation.

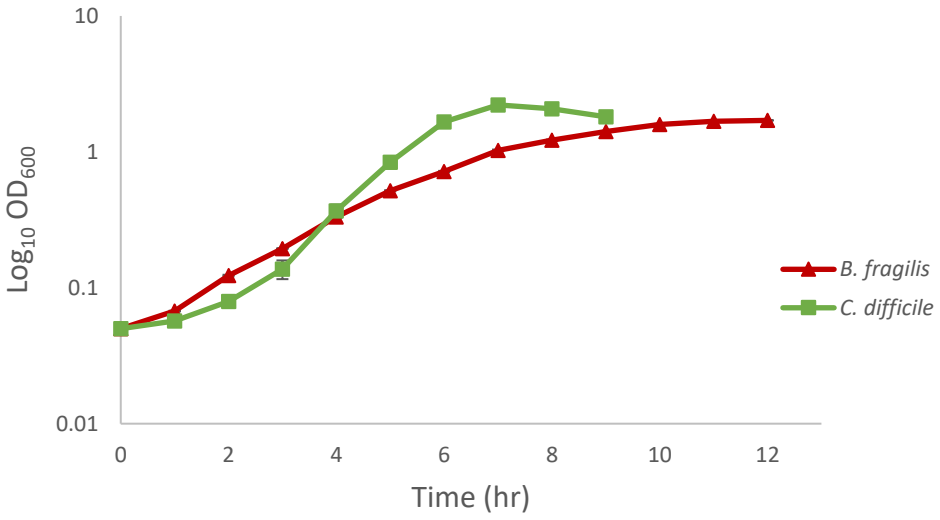

Figure 19: Growth curve of *B. fragilis* and *C. difficile* in BHIS-G

The growth of B. fragilis and C. difficile was evaluated in BHIS-G. C. difficile grew faster with a logarithmic rate of 0.380 per hour and a maximal OD600 of 2.216. Compared to B. fragilis which had a logarithmic rate of 0.208 OD600 per hour and a maximal OD600 of 1.704.

For co-culture biofilms, O/N cultures for both species were set up in BHIS-G and the OD_{600} was adjusted to 1 after 12-16 hrs of growth. Both species were diluted 1:100 into 24 well dishes, and incubated for different times. During

initial investigation using CV biofilm assay, it was noted that *B. fragilis* mono-culture formed limited levels of biofilm, compared with *C. difficile.* When *C. difficile* was co-cultured with *B. fragilis*, significantly less total biofilm was produced (by CV staining), compared to the *C. difficile* monoculture biofilms (Figure 20A).

The number of CFUs within mixed biofilms was determined as described in Chapter 2. A distinct colony morphology was observed for both species when plated on BHIS plates selective for *C. difficile*; *C. difficile* produced large opaque colonies appearing slightly yellow/green in colour with irregular edges, while *B. fragilis* produced pin prick transparent colonies. When incubated for a longer time point (48 – 72 hrs) these colonies became white opaque in colour with smooth edges. CFU counts obtained from the mono and co-culture biofilms, confirmed that *B. fragilis* was a poor biofilm producer during mono-culture. Interestingly, when both species were cultured together the CFU/ml for *C. difficile* was significantly reduced (Figure 20B), while the CFU/ml for *B. fragilis* were significantly increased. The reduction in colony counts of *C. difficile* was observed at both 24 and 72 hrs (data not shown).

To observe biofilms by confocal microscopy, strains were inoculated into 4-well glass chamber slides and stained with live/dead (Syto 9 and propidium iodide dye, respectively) after 48 hrs. Monoculture biofilms (Figure 21A) contained more live bacteria, denoted by the greener colour, with co-culture biofilms (Figure 21B) containing more dead cells.

These data suggest that the presence of *B. fragilis* in co-culture results in inhibition of *C. difficile* growth within biofilms.

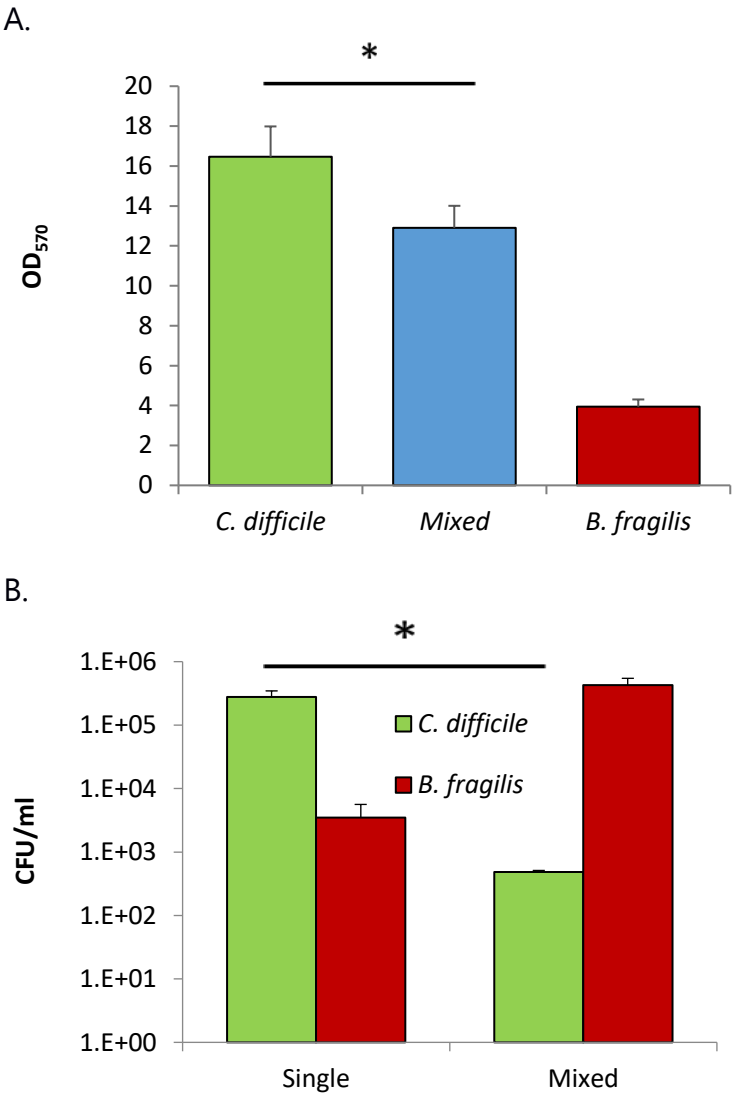

Figure 20: *B. fragilis* mediated inhibition of *C. difficile* in mixed biofilms.

(A) Biofilm formation of *C. difficile, B. fragilis* and both species co-cultured (mixed) as measured by crystal violet. (B) CFU / ml for both *C. difficile* and *B. fragilis* from mono and co-culture biofilms. A logarithmic scale is used on the Y-axis. The error bars represent standard deviations ($P<0.05$), N=3.

A B

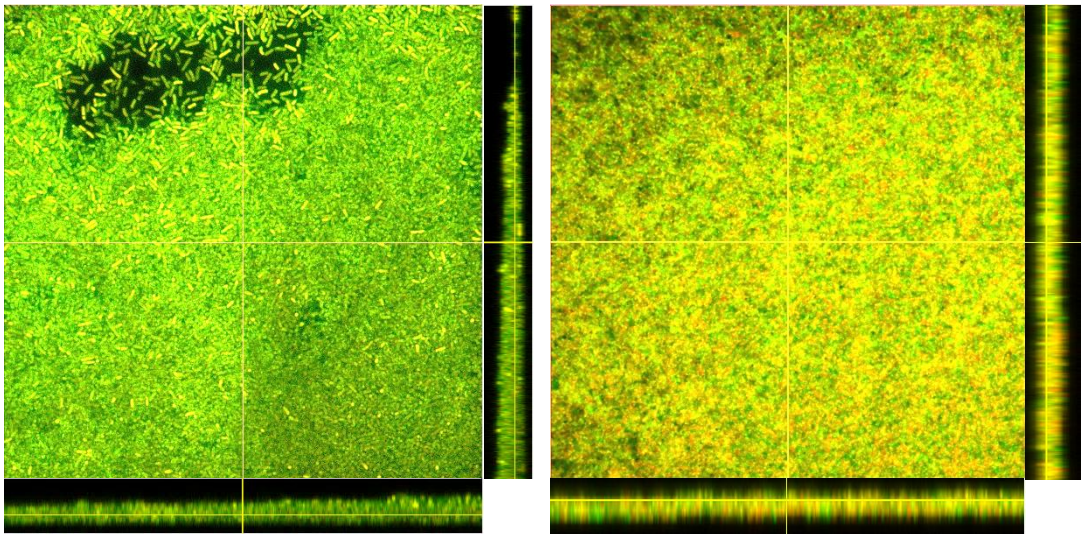

Figure 21: Confocal microscopy of *C. difficile* and co-culture biofilms.

Live/dead staining shows dead (red) and live (green) bacteria (Syto 9 and propidium iodide dye, respectively) in monoculture *C. difficile* WT (A), and co-culture with *B. fragilis* (B).

To investigate this *B. fragilis*-mediated inhibition further, *C. difficile and B. fragilis* were co-cultured under planktonic conditions, at both 6 and 10 hrs. This was performed in BHIS-G liquid culture, in falcon tubes. Interestingly, at both of these timepoints the colony counts for *C. difficile* remained at comparable levels, in both mono and co-culture conditions (Figure 22).

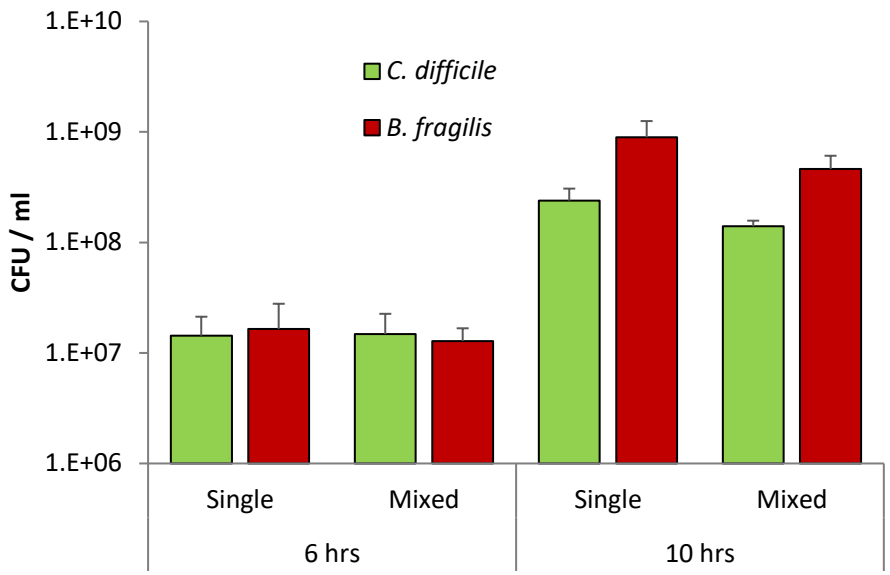

Figure 22: No inhibition of *C. difficile* during planktonic growth.

CFU / ml for both *C. difficile* and *B. fragilis* from mono and co-culture during planktonic growth. A logarithmic scale is used on the Y-axis. The error bars represent standard deviations.

4.2.2 LuxS in co-culture

To investigate potential signalling functions of LuxS in *C. difficile* interactions with other bacterial species, we then investigated the role of LuxS in *C. difficile – B. fragilis* interactions. To do this, both *C. difficile* WT and *luxS* mutant were individually co-cultured with *B. fragilis* as biofilms at a 1:1 ratio (by OD_{600}) in 24 well tissue culture dishes.

A reduction in biofilm biomass as measured by CV was observed for both *C. difficile* WT and *LuxS* in co-culture with *B. fragilis* (Figure 23A). Colony counts of *C. difficile* in monoculture were similar for both WT and *LuxS*, with maximal numbers observed at 24h for both strains. As described earlier, when both strains were co-cultured with *B. fragilis* the colony counts for *C.*

difficile were significantly reduced. Interestingly, this reduction is more pronounced for the WT than the *luxS* mutant (Figure 23B) with a ten-fold reduction in mean CFU/ml being observed for the *luxS* mutant compared to a 2 log reduction for the WT.

C. difficile

A

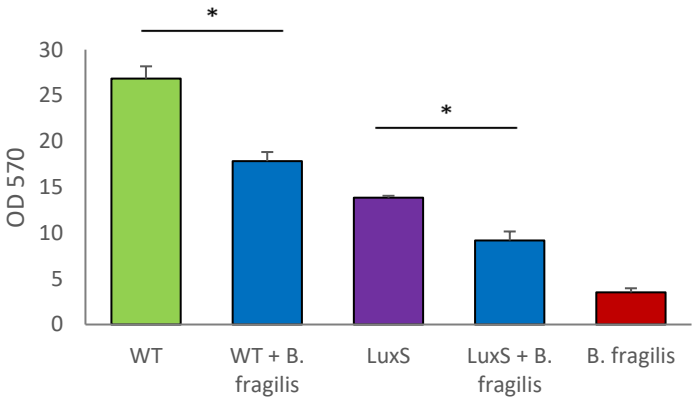

B.

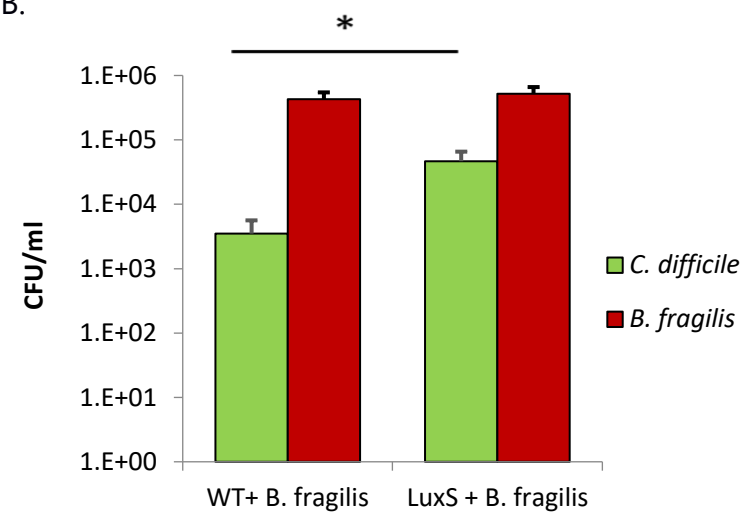

Figure 23: *B. fragilis* inhibition of *C. difficile* is more prominent for WT than *LuxS*

(**A**) CV assay for mono- and co-cultures of *C. difficile* WT and *LuxS* with *B. fragilis*. The error bars represent standard deviations (P<0.05), N=9. (**B**) CFU / ml for *C. difficile* WT, *C. difficile LuxS* during co-culture with B. fragilis. A logarithmic scale is used on the Y-axis. The error bars represent standard deviations (P<0.05), N=3.

Confocal imaging (Figure 24) showed that *C. difficile LuxS* had reduced biofilms compared to WT, although clearly the mixed biofilm of *LuxS* was distinct both in structure and composition compared to the WT *C. difficile/ B. fragilis* biofilms.

A B

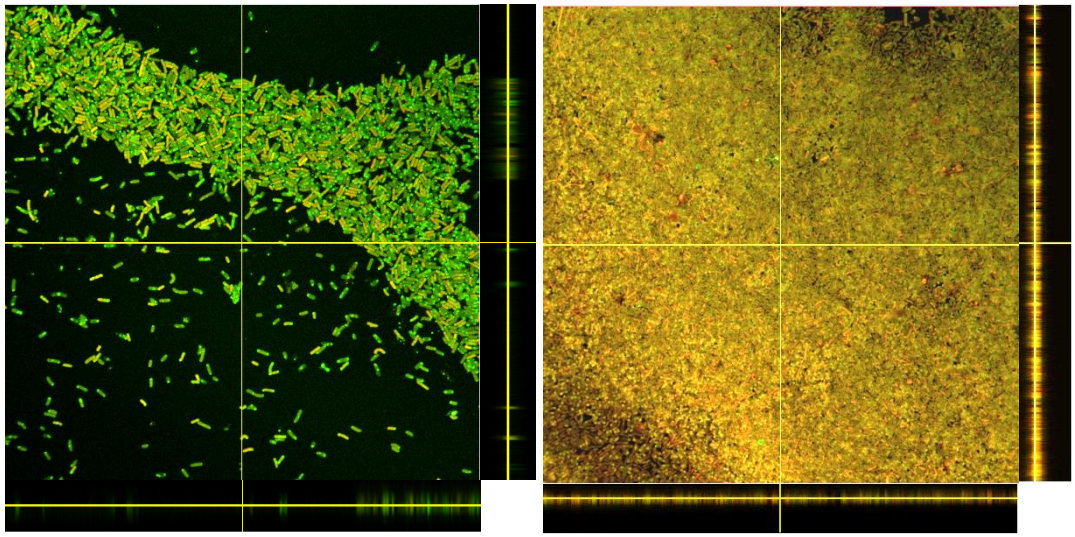

Figure 24: Confocal microscopy of *LuxS* and co-culture biofilms.

(**A**)Live/dead staining shows dead (red) and live (green) bacteria (Syto 9 and propidium iodide dye, respectively) in monoculture *C. difficile LuxS*.(**B**) Co-culture with *B. fragilis*.

LuxS may serve a metabolic function in addition to a potential role in signalling via AI-2. Hence we sought to determine the likelihood of QS being responsible for the observed *C. difficile* inhibition. As only selected members of the *Bacteroidetes* are capable of producing AI-2 (Antunes *et al.*, 2005) with this ability varying within the *B. fragilis* species (Peixoto *et al.*, 2014). We first set up an AI-2 assay to assess the ability of both monocultures and co-cultures to produce AI-2. Cell free supernatants were obtained from

monoculture biofilms of *C. difficile* WT, *C. difficile* LuxS and *B. fragilis*, together with co-cultures of both *C. difficile* strains with *B. fragilis*. Samples were taken at 36 hrs to account for differences in growth dynamics. We did not observe any AI-2 production by the *B. fragilis* strain. Whilst this strain is unable to produce AI-2 (Figure 25), some species have been shown to be QS "cheaters" capable of responding to AI-2 but lacking the ability to produce the signalling molecule. This can be evolutionarily advantageous as production of signalling molecules can be metabolically demanding for the cell (Fiegna and Velicer, 2003, Sandoz *et al.*, 2007, Jiricny *et al.*, 2010, Popat *et al.*, 2012).

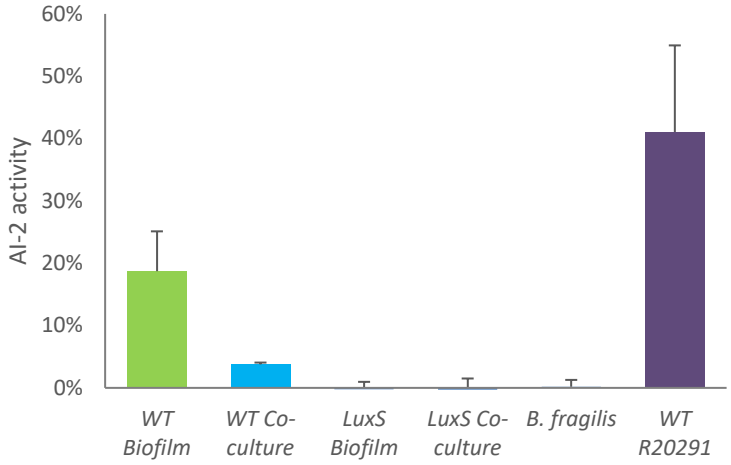

Figure 25: AI-2 production during biofilm growth in BHI.

Late log-phase *C. difficile* WT is displayed as a comparison. Cell-free supernatants were taken from each condition and assayed for AI-2 activity using *V. harveyi*. Bioluminescence is shown as a percentage of wild-type *V. harveyi* BB120 bioluminescence, which was assumed to be 100%.

As the *B. fragilis* strain is a clinical isolate, we sequenced the genome using a Nexteria XT kit on an illumina miseq to identify whether LuxS was present. We repeated this sequencing twice at different times, however, after *denovo* assembly both sequences retained >1000 contigs suggesting that regions of the genome sequence were missing. Therefore we were unable to verify the presence of a LuxS homologue, as it is possible that this gene resides on a region of the genome that failed to get sequence. However, analysis of the sequences revealed a putative two-component histone kinase which shared 36% identities and 54% similarities with the AI-2 sensor kinase/phosphatase, LuxQ of *Vibrio fischeri* (Figure 26), suggesting that *B. fragilis* may be able to detect AI-2 produced by other species.

Figure 26: Alignment of the putatitive two-component histone kinase with the LuxQ sequence from *V. fischeri*.

The sequences were aligned using the CLUSTAL w algorithm. '*' indicates positions which have a single, fully conserved residue. ':' indicates conservation between groups of strongly similar properties with a score > 0.5 in the Gonnet PAM 250 matrix.. '.' indicates conservation between groups of weakly similar properties with a score =< 0.5 in the Gonnet PAM 250 matrix..

4.2.3 Secreted inhibitors

To investigate whether any inhibitory molecules were being secreted by *B. fragilis*, we first tested cell-free supernatants from a planktonically grown O/N culture of *B. fragilis,* incubated for 48 hrs. *C. difficile* cells were

resuspended in 80% *B. fragilis* cell free supernatant and incubated for 24 hrs for biofilm formation. Whilst no inhibition was observed for *C. difficile* under these conditions (Figure 27), it is possible that any inhibitory molecule responsible for the inhibition of *C. difficile* observed in co-culture conditions, are only produced in the presence of *C. difficile*.

To test this, cell-free supernatants were prepared from monoculture biofilms of *B. fragilis* and co-culture biofilms of *C. difficile* and *B. fragilis* grown for 24 hrs. These supernatants were added to preformed biofilms at 24 hrs and incubated for a further 24 hrs. However, the biofilm *B. fragilis* supernatants also failed to inhibit the growth of *C. difficile* (Figure 28:), with enhanced growth detected with co-culture supernatants.

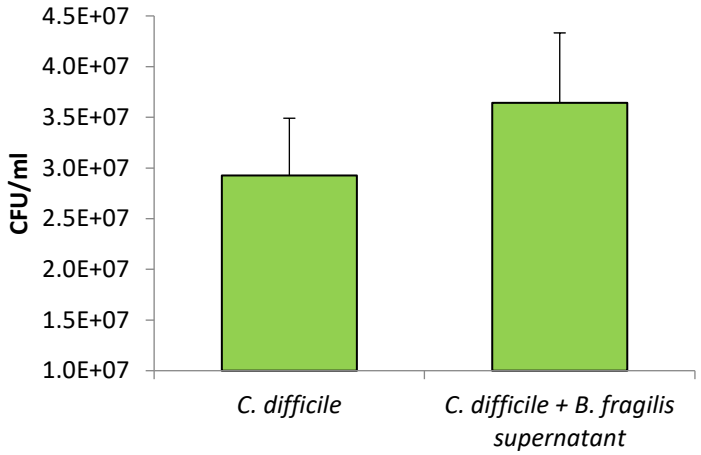

Figure 27: Cell free supernatants from planktonically cultured *B. fragilis* fail to inhibit *C. difficile*.

CFU / ml for *C. difficile* and *C. difficile* resuspended in cell-free *B. fragilis* supernatant obtained from planktonic bacteria. The error bars represent standard deviations.

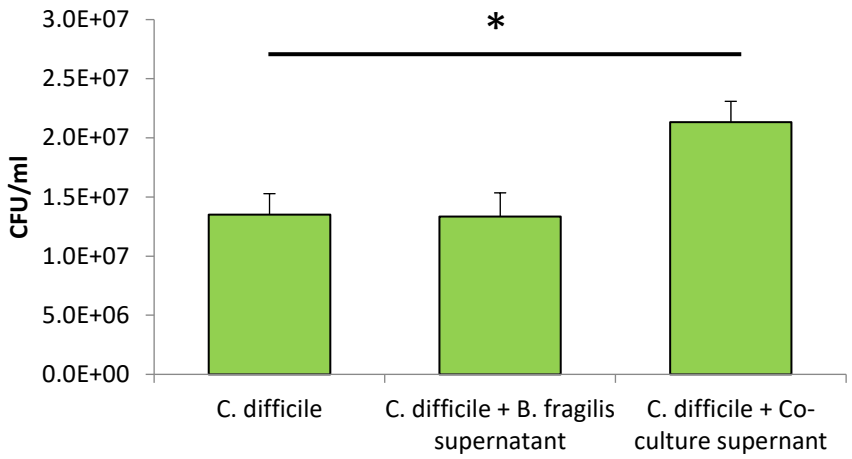

Figure 28: Cell free supernatants from *B. fragilis* biofilms fail to inhibit *C. difficile*.

CFU / ml for *C. difficile* and *C. difficile* resuspended in either cell-free *B. fragilis* biofilm supernatant or cell-free co-culture biofilm supernatant The error bars represent standard deviations ($P<0.05$).

In order to isolate any molecules that may be responsible for the observed inhibition, we used Liquid Chromatography Mass Spectrometry (Agilent 6300 Ion Trap LC/MS) in collaboration with Dr Christopher Corre and Dr Fabrizio Alterti (University of Warwick), We observed the presence of a molecule with a mass of 136 present in *B. fragilis* monocultures and the mixed samples containing *B. fragilis*. (Figure 29). Further analysis by liquid chromatography high resolution mass spectrometry yielded a predicted formula of $C_4H_9NO_4$ which corresponds to 4 known natural products: L-γ-hydroxythreonine, α-(hydroxymethyl)serine, D-erythro-2-amino-3,4-dihydroxybutanoic acid, 2-amino-2-deoxy-L-erythronic acid.

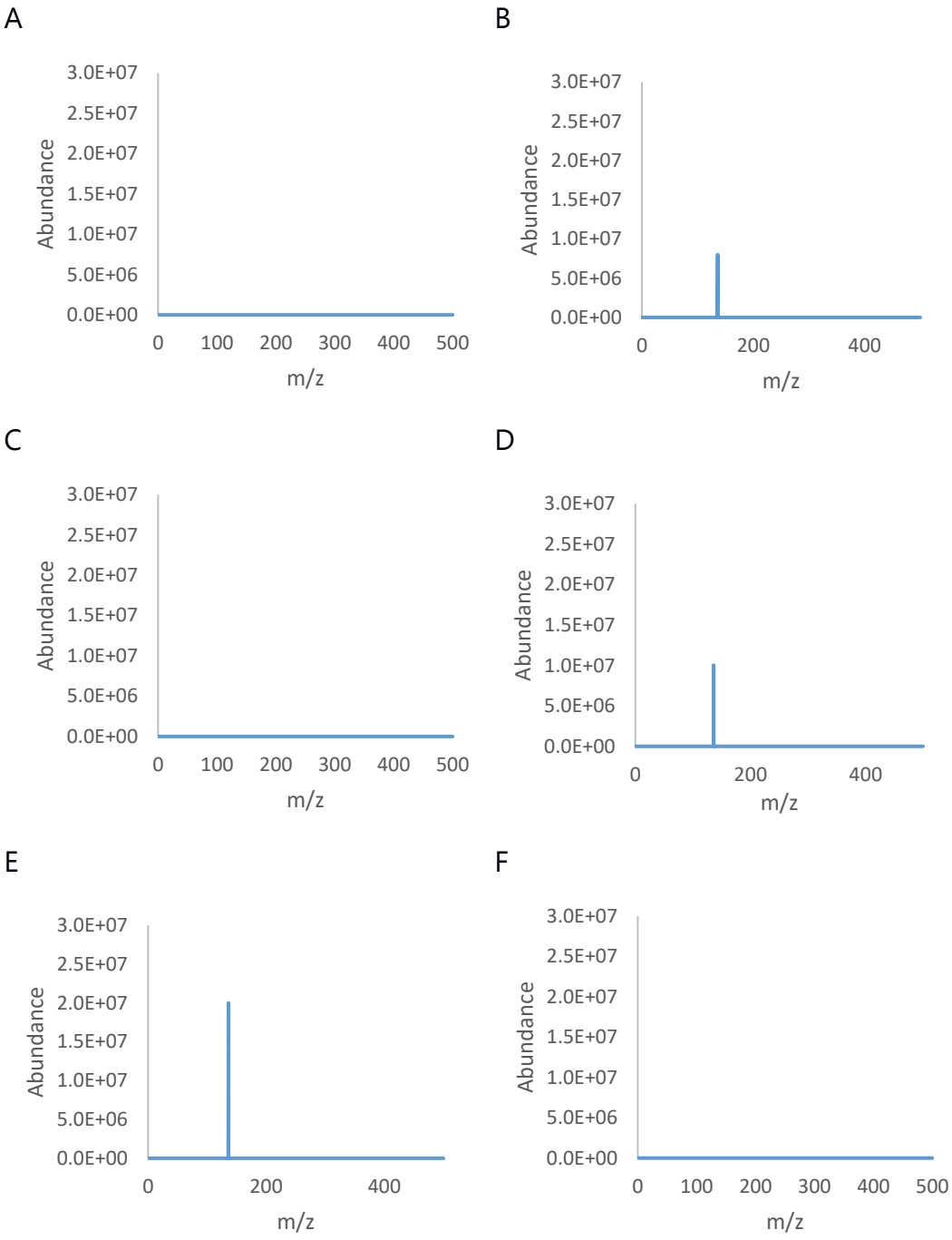

Figure 29: LCMS spectra for biofilm supernatant for *C. difficile* and *B. fragilis*.

(A) *C. difficile* WT. (B) *C. difficile* WT co-cultured with *B. fragilis*. (C) *C. difficile LuxS*. (D) *C. difficile LuxS* co-cultured with *B. fragilis*. (E) *B. fragilis*. (F) Media blank.

4.3 Discussion

With the vast number of bacterial species present within the gut (Gerritsen *et al.*, 2011), it is likely that the bacteria occupying this niche are forced to interact with one another. Some of these interactions will be mutualistic, as is seen in the oral cavity (Kuramitsu *et al.*, 2007), with bacteria forming multi-species bacterial communities allowing for bacterial cross-feeding, where the enzymes produced by one species make metabolites available for another species (Ng *et al.*, 2013). Other interactions however will be antagonistic, with bacteria directly inhibiting competing species. One method of inhibition is through the production of microbial products such as bacteriocins, microbial peptides with bactericidal activity (Majeed *et al.*, 2013, Wang and Kuramitsu, 2005). Alternatively these antagonisms can be nutrients based where specific members of the microbiota are better adapted to sequestering certain nutrients, thus exhausting the supply for others. An example being the ability for *E. coli* Nissle 1917 to out compete *S. typhimurium* through its increased ability to sequester iron (Deriu *et al.*, 2013).

Here we sought to study interactions of *C. difficile* with other gut bacteria in adherent communities, and examine the role of *luxS* in inter-bacterial interactions. We showed that *B. fragilis* has an inhibitory effect on *C. difficile* when within adherent biofilms and that LuxS may mediate the inhibition observed. Whilst the production of an inhibitory molecule by *B. fragilis* cannot be completely ruled out, our data suggests that other mechanisms such as nutritional competition are more likely candidates for the observed inhibition.

The data presented here, demonstrate the first example of *B. fragilis* inhibition of *C. difficile*. Whilst a number of studies have highlighted a negative correlation between the presence of *Bacteroides spp*. and disease instances of *C. difficile* (Seekatz and Young, 2014), few studies have been conducted to ascertain the underlying mechanisms. Studies have largely focused on the ability of *Bacteroides spp.* to metabolise bile acids, due to the evidence that secondary bile acids such as deoxycholic acid inhibit *C. difficile* growth (Sorg and Sonenshein, 2008, Buffie *et al*., 2014).

In a very recent study it was shown that production of the enzyme bile salt hydrolase, is responsible for the inhibitory effect of *Bacteroides ovatus* on *C. difficile* (Yoon *et al*., 2017). They reported that in the presence of bile acids, cell free supernatants for *B. ovatus* were capable of inhibiting the growth of *C. difficile* (Yoon *et al*., 2017). Interestingly however, it was found that in the absence of bile acids, the *Bacteroides* culture instead promoted *C. difficile* growth (Yoon *et al*., 2017). Since we do not supplement bile acids in our system, we can conclude that an alternate mechanism is responsible for *B. fragilis* mediated inhibition of *C. difficile*.

Culturing the two species together in mixed biofilms, we observed a clear defect in biofilm formation and clear decrease in CFU counts for *C. difficile*. As this inhibition was not seen during planktonic growth, we hypothesise three potential modus operandi for the observed inhibition:

Firstly, *B. fragilis* could need to detect the presence of *C. difficile.* Sequencing of the *B. fragilis* strain revealed that despite the lack of a *luxS* homolog, this *B. fragilis* strain does possess a putative two-component histidine kinase with shared homology to the AI-2 sensor kinase/phosphatase, LuxQ, suggesting that whilst *B. fragilis* is not able to produce AI-2 itself, it may be capable of responding to AI-2. There are several examples of QS cheaters or bacteria capable of detecting and responding to QS signals while lacking the ability to produce the signalling molecule themselves (Rainey and Rainey, 2003, Fiegna and Velicer, 2003, Griffin *et al.*, 2004, Diggle *et al.*, 2007, Sandoz *et al.*, 2007, Ross-Gillespie *et al.*, 2007, Jiricny *et al.*, 2010, Popat *et al.*, 2012). If true, *B. fragilis* may be altering its gene expression upon detection of *C. difficile* AI-2, thus creating an environment less favourable for *C. difficile*. As a large number of antimicrobial compounds produced by bacteria are secondary metabolites, which are metabolically costly to produce, bacteria often tightly regulate their expression (Nett *et al.*, 2009). If such a molecule were responsible for the observed inhibition then it is likely that it would only be expressed in the co-culture conditions and not when in monoculture.

Alternatively the mechanisms responsible for the observed inhibition could require the bacteria to be in close proximity. Strains of *B. fragilis* have been shown to possess the type VI secretion system (T6SS) (Russell *et al.*, 2014, Coyne *et al.*, 2016) a multiprotein complex shown to inhibit or kill other members of the Bacteroidales (Chatzidaki-Livanis *et al.*, 2016). Although such inhibition has not previously been shown between Gram-positives and

Gram-negatives, the inability of cell-free supernatants to inhibit *C. difficile*, leaves this possibility open.

Finally the inhibition observed here could simply be the result of a nutritional limitation at a later time point. It could be that *B. fragilis* gains a competitive advantage over *C. difficile* between 10 and 24 hrs post inoculation. This could be the result of the production of metabolic by products, or complex components that are broken down may be utilised by *B. fragilis*.

We detected a small molecule with an m/z of 136 and predicted molecular formula, $C_4H_9NO_4$, by LC/MS in *B. fragilis* biofilm supernatants. No known inhibitory molecule shares this formula. As it is produced by *B. fragilis* in all tested conditions and given the failure of cell free supernatants for both *B. fragilis* mono and co-cultures to inhibit *C. difficile,* this molecule seems an unlikely candidate for the observed inhibition. In addition to this, this molecule was produced in the *LuxS* co-cultures suggesting that this is not responsible for a LuxS-mediated inhibition of *C. difficile* in *B. fragilis* co-cultures.

Although our data demonstrates that LuxS is involved in *B. fragilis*-mediated inhibition of *C. difficile*, the role of LuxS or AI-2 in this inhibition remains unclear. Whilst we cannot rule out a role for signalling, the LuxPQ receptor complex has previously only been discovered in *Vibrionale* (Rezzonico and Duffy, 2008). Although our data suggests possible homology to LuxQ is

present in *B. fragilis*, further research is required to determine whether this species is capable of detecting and responding to AI-2.

As LuxS plays an important role in the detoxification of SAH (Schauder *et al.*, 2001), the metabolic implications for its inactivation cannot be ignored. During analysis of LuxS inactivation in *Lactobacillus reuteri* it was found that the subsequent transcriptional and metabolic changes were not found to be cell-density dependant, suggesting that this was likely a metabolic consequence to the inactivation of LuxS (Wilson *et al.*, 2012).

This will be explored further utilising co-culture RNA-sequencing in chapter 5.

Chapter 5 Understanding inter-species interactions within biofilms

5.1 Introduction

RNA-seq, a relatively new sequencing-based technology, can provide a snapshot of the entire transcriptome of a bacterial population at a given point in time. Transcriptomic studies can provide insight into the regulation of bacterial genes involved in metabolism and other cellular functions. RNA-seq has recently become the de facto method for transcriptome studies (Nicolas *et al.*, 2012, Choi, 2016) due to its many advantages over previous methods, such as not requiring previous knowledge of the reference sequence or coding sequence, low background noise, identification of short or poorly expressed transcripts, single nucleotide resolution, identification of transcriptional start sites, and identification of RNA processing.

As bacteria seldom exist in isolation, interspecies interactions influence the bacterial physiology and pathogenicity. During such interactions, both partners respond in a multitude of ways, often adjusting their gene expression (Wolf *et al.*, 2018). Dual species RNA-seq has enabled researchers to gain a deeper insight into such changes during a number of interspecies conditions, including host-pathogen, mutualistic and commensal interactions (Dutton *et al.*, 2016, Sugimura and Saito, 2017, Wolf *et al.*, 2018). Such studies have unveiled the importance of the carbon storage regulator system for the virulence of *Yersinia pseudotuberculosis* (Nuss *et al.*, 2017), and the ability for *Streptococcus gordonii* to promote *Candida albicans* yeast-to-hyphae transition (Dutton *et al.*, 2016).

Having established the ability for *B. fragilis* to inhibit *C. difficile* growth during biofilm conditions, with notable differences between *C. difficile* WT and *luxS* mutant (*LuxS*), we sought to identify the pathways that mediate this effect. Utilising RNA-seq, we aimed to compare the transcriptional landscapes of both *C. difficile* strains and *B. fragilis*, in mono and co-culture.

Results

Dual and mono species RNA seq from biofilms

C. difficile WT and *LuxS*, together with *B. fragilis* were grown in both mono and co-culture, in BHIS-G at 37°C in anaerobic conditions, in 24-well tissue culture plates (Figure 30). To avoid RNA degradation, RNA was extracted from bacterial biofilms after 18 hrs, post inoculation. 3 wells per sample were combined and the RNA was extracted and cDNA libraries were prepared using TruSeq stranded total RNA kit (Illumina) as described in Chapter 2. 3 biological replicates were used per condition.

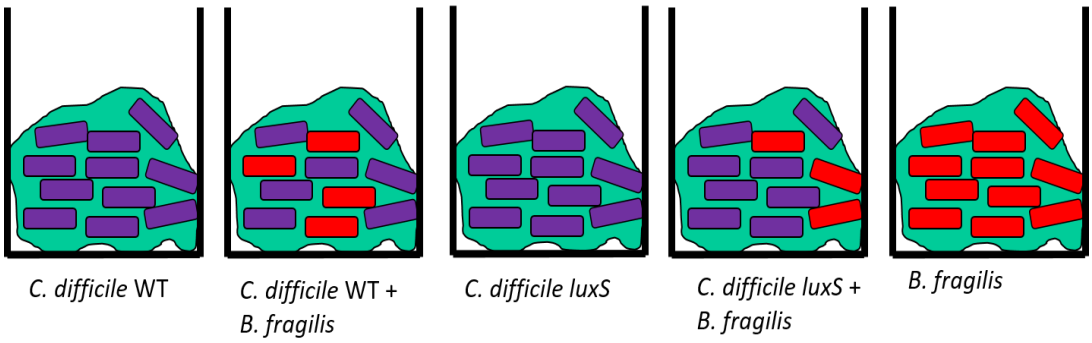

Figure 30: Mono and Co-culture condition for *C. difficile* WT and LuxS (Purple) and *B. fragilis* (Red).

RNA was isolated at 18 hrs from three wells per samples.

Analysis by BLAST (NCBI) demonstrated species specificity for mapping, co-culture samples were mapped to each species reference separately. Initial mapping of the *B. fragilis* strain to a published reference proved unsuccessful, offering a poor rate of alignment of 60%. As the *B. fragilis* strain has not been previously sequenced, and because we were not successful in generating high quality genome sequence, a reference was generated from RNA library of *B. fragilis* using the software rnaSPAdes (Bankevich *et al.*, 2012) and annotated using Prokka (Seemann, 2014). The reads from each condition were mapped to their respective reference sequence using BWA (Li and Durbin, 2009, Li and Durbin, 2010) and counted using coverageBed (Quinlan, 2014).

Metabolic pathways in *C. difficile* were identified using the KEGG mapper (Kanehisa and Goto, 2000), a tool that identifies the function of genes in a published genome. As the *B. fragilis* strain used in this study does not have a published reference genome, blastKOALA (Kanehisa *et al.*, 2016) was used to search for gene homology within metabolic pathways.

5.1.4 Transcriptional responses of *C. difficile* WT and luxS mutant strains during co-culture with *B. fragilis*.

A total of 45 genes were differentially expressed in WT *C. difficile*, during co-culture with *B. fragilis*. Of these 21 were down-regulated and 24 were up-regulated. 69 genes were differentially expressed in *C. difficile LuxS* during co-culture with *B. fragilis,* 34 of with were down-regulated and 35 up-regulated (Figure 31). A total of 26 genes were up or down-regulated in both WT and *LuxS* (Table 7). These include 6 up-regulated genes (*accB, abfH, abfT,*

abfD, sucD and *cat1*) involved in carbon and butanoate metabolism (Figures 32 and 33 respectively), with *cat1* encoding succinyl-CoA:coenzyme A transferase being the most highly up-regulated gene for both WT and *LuxS* (Table 7). *nanE,* which encodes a putative N-acetylmannosamine-6-phosphate 2-epimerase was also up-regulated while gene *bcd2,* which encodes butyryl-CoA dehydrogenase, an enzyme involved in butanoate metabolism was down-regulated in both strains.

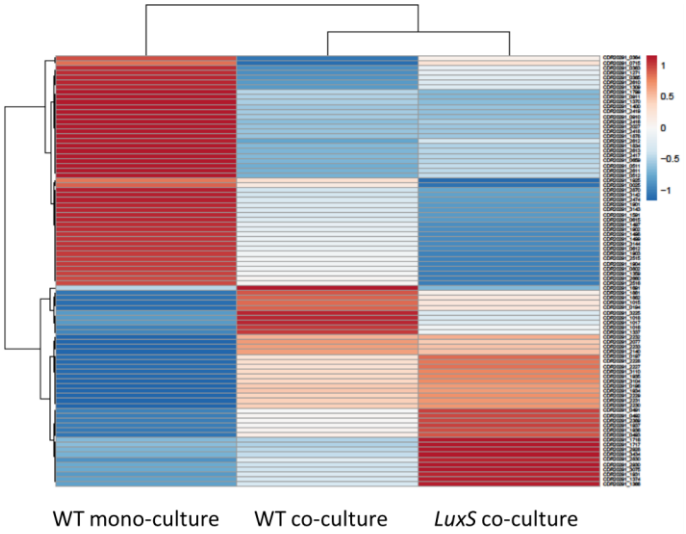

Figure 31: Heat map comparing differentially expressed genes of *C. difficile.*

A total of 88 genes were differentially expressed between WT and *LuxS.*

8 genes of the up-regulated genes were specific to WT during co-culture. Of these, 4 genes involved in fatty acid biosynthesis and metabolism are noted to be up-regulated: *fabH* encoding 3-oxoacyl-[acyl-carrier protein] synthase III, *fabK* encoding trans-2-enoyl-ACP reductase, *accC* biotin carboxylase (acetyl-CoA carboxylase subunit A), and *accB* biotin carboxyl carrier protein of acetyl-CoA carboxylase (Figure 34). Additionally *plsX* encoding fatty acid / phospholipid synthesis protein, was also up-regulated.

18 up-regulated genes were specific to *LuxS* in co culture. These include a putative homocysteine S-methyltransferase, a putative osmoprotectant ABC transporter, substrate binding/ permease protein, ribonucleoside-diphosphate reductase alpha chain (*nrdE*) and two genes from the trehalose operon: a PTS system II ABC transporter, and trehalose-6-phosphate hydrolase *(treA*).

11 genes were found to be down-regulated exclusively in WT (Table 8). These include *idhA*, *hisH*, *eutB* and a putative radical SAM superfamily protein.

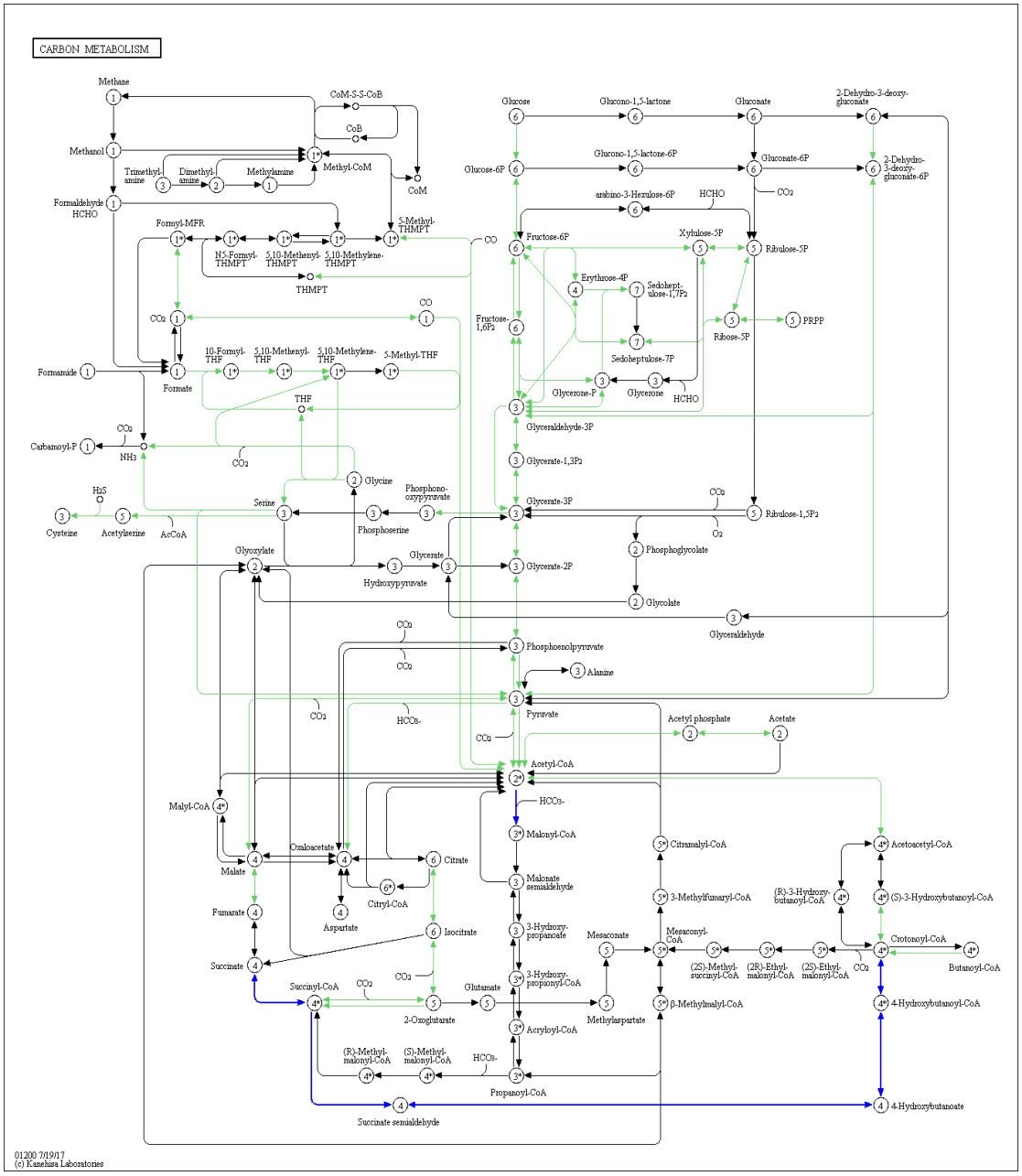

Figure 32: Metabolic pathway for Carbon metabolism.

Carbon metabolism genes present in *C. difficile* (green). 6 genes are found to be up-regulated in both WT and *LuxS* (*accB, abfH, abfT, abfD, sucD* and *cat1*) (blue).

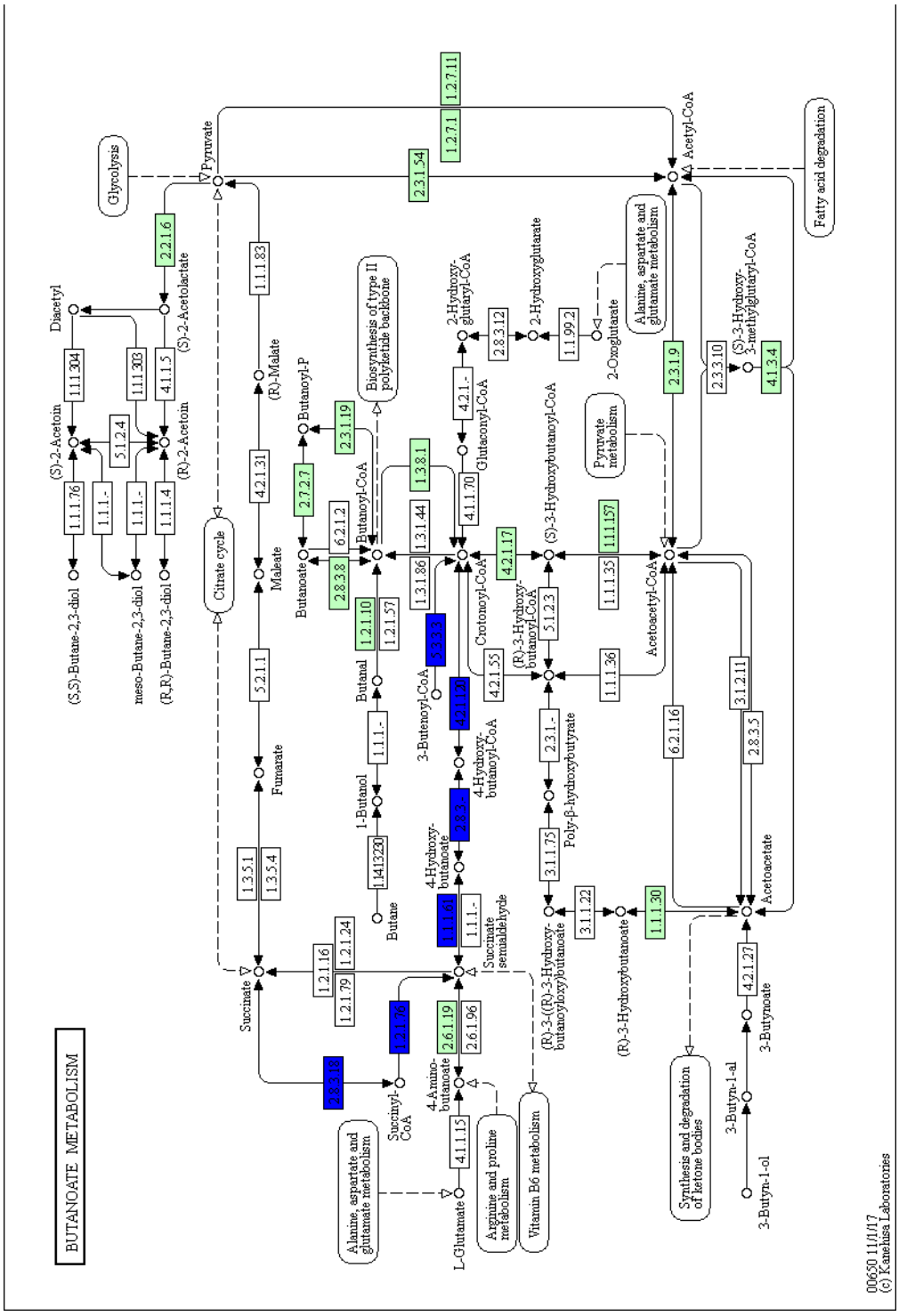

Figure 33: Metabolic pathway for Butanoate metabolism.

Butanoate metabolism genes present in *C. difficile* (green). 6 genes found to be up-regulated in both WT and *LuxS* (*accB, abfH, abfT, abfD, sucD* and *cat1*) (blue).

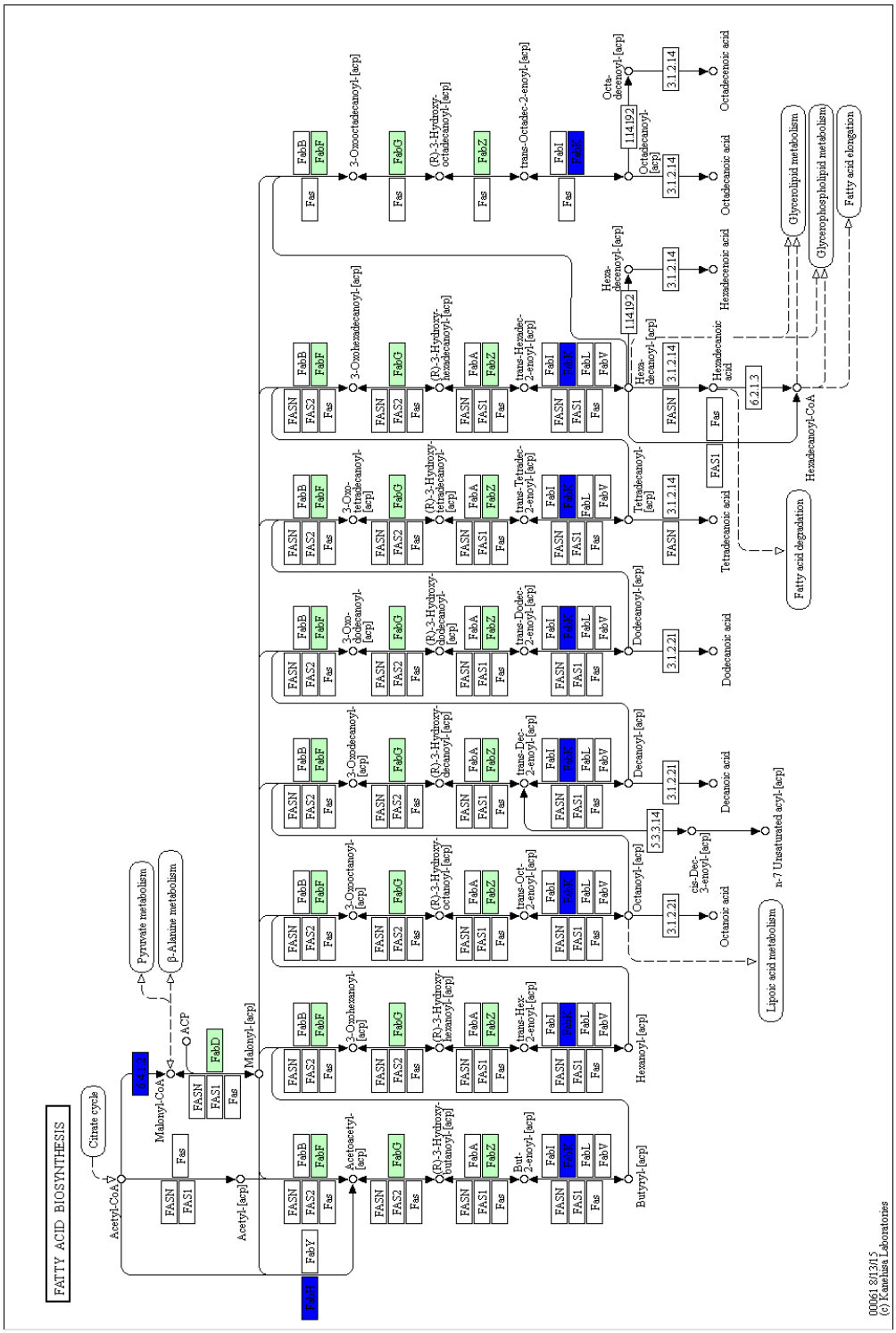

Figure 34: Metabolic pathway for Fatty Acid Biosynthesis.
Fatty acid biosynthesis genes present in *C. difficile* (green). 4 genes, *fabH, fabK, accC* and *accB,* are found to be up-regulated in *C. difficile* WT only (blue).

24 genes are found to be down-regulated only in *LuxS* (Table 9). These include 3 genes involved in thiamine metabolism *thiD*, *thiK* and *thiE1*, (CDR20291_1497, CDR20291_1498 and CDR20291_1499 respectively) which encode a putative phosphomethylpyrimidine kinase, 4-methyl-5-beta-hydroxyethylthiazole kinase and thiamine-phosphate pyrophosphorylase respectively (Figure 35). Other genes also down-regulated include: *pflD*; putative formate acetyltransferase and *proC2* pyroline-5-carboxylate reductase.

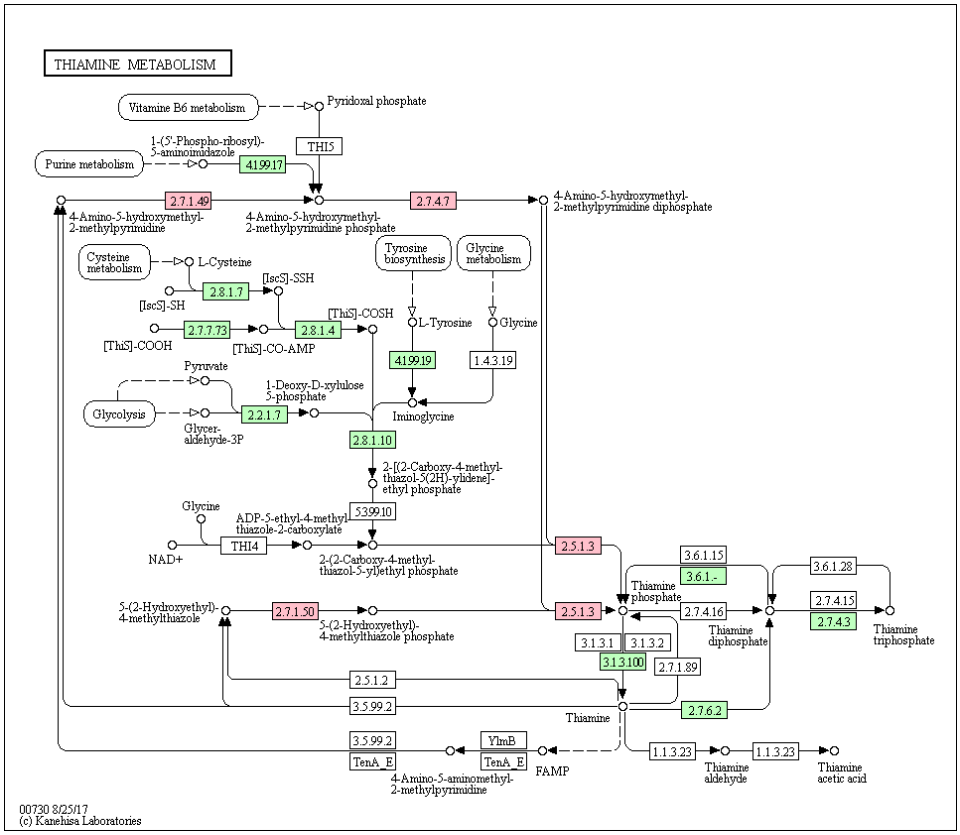

Figure 35: Metabolic pathway for Thiamine metabolism.

Thiamine metabolism genes presents in *C. difficile* (green). 3 *thiD*, *thiK* and, *thiE1* genes were found to be down-regulated in *LuxS* (pink).

Table 8: Genes up- and down-regulated in **both** *C. difficile* WT and *LuxS,* in *C. difficile-Bacteroides fragilis* co-cultures relative to WT *C. difficile.*

Gene ID	Log2foldchange	Gene Annotation
CDR20291_0196	1.242760946	hypothetical protein
CDR20291_0197	1.024719474	hypothetical protein
CDR20291_0511	-1.947939847	hypothetical protein
CDR20291_0512	-1.790659218	hypothetical protein
CDR20291_0910	-1.118039675	butyryl-CoA dehydrogenase
CDR20291_1015	1.855396639	fatty acid biosynthesis transcriptional regulator
CDR20291_1799	-1.559955287	hypothetical protein
CDR20291_1862	1.571375262	biotin carboxyl carrier protein of acetyl-CoA carboxylase
CDR20291_1878	-1.084562908	ABC transporter ATP-binding protein
CDR20291_1931	1.501260024	AraC family transcriptional regulator
CDR20291_1935	1.754871647	hypothetical protein
CDR20291_2077	1.310107407	Sodium:dicarboxylate symporter
CDR20291_2140	2.555234046	N-acetylmannosamine-6-phosphate 2-epimerase
CDR20291_2227	3.630122723	NAD-dependent 4-hydroxybutyrate dehydrogenase
CDR20291_2228	3.789825947	4-hydroxybutyrate CoA transferase
CDR20291_2229	3.695347944	hypothetical protein
CDR20291_2230	3.544168193	gamma-aminobutyrate metabolism dehydratase/isomerase
CDR20291_2231	3.864728796	succinate-semialdehyde dehydrogenase [NAD(P)+]
CDR20291_2232	4.2239099	succinyl-CoA:coenzyme A transferase
CDR20291_2233	4.339535053	hypothetical protein
CDR20291_2418	-1.624152909	hypothetical protein
CDR20291_2419	-1.384788131	aminotransferase

CDR20291_2611	-1.45763049	two-component response regulator
CDR20291_2612	-1.940640211	hypothetical protein
CDR20291_2613	-1.569696353	polysaccharide deacetylase
CDR20291_3110	1.176093028	hypothetical protein

Note: P adjusted value< 0.05. Green text denotes up-regulated genes, blue text denotes down-regulated genes.

Table 9: Genes up- and down-regulated in ***C. difficile*** **WT,** in *C. difficile-Bacteroides fragilis* co-cultures relative to WT *C. difficile*

Gene ID	log2FoldChange	Gene Annotation
CDR20291_0194	1.38220809	10 kDa chaperonin
CDR20291_0363	-1.377088342	radical SAM protein
CDR20291_0364	-1.003594522	hypothetical protein
CDR20291_0365	-1.461206801	(R)-2-hydroxyisocaproate dehydrogenase
CDR20291_0659	-1.24853552	radical SAM protein
CDR20291_1016	1.708784707	glycerol-3-phosphate acyltransferase PlsX
CDR20291_1017	1.701199239	3-oxoacyl-ACP synthase III
CDR20291_1018	1.246932597	trans-2-enoyl-ACP reductase
CDR20291_1271	-1.156719781	hypothetical protein
CDR20291_1309	-1.208810668	phosphohydrolase
CDR20291_1337	1.329049949	transcriptional regulator
CDR20291_1400	-1.833327377	imidazole glycerol phosphate synthase subunit HisH
CDR20291_1834	-1.411634275	ethanolamine/propanediol ammonia-lyase heavy chain
CDR20291_1861	1.412304008	biotin carboxylase acetyl-CoA carboxylase subunit A
CDR20291_2027	1.63094576	2-nitropropane dioxygenase

CDR20291_2416	-1.231650825	hypothetical protein
CDR20291_2417	-1.574982111	hypothetical protein
CDR20291_2610	-1.046806871	two-component sensor histidine kinase
CDR20291_3225	1.022902487	formate/nitrite transporter

Note: P adjusted value< 0.05. Green text denotes up-regulated genes, blue text denotes down-regulated genes.

Table 10: Genes up and down-regulated in ***C. difficile LuxS*** in in *C. difficile-Bacteroides fragilis* co-cultures relative to WT *C. difficile.*

LuxSmix	**log2FoldChange**	Gene Annotation
CDR20291_0025	-1.320529858	acetoin:2%2C6-dichlorophenolindophenol oxidoreductase subunit alpha
CDR20291_0491	1.096435454	RNA methylase
CDR20291_0492	1.180203419	hypothetical protein
CDR20291_0493	1.007610513	outer membrane lipoprotein
CDR20291_0615	-0.869149983	nucleotide phosphodiesterase
CDR20291_0715	1.624572548	N-acetylmuramoyl-L-alanine amidase
CDR20291_0802	-2.260047134	ABC transporter substrate-binding protein
CDR20291_0911	-1.241809993	electron transfer flavoprotein subunit beta
CDR20291_1359	-0.850952233	hypothetical protein
CDR20291_1366	0.92740269	ferrous ion transport protein
CDR20291_1370	-1.124726418	tyrosyl-tRNA synthetase
CDR20291_1374	1.165117564	iron-sulfur protein
CDR20291_1497	-1.456295839	phosphomethylpyrimidine kinase
CDR20291_1498	-1.727285435	hydroxyethylthiazole kinase
CDR20291_1499	-1.276386794	thiamine-phosphate pyrophosphorylase

CDR20291_1591	-1.517990203	dinitrogenase iron-molybdenum cofactor
CDR20291_1691	1.418730417	nitrite and sulfite reductase subunit
CDR20291_1716	1.314365385	thiol peroxidase
CDR20291_1717	1.110872045	hypothetical protein
CDR20291_1901	-1.832663158	ABC transporter ATP-binding protein
CDR20291_1902	-1.875507101	ABC transporter substrate-binding protein
CDR20291_1903	-1.659329494	ABC transporter permease
CDR20291_1904	-1.638608704	hypothetical protein
CDR20291_1925	-1.548059893	flavodoxin
CDR20291_1934	1.545622858	hypothetical protein
CDR20291_1936	1.336887442	GntR family transcriptional regulator
CDR20291_1937	1.373694549	ABC transporter ATP-binding protein
CDR20291_2389	1.261970927	competence protein
CDR20291_2474	-1.434272008	DNA-directed RNA polymerase subunit omega
CDR20291_2515	-1.6039508	amino acid permease family protein
CDR20291_2516	-1.176482249	cobalt dependent x-pro dipeptidase
CDR20291_2660	-0.958813531	teichuronic acid biosynthesis glycosyl transferase
CDR20291_2830	1.113329954	ribonucleoside-diphosphate reductase subunit alpha
CDR20291_2870	-2.33551794	hypothetical protein
CDR20291_2928	1.753815574	PTS system transporter subunit IIABC
CDR20291_2930	1.571316791	trehalose-6-phosphate hydrolase
CDR20291_3075	1.364968728	osmoprotectant ABC transporter substrate-binding/permease
CDR20291_3104	0.809909777	sigma-54-dependent transcriptional activator
CDR20291_3142	-1.665916251	pyrroline-5-carboxylate reductase

CDR20291_3143	-1.830480704	formate acetyltransferase
CDR20291_3144	-1.643573257	pyruvate formate-lyase 3 activating enzyme
CDR20291_3434	1.44024185	homocysteine S-methyltransferase

Note: P adjusted value< 0.05. Green text denotes up-regulated genes, blue text denotes down-regulated genes.

As *C. difficile* WT is more susceptible to *B. fragilis* mediated inhibition compared to *LuxS*, we sought to identify transcriptional differences between the two strains. With the ability for *C. difficile* to gain a competitive advantage against other members of the gut microbiota through its ability to utilise trehalose (Collins *et al.*, 2018a), it is interesting to note an upregulation of two genes from the trehalose operon: *treA* (CDR20291_2930) and a PTS system transporter (CDR20291_2928) in LuxS. To investigate if the upregulation of the trehalose operon in *C. difficile LuxS* provided the mutant with a competitive advantage over the WT, we first tested the ability of both WT to produce a biofilm in the presence of 1 µM, 10 µM, 100 µM and 1000 µM trehalose (Figure 36A). Since supplementing the medium with additional levels of glucose, equivalent to trehalose, also had an inhibitory effect (Figure 36A), we switched the medium to BHIS, removing the glucose entirely (Figure 36B). In the absence of glucose, the levels of trehalose tested had no effect on the biofilm formation of WT, with slight inhibition seen at higher concentration in *LuxS*.

A

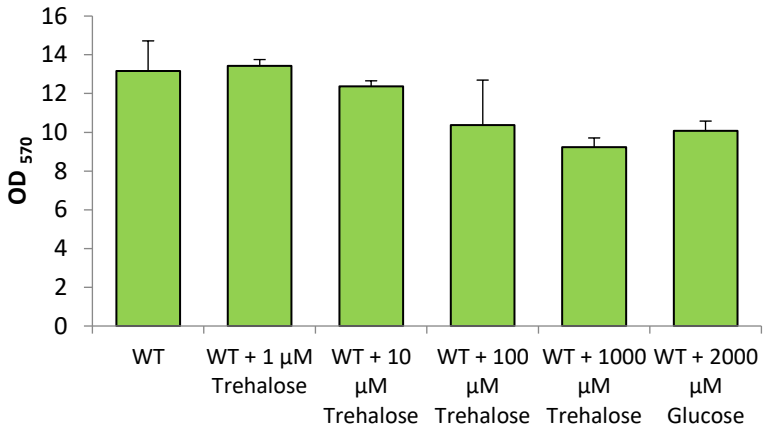

B

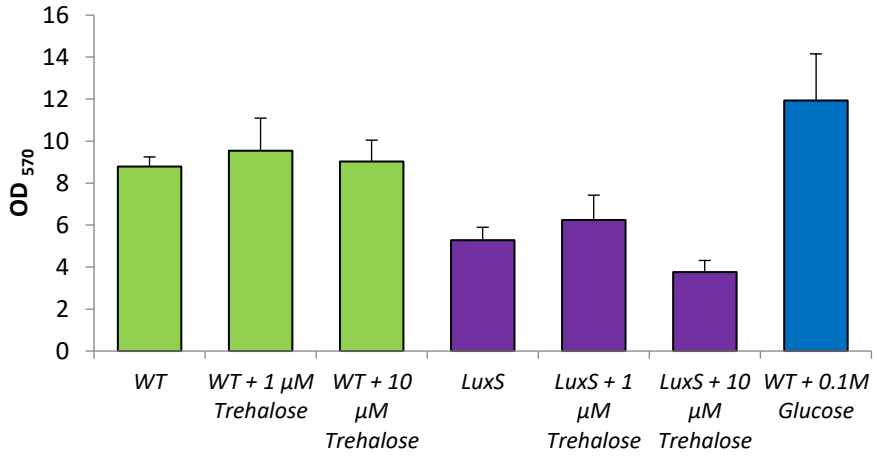

Figure 36: Biofilm formation of *C. difficile* WT and LuxS with and without trehalose as measured by crystal violet.

(**A**) WT was tested with 1 µM, 10 µM, 100 µM and 1000 µM trehalose together with 2000 µM Glucose in BHIS-G. (**B**) Both WT and *LuxS* were tested with lower concentrations of 1 µM, 10 µM trehalose. WT grown in BHIS-G was used as for comparison. N=3 with error bars representing standard deviation.

4.2.5 Transcriptional profiles of *B. fragilis* during co-culture with *C. difficile* WT and LuxS

When co-cultured with *C. difficile* WT, 335 genes were differentially expressed in *B. fragilis* compared to monoculture biofilms, with 139 genes

being up-regulated and 196 down-regulated. 324 genes were differentially expressed during *B. fragilis* co-culture with LuxS compared to *B. fragilis* monoculture. Of these 150 were up-regulated and 174 down-regulated. In total, 266 shared genes were found to be up and down-regulated in both co-culture conditions. Of these the 28 highest up- and down- regulated genes are shown in Table 11 & 12 respectively. Whilst the highest up-regulated gene in both conditions encodes a virus attachment protein, no other viral genes were shown to be up-regulated. The next highest up-regulated genes in both conditions encoding desulfoferrodoxin and rubrerythrin. With both of these proteins containing iron, it is curious that multiple copies of *fecR*, a key regulator for the ferric citrate transport system (Andrews *et al.*, 2003), and ferrous iron transport protein B were also up-regulated. It should be noted that many of the other up-regulated genes corresponded to hypothetical proteins of unknown function.

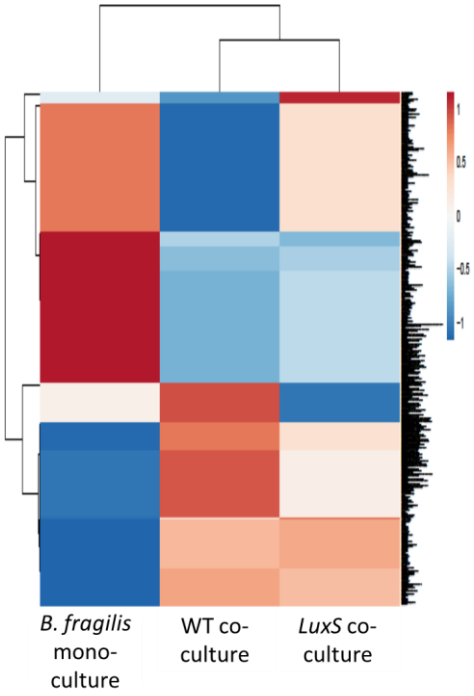

Figure 37: Heat map comparing differentially expressed genes of *B. fragilis*.

Differentially expressed genes in *B. fragilis* were compared between all culture conditions.

Table 11: Genes up-regulated in ***B. fragilis***, in both *C. difficile* **WT and *LuxS*-** *Bacteroides fragilis* co-cultures relative to *B. fragilis* mono-culture.

log2FoldChange	Gene Annotation
9.287946	Virus attachment protein p12 family protein
7.634947	Desulfoferrodoxin
6.03326	Rubrerythrin
4.659762	hypothetical protein
2.93005	hypothetical protein
2.652998	hypothetical protein
2.266419	DNA-binding transcriptional repressor MngR
2.231958	hypothetical protein
1.932819	L-fucose isomerase
1.759508	NADP-dependent 7-alpha-hydroxysteroid dehydrogenase

1.698321	Alkyl hydroperoxide reductase subunit F
1.623389	2-isopropylmalate synthase
1.569406	Sensor histidine kinase RcsC
1.56776	Galactokinase
1.546709	Carbamoyl-phosphate synthase large chain
1.519255	fec operon regulator FecR
1.495672	UDP-glucose 4-epimerase
1.491419	3-isopropylmalate dehydratase small subunit
1.462756	indolepyruvate oxidoreductase subunit beta
1.452842	3-isopropylmalate dehydrogenase
1.431211	fec operon regulator FecR
1.412666	fec operon regulator FecR
1.38758	fec operon regulator FecR
1.372355	hypothetical protein
1.355325	hypothetical protein
1.312292	integration host factor subunit alpha
1.304238	hypothetical protein
1.295602	3-isopropylmalate dehydratase large subunit

Note: P adjusted value< 0.05.

Table 12: Genes down-regulated in ***B. fragilis***, in *C. difficile* **WT and *LuxS*-**
Bacteroides fragilis co-cultures relative to *B. fragilis* mono-culture.

log2FoldChange	**Gene Annotation**
-2.98798	hypothetical protein
-2.80775	Biopolymer transport protein ExbD/TolR
-2.75952	Biopolymer transport protein ExbD/TolR
-2.45804	hypothetical protein
-2.45438	ECF RNA polymerase sigma factor SigW
-2.36995	Efflux pump periplasmic linker BepF

-2.28626	Inner membrane protein YhiM
-2.27704	Gram-negative bacterial tonB protein
-2.24283	colicin uptake protein TolQ
-2.21503	Histidine decarboxylase proenzyme precursor
-2.17528	hypothetical protein
-2.12616	hypothetical protein
-2.12196	putative TonB-dependent receptor precursor
-2.11095	hypothetical protein
-2.0886	hypothetical protein
-2.0541	hypothetical protein
-2.02612	Acetylxylan esterase precursor
-2.02381	Porin subfamily protein
-2.02379	tetratricopeptide repeat protein
-2.0236	hypothetical protein
-1.95909	Outer membrane protein OprM precursor
-1.94728	TonB-dependent Receptor Plug Domain protein
-1.89613	hypothetical protein
-1.88633	Choloylglycine hydrolase
-1.8758	Putative NAD(P)H-dependent FMN-containing oxidoreductase YwqN
-1.86516	ISXO2-like transposase domain protein

Note: P adjusted value< 0.05.

Additionally there are a number of metabolic pathways up-regulated in both, these include 4 genes (encoding 3-isopropylmalate dehydratase small subunit, 3-isopropylmalate dehydrogenase, Galactokinase and 3-isopropylmalate dehydratase large subunit) involved in valine, leucine and isoleucine biosynthesis and C5-Branched dibasic acid metabolism (Figure 38 and 39 respectively).

Similarly, several metabolic pathways are down-regulated in both co-culture conditions. These include 6 genes involved in carbon metabolism (Figure 40), 4 genes involved in alanine, aspartate and glutamate metabolism, and 4 genes involved in the biosynthesis of amino acids, however these appear to be single genes rather than specific pathways (Figure 41).

Despite both co-culture conditions only sharing 82% of differentially expressed genes compared to the monoculture, analysis by blastKOALA (Kanehisa *et al.*, 2016) did not clearly highlight any metabolic pathways as being differentially expressed between the co-culture conditions, with many of the genes being annotated as hypothetical genes.

A total of 67 genes were found to be specific to *C. difficile* WT co-culture, with 29 of these up-regulated (Table 12) and 38 down-regulated (Table 13). Similarly 58 genes were found to be specific to *C. difficile LuxS* co-culture, with 38 of these up-regulated (Table 14) and 20 down-regulated (Tables 15).

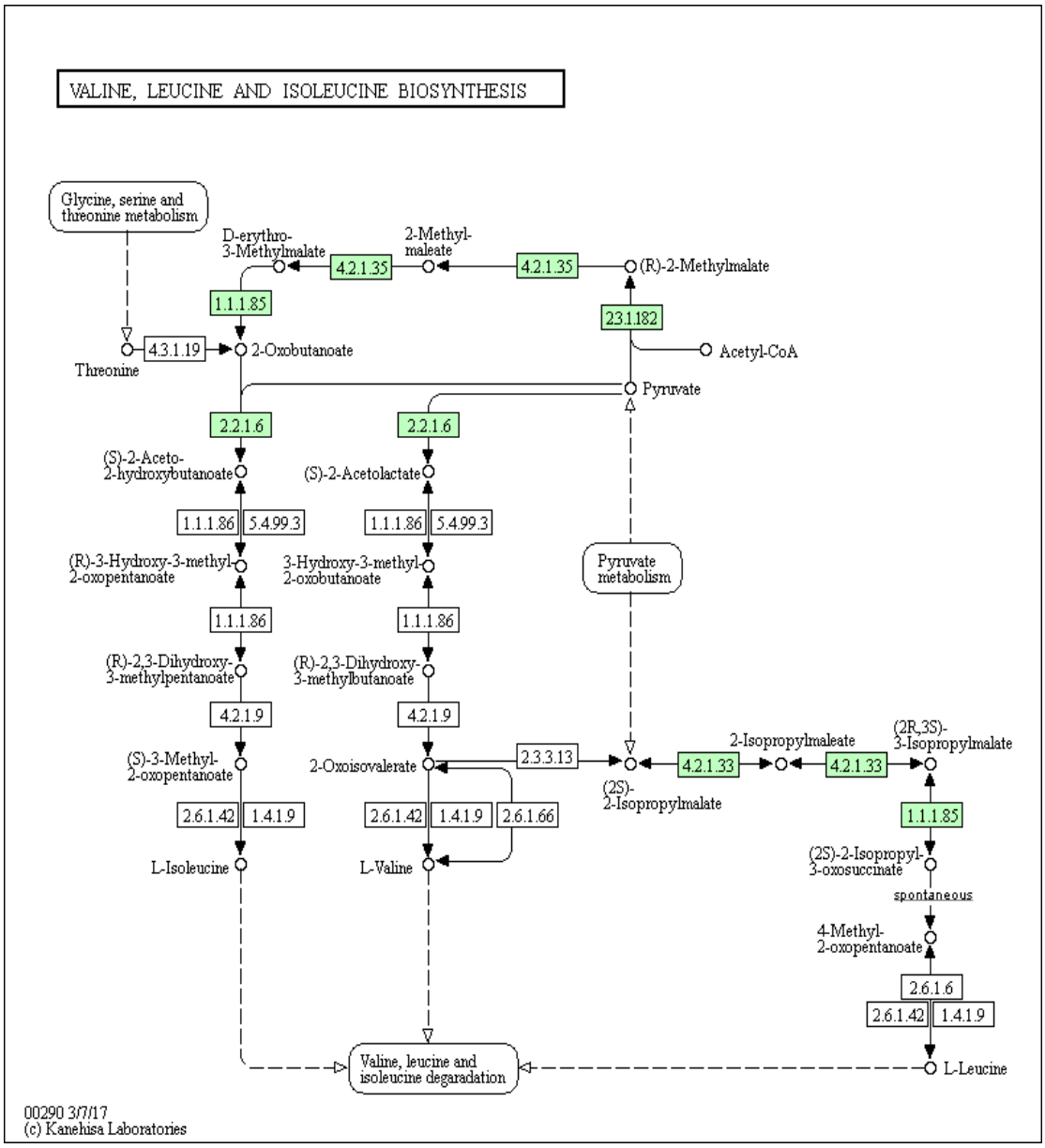

Figure 38: Metabolic pathway for valine, leucine and isoleucine biosynthesis.

4 genes were found to be differentially expressed in *B. fragilis* during co-culture with *C. difficile* WT and *LuxS* (green).

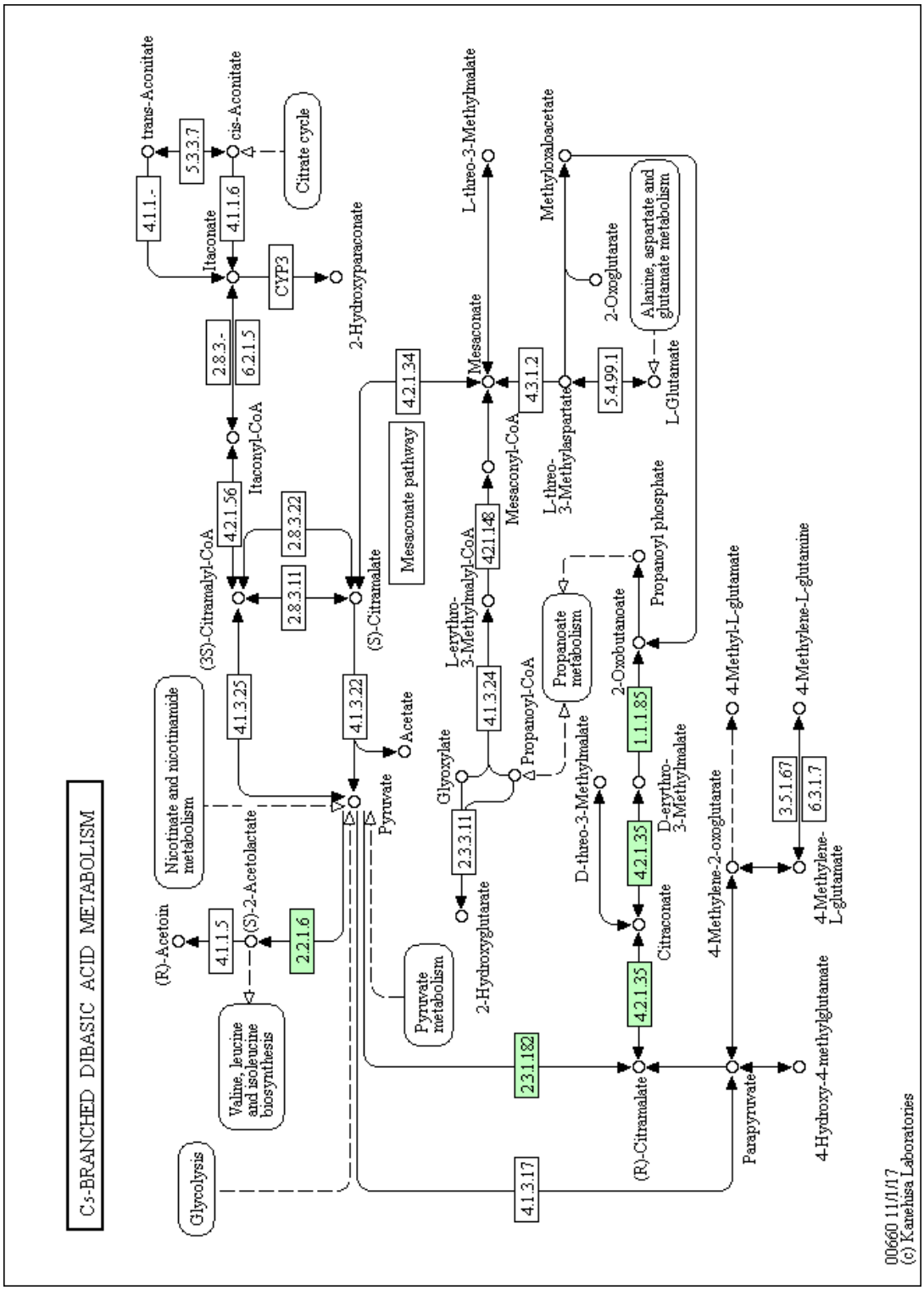

Figure 39: Metabolic pathway for C5-branched diabasic acid metabolism.

4 genes were found to be differentially expressed in *B. fragilis* during co-culture with *C. difficile* WT and *LuxS* (green).

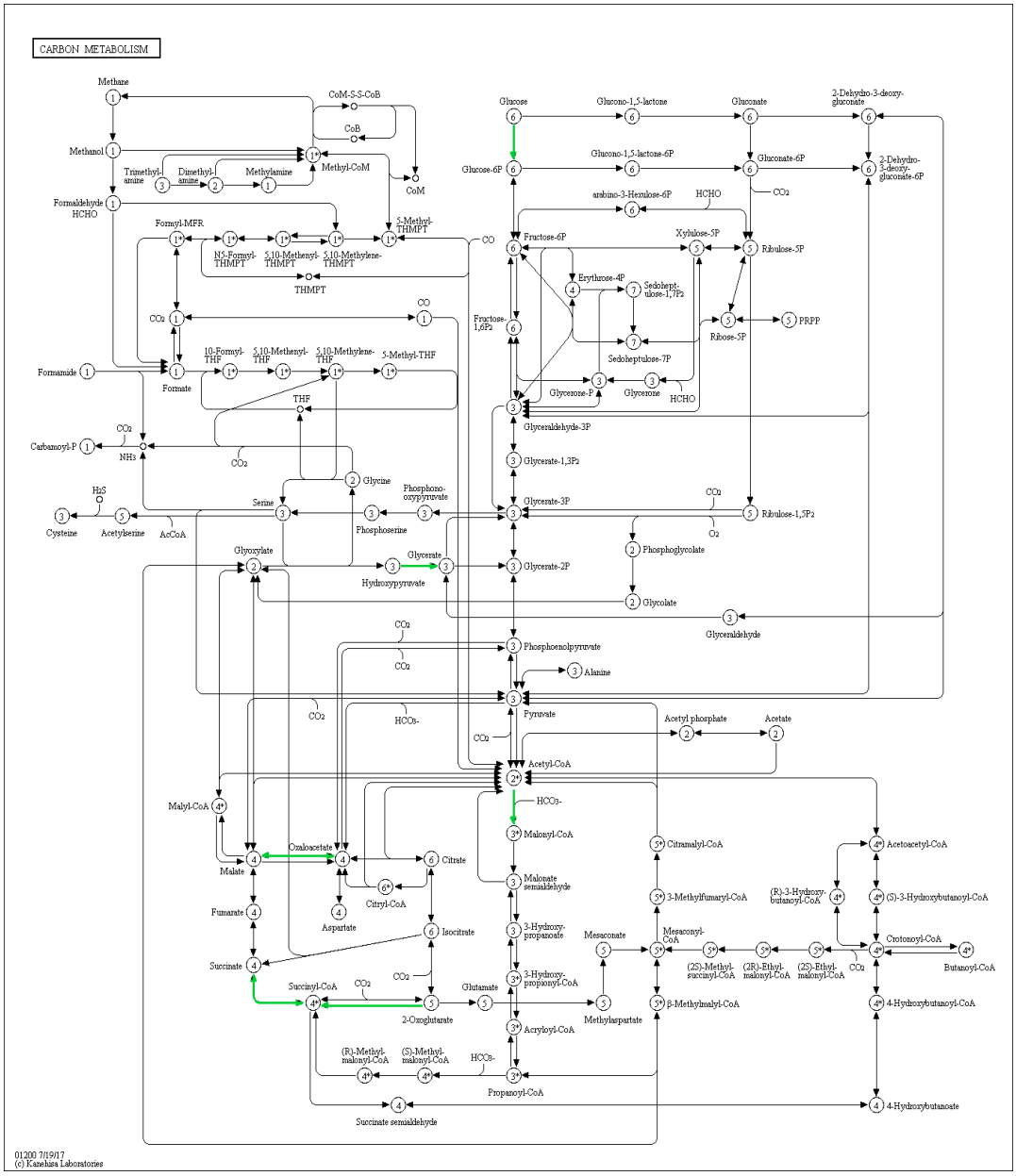

Figure 40: Metabolic pathway for carbon metabolism.

4 genes involved in carbon metabolism are down-regulated in *B. fragilis* co-cultured with *C. difficile* WT and *LuxS* (green).

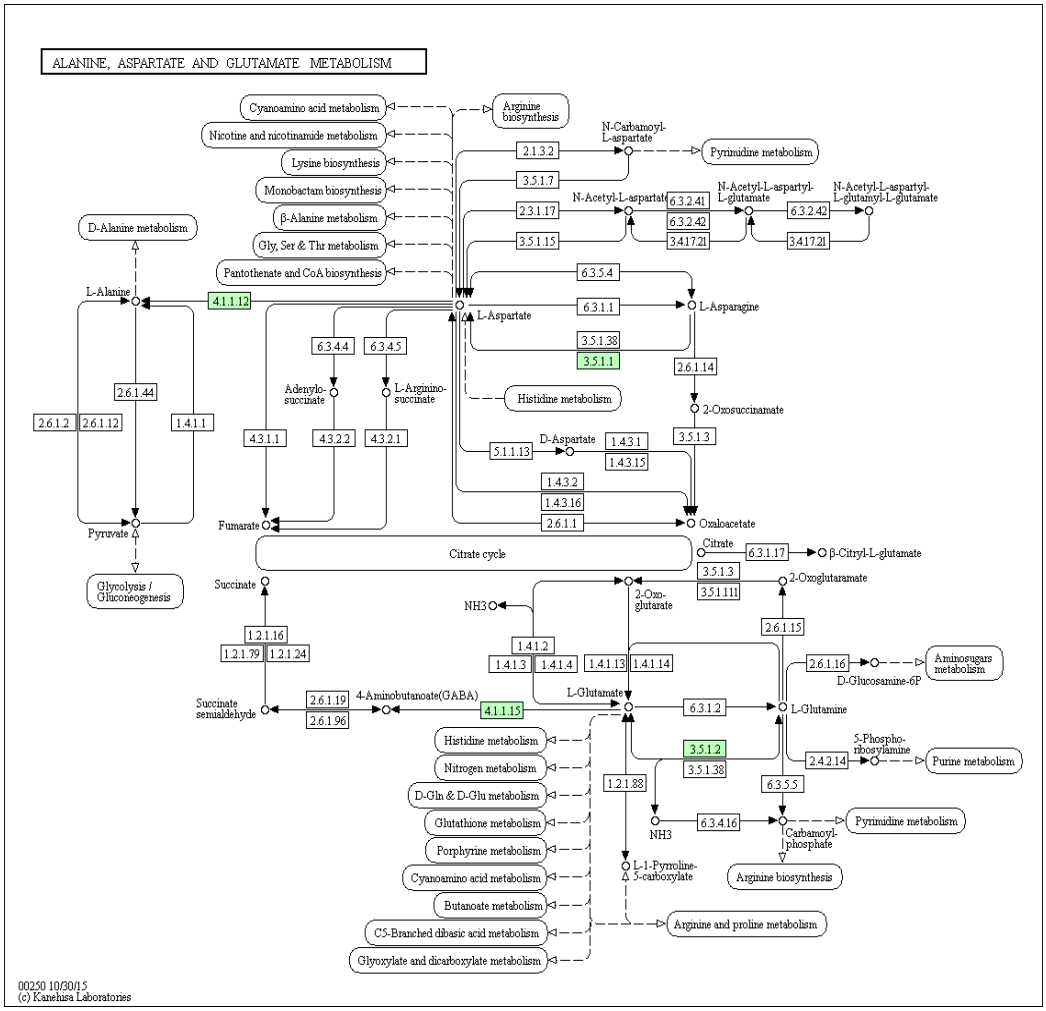

Figure 41: Metabolic pathway for Alanine, Aspartate and Glutamate metabolism.

4 genes involved in Alanine, Aspartate and Glutamate metabolism are down-regulated in *B. fragilis* co-cultured with *C. difficile* WT and *LuxS* (green).

Table 13: Genes up-regulated in ***B. fragilis***, in C. difficile **WT**-*Bacteroides fragilis* co-cultures relative to *B. fragilis* mono-culture

log2FoldChange	Gene Annotation
1.311516	RNA polymerase sigma factor
1.30583	N-acetylmuramoyl-L-alanine amidase
1.296892	tRNA-Arg(ccg)
1.287475	Phytochrome-like protein cph1
1.273862	L-fucose-proton symporter
1.192976	SusD family protein
1.125756	putative N-acetyltransferase YvbK
1.046014	hypothetical protein
0.929316	hypothetical protein
0.918517	7-cyano-7-deazaguanine synthase
0.895506	3-deoxy-D-manno-octulosonic acid transferase
0.894201	hypothetical protein
0.892291	Putative multidrug export ATP-binding/permease protein
0.880993	hypothetical protein
0.880608	NADPH-dependent 7-cyano-7-deazaguanine reductase
0.876389	Nicotinamide-nucleotide amidohydrolase PncC
0.862807	hypothetical protein
0.845284	50S ribosomal protein L35
0.844678	Peptide-N-glycosidase F%2C N terminal
0.843493	Abhydrolase family protein
0.839781	Phospho-N-acetylmuramoyl-pentapeptide-transferase
0.829317	hypothetical protein
0.825833	Beta-1%2C4-mannooligosaccharide phosphorylase
0.811321	lipid-A-disaccharide synthase
0.811099	hypothetical protein
0.81081	Aspartate/alanine antiporter
0.807753	Arylsulfatase
0.802685	DNA-invertase hin
0.801621	D-3-phosphoglycerate dehydrogenase

Note: P adjusted value< 0.05.

Table 14: Genes down-regulated in ***B. fragilis***, in *C. difficile* **WT**-*Bacteroides fragilis* co-cultures relative to *B. fragilis* mono-culture.

log2FoldChange	Gene Annotation
-1.40341	hypothetical protein
-1.37746	hypothetical protein
-1.37108	hypothetical protein
-1.36255	hypothetical protein
-1.28886	Fimbrillin-A associated anchor proteins Mfa1 and Mfa2
-1.22553	hypothetical protein
-1.19669	hypothetical protein
-1.19434	hypothetical protein
-1.19075	Nitroreductase family protein
-1.15186	hypothetical protein
-1.12987	hypothetical protein
-1.1191	hypothetical protein
-1.11384	hypothetical protein
-1.09063	hypothetical protein
-1.0769	Quercetin 2%2C3-dioxygenase
-1.07478	Hydroxylamine reductase
-1.07286	ECF RNA polymerase sigma factor SigH
-1.07215	Multidrug resistance protein MdtA precursor
-1.05139	Chagasin family peptidase inhibitor I42
-1.01228	Dihydrolipoyllysine-residue acetyltransferase component of pyruvate dehydrogenase complex
-1.00722	hypothetical protein
-0.99411	Putative pyridoxal phosphate-dependent aminotransferase EpsN
-0.9932	Alpha-amylase precursor
-0.9877	hypothetical protein
-0.98757	putative deferrochelatase/peroxidase YfeX
-0.98646	hypothetical protein
-0.97934	Hexokinase
-0.95502	Flavodoxin
-0.93045	Succinyl-CoA ligase [ADP-forming] subunit beta
-0.92318	Carboxymuconolactone decarboxylase family protein
-0.89637	tRNA 2'-O-methylase

-0.88426	Putative SOS response-associated peptidase YedK
-0.86662	Helix-turn-helix
-0.86218	hypothetical protein
-0.86014	Tyrocidine synthase 1
-0.85888	GDP-mannose 4%2C6-dehydratase
-0.83579	hypothetical protein
-0.82748	Putative zinc ribbon domain protein

Note: P adjusted value< 0.05.

Table 15: Genes up-regulated in ***B. fragilis***, in C. difficile ***LuxS***-*Bacteroides fragilis* co-cultures relative to *B. fragilis* mono-culture

log2FoldChange	**Gene Annotation**
1.50249	hypothetical protein
1.48934	Tyrosine recombinase XerD
1.295481	fec operon regulator FecR
1.280656	tRNA-Leu(caa)
1.235375	Reverse rubrerythrin-1
1.220847	hypothetical protein
1.200963	ATP-dependent Clp protease ATP-binding subunit ClpC
1.188287	hypothetical protein
1.176729	tRNA-Thr(cgt)
1.133713	hypothetical protein
1.109684	60 kDa chaperonin
1.09403	10 kDa chaperonin
1.08306	Tyrosine recombinase XerC
1.066955	NAD-specific glutamate dehydrogenase
1.063195	fec operon regulator FecR
1.03149	fec operon regulator FecR
1.021451	hypothetical protein
1.015769	tRNA-Phe(gaa)
0.990297	hypothetical protein
0.98787	tRNA-Arg(gcg)
0.980119	MarR family protein
0.956639	hypothetical protein
0.951389	hypothetical protein

0.938171	Septum formation protein Maf
0.932255	ATP synthase subunit beta
0.92593	hypothetical protein
0.921887	hypothetical protein
0.905375	30S ribosomal protein S20
0.89716	hypothetical protein
0.885735	hypothetical protein
0.871156	hypothetical protein
0.865619	50S ribosomal protein L34
0.843942	tRNA-Asp(gtc)
0.843727	Cellobiose 2-epimerase
0.835563	50S ribosomal protein L36
0.817012	30S ribosomal protein S21
0.802377	tRNA-Lys(ttt)
0.800503	50S ribosomal protein L31 type B

Note: P adjusted value< 0.05.

Table 16: Genes down-regulated in ***B. fragilis***, in C. difficile ***LuxS***-*Bacteroides fragilis* co-cultures relative to *B. fragilis* mono-culture.

log2FoldChange	**Gene Annotation**
-1.4039	hypothetical protein
-1.33473	hypothetical protein
-1.33023	hypothetical protein
-1.19678	hypothetical protein
-1.11145	Lactate utilization protein C
-1.06955	Molecular chaperone Hsp31 and glyoxalase 3
-1.03246	hypothetical protein
-1.01929	putative metallo-hydrolase
-1.01713	Colicin I receptor precursor
-0.98589	Cadmium%2C zinc and cobalt-transporting ATPase
-0.9256	Bifunctional transcriptional activator/DNA repair enzyme Ada
-0.91437	Pyruvate formate-lyase 1-activating enzyme
-0.9142	hypothetical protein
-0.87106	putative A/G-specific adenine glycosylase YfhQ

-0.86216	Lipoprotein-releasing system transmembrane protein LolE
-0.8445	FMN reductase [NAD(P)H]
-0.83554	putative oxidoreductase
-0.81525	Transaldolase
-0.8053	Aminopeptidase YwaD precursor
-0.80259	dTDP-4-dehydrorhamnose reductase

Note: P adjusted value < 0.05.

Discussion

In this Chapter we have described RNA-seq of co-cultures of *C. difficile* and *B. fragilis.* The purpose of this study was to determine the mechanisms responsible for the observed *B. fragilis* mediated inhibition of *C. difficile*. Although our data does not predict a single mechanism responsible for the *B. fragilis* mediated inhibition of *C. difficile*, we identified a number of potentially important metabolic pathways differentially expressed in both organisms in the conditions tested.

Although upregulation was observed for 6 genes involved in carbon and butanoate metabolism for both *C. difficile* WT and *LuxS*, these genes (*accB, abfH, abfT, abfD, sucD* and *cat1*) are all involved in the utilisation of succinate as a carbon source. As *B. fragilis* is known to produce succinate (Macy *et al.*, 1978), it is likely that the upregulation in these pathways results from the increased levels of succinate in the culture medium. However, since gut microbiota-produced succinate promotes *C. difficile* growth *in vivo* (Ferreyra *et al.*, 2014), it is unlikely that these changes are directly responsible for the observed inhibition of *C. difficile*. However, bacteria utilise carbohydrates in a sequential manner (Bruckner and Titgemeyer, 2002). Consistent with this, we

observed a down regulation of genes important for the utilisation of pyruvate such as *bcd2* and *idhA* encoding for butyryl-CoA dehydrogenase and (r)-2-hydroxyisocaproate dehydrogenase respectively. Such a shift in metabolism could allow *B. fragilis* to fully consume other metabolites, and thus enabling it to outcompete *C. difficile*.

Interestingly, the ability of *C. difficile* to utilise trehalose as a carbon source through the expression of the trehalose operon, has been shown to provide a growth advantage to *C. difficile* against other bacteria (Collins *et al.*, 2018a). As such, the *LuxS* upregulation of a phosphotransferase system component and *treA* (both in the trehalose operon), likely enables increased utilisation of trehalose, providing an additional carbon source. Like glucose, trehalose acts as an osmoprotectant (Tanghe *et al.*, 2003). As such its presence within the cell likely helps to maintain the conformation of proteins during cellular dehydration (Pareek *et al.*, 2010). Therefore its increased utilisation could negatively impact biofilm formation (as seen in chapter 3). Although exogenous trehalose levels similar to those used by Collins *et al.* (2018) had an inhibitory effect on biofilm formation of both WT and *LuxS*, this trehalose induced inhibition appears to be concentration dependent. Therefore it is possible that the ideal concentration of trehalose would have a differential effect on *LuxS* and WT. It would also be useful to assess the impact of trehalose on the CFU of WT and *LuxS.*

Fatty acids are an essential component of bacterial cell membranes (Fujita *et al.*, 2007) and thus important for bacterial growth. During co-culture we observed upregulation of 5 genes responsible for fatty acid synthesis (*plsX*,

fabH, *fabK, accB and accC*) in *C. difficile* WT. In *Bacillus subtilis* the upregulation of fatty acid synthesis genes have been associated with the response to environmental stresses due to the changes offered to membrane fluidity and diffusion rate (Ter Beek *et al.*, 2008). The upregulation of these genes in *C. difficile* could be indicative of a response to a *B. fragilis* produced inhibitory molecule.

Interestingly, *C. difficile* LuxS demonstrates a down regulation of genes involved in the salvage of thiamine *thiD*, *thiK* and *thiE1* (Melnick *et al.*, 2004). As the active form of thiamine, thiamin diphosphate (ThDP), is indispensable for the carbohydrate and branched-chain amino acid metabolic enzymes (Melnick *et al.*, 2004), a defect in its production could prove fatal to the bacteria concerned. However, as *C. difficile LuxS* survives better than the WT during co-culture conditions, further work would be necessary to assess the role of thiamine during *C. difficile* co-cultures.

Since many bacteria require branched-chain amino acids (isoleucine, leucine and, valine) for protein synthesis, branched-chain fatty acid synthesis, and environmental adaptation (Kaiser *et al.*, 2018). The observed upregulation of genes involved in valine, leucine and isoleucine biosynthesis during co-culture with *C. difficile* is likely due to changes in the abundance of these amino acids in the growth medium.

Iron is essential for virtually all organisms and bacterial elaborate a number of mechanisms to sequester iron. It is interesting to note that a number of copies of the ferric citrate transport system regulator, *fecR,* are found to be

up-regulated in *B. fragilis* during both culture conditions. The ferric citrate transport system is an iron uptake system that responds to the presence of citrate (Wagegg and Braun, 1981, Staudenmaier *et al.*, 1989, Andrews *et al.*, 2003). Interestingly, analysis of the *C. difficile* genome using BLAST (NCBI) found that *C. difficile* does not possess this iron uptake system. Additionally there is some evidence of ferric citrate being an iron source in the gut (Andrews *et al.*, 2003). Hence *B. fragilis* may have a possible advantage in sequestering iron, and outcompeting *C. difficile* and preventing it from colonising the gut

Finally, with a large number of hypothetical genes being differentially expressed in *B. fragilis*, homology analysis would need to be performed in order to rule out the possibility of these genes producing an inhibitory molecule.

Chapter 6 Discussion

Recurrent infections caused by many pathogens, have been associated with the ability to form biofilms (Romling and Balsalobre, 2012). Biofilms offer the bacteria within increased resistance to a range of environmental stresses, including, antibiotic and oxygen stress and protection from phagocytosis (Davey and O'Toole G, 2000, Hall-Stoodley and Stoodley, 2009). In recent years it has become clear that the causative agent of CDI, *C. difficile*, is not only capable of forming biofilms *in vitro* (Dawson *et al.*, 2012, Đapa *et al.*, 2013, Crowther *et al.*, 2014, Walter *et al.*, 2015, Pantaleon *et al.*, 2015, Maldarelli *et al.*, 2016) but that some clinical relevant strains, are also capable of forming biofilm like structures *in vivo* (Soavelomandroso *et al.*, 2017). With 20-36% of instances of CDI resulting in recurrent infections (Barbut *et al.*, 2000, Rupnik *et al.*, 2009, Smits *et al.*, 2016) the mechanisms responsible need to be understood.

Quorum sensing is thought to regulate biofilm formation, development and dispersal of many bacterial species by enabling the bacteria to coordinate gene expression (Zhu and Mekalanos, 2003, Hammer and Bassler, 2003, Sakuragi and Kolter, 2007, Hardie and Heurlier, 2008, De Araujo *et al.*, 2010, Li and Tian, 2012, Solano *et al.*, 2014). The LuxS/AI-2 QS system has been of particular interest to researchers (Hardie and Heurlier, 2008). LuxS, an enzyme in the activated methyl cycle, is responsible for the production of the potent, cross-species QS signalling molecule, AI-2 (Bassler *et al.*, 1997, Schauder *et al.*, 2001, Federle and Bassler, 2003). Given the role for LuxS during the biofilm formation, development or dispersal of many species

(Chen *et al.*, 2002, Yoshida *et al.*, 2005, De Keersmaecker *et al.*, 2005, Auger *et al.*, 2006, Rickard *et al.*, 2006, Gonzalez Barrios *et al.*, 2006, Shao *et al.*, 2007, Sztajer *et al.*, 2008, Huang *et al.*, 2009, Ahmed *et al.*, 2009, De Araujo *et al.*, 2010, Cao *et al.*, 2011, Karim *et al.*, 2013, Li *et al.*, 2015), it has been proposed that AI-2 is the "universal language" of bacteria (Federle and Bassler, 2003, Hardie and Heurlier, 2008). However, with many species lacking the two characterised AI-2 receptors, others have hypothesised that the metabolic function of LuxS is responsible for the observed phenotypes in many of these species (Rezzonico and Duffy, 2008, Wilson *et al.*, 2012).

The role for LuxS in *C. difficile* has remained clouded, with conflicting studies for its role in toxin production (Carter *et al.*, 2005, Lee and Song, 2005). More recently it has been demonstrated that a *C. difficile luxS* mutant (*LuxS*) exhibits a severe defect during biofilm formation (Đapa *et al.*, 2013). This study aimed to utilise a number of molecular biology techniques in order to characterise the role of LuxS during *in vitro* biofilm formation. With the implicated cross-species signalling role for LuxS/AI-2 (Federle and Bassler, 2003), coupled with the ability for other members of the gut microbiota (including Bacteroidies) to provide colonisation resistance to *C. difficile* (Lawley *et al.*, 2012), we also sought to investigate how *luxS* influences the interactions between *C. difficile* and a gut commensal and pathogen, *B. fragilis*.

During *C. difficile* mono-culture, we observed a defect in biofilm formation at both 24 and 72 hrs which was consistent with the findings of Dapa *et al.* (2013). Similarly to Carter *et al.* (2005), the addition of MHF, a chemical form

of AI-2, had no effect on *LuxS*. However, through the exogenous addition of DPD, the precursor to AI-2, we were able to partially restore the biofilm formation of *LuxS* in a dose-dependent manner. These results suggest a role of LuxS/AI-2 QS in *C. difficile* biofilm formation.

Utilising RNA-sequencing, we identified two prophage regions down-regulated during the early stages of biofilm formation (18 hrs). In other bacteria, prophage have been associated with both the development of *Pseudomonas aeruginosa* biofilms and dispersal of *Enterococcus faecalis* (Secor, 2016, Rossmann *et al.*, 2015). Furthermore, the phage mediated biofilm dispersal of *E. faecalis* is regulated by AI-2 (Rossmann *et al.*, 2015). Through PCR analysis we were able to confirm the presence of these prophage within *C. difficile* biofilms. Since the expression of prophage results in the lysis of the host cell (Young, 1992), coupled with the observation by Đapa *et al.* (2013) that e-DNA is a key component of *C. difficile* biofilm, we hypothesise *C. difficile* is utilising prophage induction for the purpose of releasing the cell contents and e-DNA from a subset of the bacterial population. With the ability for clinically relevant *C. difficile* strains to produce biofilm-like structures *in vivo* (Soavelomandroso *et al.*, 2017) combined with the increased antibiotic resistance biofilms offer *C. difficile in vitro* (Đapa *et al.*, 2013), we believe that this mode of growth could offer a reservoir for recurrent infections.

Since microbial dysbiosis in the gut is the major risk factor for developing CDI, the replenishment of "normal" members of the gut microbiota by means of faecal microbiota transplantation has proved to be an effective treatment

for the most severe cases of CDI (Smits *et al*., 2016). However, due to the complex nature of the gut microbiota, the mechanisms responsible for colonisation resistance are poorly understood. With a number of sequencing studies indicating the ability for members of the *Bacteroidetes* to resist *C. difficile* colonisation (Seekatz and Young, 2014) and evidence that selected strains of *B. fragilis* have the ability to produce AI-2 (Antunes *et al*., 2005). Coupled with the evidence that *C. difficile* is capable of forming mixed species communities in mice (Semenyuk *et al*., 2015), we sought to investigate how *C. difficile luxS* influences interaction with *B. fragilis* during biofilm formation.

First we studied the interactions of WT *C. difficile* and *B. fragilis* when co-cultured in biofilms. Interestingly we found that *B. fragilis* had an inhibitory effect on *C. difficile* during biofilm growth (as measured by CFU) that was not observed during planktonic co-culture conditions. Furthermore cell free supernatants of *B. fragilis* failed to inhibit *C. difficile* growth. A very recent study demonstrated that production of the enzyme: bile salt hydrolase, is responsible for the inhibitory effect of *B. ovatus* on *C. difficile* (Yoon *et al*., 2017). They reported that in the presence of bile acids, cell free supernatants for *B. ovatus* were capable of inhibiting the growth of *C. difficile* whereas, in the absence of bile acids *C. difficile* growth was promoted (Yoon *et al.* 2017). Since bile acids are not supplemented into our media, a different mechanism is likely responsible for *B. fragilis* mediated inhibition of *C. difficile*.

In comparison, we found that whilst *LuxS* was inhibited during co-culture with *B. fragilis*, the levels of inhibition were far greater for WT. Although we

cannot rule out the possibility of an inhibitory molecule being produced by *B. fragilis* upon detection of *C. difficile*, the dual species RNA-seq data hints at involvement of metabolic pathways or nutritional inhibition in the inhibition of *C. difficile*.

The incorporation of iron into proteins is key for survival of all organisms. It is therefore interesting to note a clear upregulation of multiple copies of the ferric citrate transport system in *B. fragilis*, during co-culture with *C. difficile*. Ferric citrate is actively transported across the outer membrane by FecA, and across the inner membrane by FecBCDE proteins (Wagegg and Braun, 1981, Pressler *et al.*, 1988, Staudenmaier *et al.*, 1989). As *C. difficile* does not possess the ferric citrate transport system, we suspect that *B. fragilis* is better adapted at sequestering iron. With the presence of ferric citrate in the gut (Kortman *et al.*, 2014), iron starvation could play an important role in colonisation resistance.

The differences in *B. fragilis* mediated inhibition of *C. difficile* between WT and *LuxS* could also be attributed to the observed upregulation in *LuxS,* of two genes on the trehalose operon (a PTS system component and TreA). Although the effect on CFU and an increased range of Trehalose concentrations would need to be further investigated. Recent studies have suggested that upregulation of these genes afford the bacteria a fitness advantage *in vivo* (Robinson *et al.*, 2014, Collins *et al.*, 2018a). Additional, with the role of trehalose as an osmoprotectant, the increased utilisation in *LuxS* could be having a negative effect on the biofilm formation of this strain.

In conclusion, we demonstrated strong evidence to suggest a signalling role for LuxS/AI-2 in *C. difficile* that likely induces the release of prophage. We speculate that this in turn increases lyses a subset of the bacterial population, releasing eDNA and increasing the levels of biofilm formation. Additionally we demonstrated the ability for *B. fragilis* to inhibit *C. difficile* during the biofilm mode of growth. Co-culture RNA-seq analysis has demonstrated a possible metabolic effect causing the observed inhibition. However, with the large number of hypothetical genes differentially expressed in *B. fragilis*, the possibility of the synthesis of an inhibitory molecule cannot be ruled out.

Future work

This work has given insight into the role of prophage during *in vitro C. difficile* biofilm formation. Several key steps forward would include the quantification of biofilm eDNA to confirm that the observed differential regulation of prophage genes between WT and *LuxS,* results in changes to the level of eDNA. As *C. difficile* has been shown to produce biofilm like structures *in vivo* (Semenyuk *et al.*, 2015, Soavelomandroso *et al.*, 2017). It would also be important to determine whether LuxS affects adherence to tissue culture cells with an aim of characterising its effect *in vivo*. The final step for this work would also be to establish the role of this enzyme in virulence.

For the observed *B. fragilis* mediated inhibition of *C. difficile,* further analysis is required to fully characterise the mechanisms responsible. With inhibition only observed during biofilm growth, metabolomics studies including proteomic and RNA-seq analysis could be used to track metabolic changes at multiple timepoints, rather than the "snapshot" approach used. Additionally it would be useful to expand these studies to other members of the *Bacteroidetes* to identify whether the mechanism utilised by *B. fragilis* to inhibit *C. difficile* is species specific, or whether this is conserved amongst other species.

As the key risk factor for the development of CDI is disruption to the gut microbiota, it would be interesting to further these studies with a number of species representative of both a healthy and diseased gut. Such studies in a physiologically relevant model, such as the vertical diffusion chamber model

developed in our laboratory, could help to shed light on the complex inter-microbial interactions that are responsible for the colonisation resistance of the healthy microbiota.

As a number of differentially expressed genes in *B. fragilis*, are annotated as hypothetical proteins with unknown function. Further analysis is needed to assess their impact during co-culture. Such work could yield the production of an inhibitory molecule against *C. difficile*.

Finally, given the consistent up-regulation of the trehalose operon in *LuxS.* It would be interesting to fully assess its role during co-culture. This could be done by testing a wider range of concentrations and assessing its impact on the CFU of both WT and *LuxS*.

Appendix

Table S1: All Genes up- and down-regulated in ***B. fragilis***, in C. difficile ***WT***-*Bacteroides fragilis* co-cultures relative to *B. fragilis* mono-culture.

Gene identifier	log2FoldChange	Product
bf_rs_03152	1.31151618	RNA polymerase sigma factor
bf_rs_01567	1.30582995	N-acetylmuramoyl-L-alanine amidase
bf_rs_02264	1.29689246	tRNA-Arg(ccg)
bf_rs_01254	1.28747467	Phytochrome-like protein cph1
bf_rs_01030	1.27386249	L-fucose-proton symporter
bf_rs_01257	1.19297587	SusD family protein
bf_rs_01509	1.12575629	putative N-acetyltransferase YvbK
bf_rs_01907	1.04601422	hypothetical protein
bf_rs_02466	0.9293162	hypothetical protein
bf_rs_00894	0.91851713	7-cyano-7-deazaguanine synthase
bf_rs_02556	0.895506	3-deoxy-D-manno-octulosonic acid transferase
bf_rs_00770	0.89420097	hypothetical protein
bf_rs_01245	0.89229059	Putative multidrug export ATP-binding/permease protein
bf_rs_01085	0.88099287	hypothetical protein
bf_rs_00895	0.88060769	NADPH-dependent 7-cyano-7-deazaguanine reductase
bf_rs_01448	0.87638903	Nicotinamide-nucleotide amidohydrolase PncC
bf_rs_01836	0.86280653	hypothetical protein
bf_rs_01057	0.84528417	50S ribosomal protein L35
bf_rs_00537	0.84467834	Peptide-N-glycosidase F%2C N terminal
bf_rs_01075	0.84349289	Abhydrolase family protein
bf_rs_00189	0.83978061	Phospho-N-acetylmuramoyl-pentapeptide-transferase
bf_rs_03080	0.82931744	hypothetical protein
bf_rs_00834	0.82583297	Beta-1%2C4-mannooligosaccharide phosphorylase
bf_rs_02026	0.81132105	lipid-A-disaccharide synthase
bf_rs_01653	0.81109879	hypothetical protein
bf_rs_02254	0.81081041	Aspartate/alanine antiporter
bf_rs_02339	0.80775334	Arylsulfatase
bf_rs_03030	0.80268521	DNA-invertase hin
bf_rs_01201	0.80162109	D-3-phosphoglycerate dehydrogenase
bf_rs_01736	-0.8274754	Putative zinc ribbon domain protein
bf_rs_01302	-0.8357887	hypothetical protein

bf_rs_01112	-0.8588795	GDP-mannose 4%2C6-dehydratase
bf_rs_01884	-0.8601448	Tyrocidine synthase 1
bf_rs_02192	-0.8621834	hypothetical protein
bf_rs_01418	-0.8666213	Helix-turn-helix
bf_rs_01339	-0.8842581	Putative SOS response-associated peptidase YedK
bf_rs_02268	-0.8963737	tRNA 2'-O-methylase
bf_rs_02955	-0.9231776	Carboxymuconolactone decarboxylase family protein
bf_rs_01351	-0.9304549	Succinyl-CoA ligase [ADP-forming] subunit beta
bf_rs_01007	-0.955022	Flavodoxin
bf_rs_01605	-0.979336	Hexokinase
bf_rs_00279	-0.9864582	hypothetical protein
bf_rs_01321	-0.9875694	putative deferrochelatase/peroxidase YfeX
bf_rs_02874	-0.9876972	hypothetical protein
bf_rs_01816	-0.9932022	Alpha-amylase precursor
bf_rs_00505	-0.9941066	Putative pyridoxal phosphate-dependent aminotransferase EpsN
bf_rs_02297	-1.0072175	hypothetical protein
bf_rs_01005	-1.0122806	Dihydrolipoyllysine-residue acetyltransferase component of pyruvate dehydrogenase complex
bf_rs_00888	-1.0513925	Chagasin family peptidase inhibitor I42
bf_rs_00419	-1.0721486	Multidrug resistance protein MdtA precursor
bf_rs_01154	-1.0728616	ECF RNA polymerase sigma factor SigH
bf_rs_01264	-1.0747784	Hydroxylamine reductase
bf_rs_00886	-1.0769047	Quercetin 2%2C3-dioxygenase
bf_rs_01818	-1.090627	hypothetical protein
bf_rs_00666	-1.1138356	hypothetical protein
bf_rs_01014	-1.1191019	hypothetical protein
bf_rs_00957	-1.1298746	hypothetical protein
bf_rs_02248	-1.151859	hypothetical protein
bf_rs_00131	-1.1907486	Nitroreductase family protein
bf_rs_03151	-1.1943367	hypothetical protein
bf_rs_00525	-1.1966945	hypothetical protein
bf_rs_02975	-1.2255261	hypothetical protein
bf_rs_01315	-1.2888614	Fimbrillin-A associated anchor proteins Mfa1 and Mfa2
bf_rs_02081	-1.3625527	hypothetical protein
bf_rs_01958	-1.3710842	hypothetical protein
bf_rs_03077	-1.377462	hypothetical protein
bf_rs_03003	-1.4034069	hypothetical protein

bf_rs_03155	9.28794563	Virus attachment protein p12 family protein
bf_rs_03086	7.6349471	Desulfoferrodoxin
bf_rs_03072	6.03325998	Rubrerythrin
bf_rs_03166	4.65976216	hypothetical protein
bf_rs_00677	2.93004973	hypothetical protein
bf_rs_00222	2.65299814	hypothetical protein
bf_rs_00221	2.26641901	DNA-binding transcriptional repressor MngR
bf_rs_01618	2.23195774	hypothetical protein
bf_rs_00148	1.93281884	L-fucose isomerase
bf_rs_02052	1.75950799	NADP-dependent 7-alpha-hydroxysteroid dehydrogenase
bf_rs_01338	1.72164992	tRNA-Arg(tct)
bf_rs_00791	1.69832127	Alkyl hydroperoxide reductase subunit F
bf_rs_02029	1.62338926	2-isopropylmalate synthase
bf_rs_00043	1.58578594	tRNA-Gln(ttg)
bf_rs_01305	1.56940593	Sensor histidine kinase RcsC
bf_rs_01029	1.56776049	Galactokinase
bf_rs_02411	1.54670918	Carbamoyl-phosphate synthase large chain
bf_rs_02599	1.51925504	fec operon regulator FecR
bf_rs_01253	1.49567239	UDP-glucose 4-epimerase
bf_rs_02030	1.49141904	3-isopropylmalate dehydratase small subunit
bf_rs_01061	1.46275613	indolepyruvate oxidoreductase subunit beta
bf_rs_02028	1.45284187	3-isopropylmalate dehydrogenase
bf_rs_02940	1.43121061	fec operon regulator FecR
bf_rs_02241	1.41266608	fec operon regulator FecR
bf_rs_02743	1.41160764	RNA polymerase sigma factor SigV
bf_rs_00674	1.38757997	fec operon regulator FecR
bf_rs_01987	1.37235468	hypothetical protein
bf_rs_01783	1.35532527	hypothetical protein
bf_rs_01568	1.31229239	integration host factor subunit alpha
bf_rs_01699	1.30423791	hypothetical protein
bf_rs_02031	1.295602	3-isopropylmalate dehydratase large subunit
bf_rs_02841	1.28810105	hypothetical protein
bf_rs_02675	1.24759394	Autoinducer 2 sensor kinase/phosphatase LuxQ
bf_rs_00577	1.2413622	HTH-type transcriptional activator Btr
bf_rs_01202	1.23666221	hypothetical protein
bf_rs_01668	1.22879006	ACT domain protein
bf_rs_03031	1.21730538	hypothetical protein
bf_rs_02926	1.21276045	hypothetical protein

bf_rs_01426	1.19936263	Chaperone protein HtpG
bf_rs_00627	1.18162145	Glycosyl hydrolase family 57
bf_rs_03008	1.17199863	mRNA interferase YafQ
bf_rs_02150	1.15409411	hypothetical protein
bf_rs_00864	1.14407471	hypothetical protein
bf_rs_00365	1.13961018	fec operon regulator FecR
bf_rs_02832	1.13922453	23S ribosomal RNA
bf_rs_01838	1.13912045	hypothetical protein
bf_rs_00811	1.13837215	Outer membrane protein 41 precursor
bf_rs_03132	1.13002777	hypothetical protein
bf_rs_01239	1.10929565	Leucine Rich repeats (2 copies)
bf_rs_03037	1.10816435	hypothetical protein
bf_rs_02408	1.10660339	Fimbrillin-A associated anchor proteins Mfa1 and Mfa2
bf_rs_02230	1.09961947	Acetolactate synthase isozyme 2 large subunit
bf_rs_02399	1.08407984	hypothetical protein
bf_rs_01086	1.08407605	hypothetical protein
bf_rs_02433	1.07391745	Transcriptional regulatory protein DegU
bf_rs_03138	1.07014526	hypothetical protein
bf_rs_01784	1.06893257	hypothetical protein
bf_rs_01566	1.06865561	transcriptional repressor DicA
bf_rs_02590	1.06407662	site-specific tyrosine recombinase XerC
bf_rs_00865	1.06398909	tRNA-Cys(gca)
bf_rs_01565	1.04563885	hypothetical protein
bf_rs_01379	1.03485885	tRNA-Lys(ctt)
bf_rs_02389	1.02328388	30S ribosomal protein S2
bf_rs_01277	1.02164857	Undecaprenol kinase
bf_rs_00371	1.02120257	tRNA-Met(cat)
bf_rs_02946	1.01803948	Tyrosine recombinase XerC
bf_rs_01794	0.9987764	Inner membrane protein YhaI
bf_rs_02390	0.99872926	30S ribosomal protein S9
bf_rs_02252	0.99613625	Methylmalonyl-CoA mutase large subunit
bf_rs_00843	0.98987401	Alpha-xylosidase
bf_rs_00756	0.98619346	50S ribosomal protein L25
bf_rs_03100	0.9843561	hypothetical protein
bf_rs_00150	0.97580954	Lactaldehyde reductase
bf_rs_01445	0.96350482	hypothetical protein
bf_rs_00793	0.95952031	Alkyl hydroperoxide reductase subunit C
bf_rs_01284	0.93733378	hypothetical protein

bf_rs_00846	0.93382112	hypothetical protein
bf_rs_03009	0.93278166	hypothetical protein
bf_rs_00863	0.92145531	Ferrous iron transport protein B
bf_rs_02388	0.91253771	Elongation factor Ts
bf_rs_03154	0.90735125	tRNA-Leu(taa)
bf_rs_01704	0.90636011	Oxygen regulatory protein NreC
bf_rs_03094	0.90350551	hypothetical protein
bf_rs_00831	0.90337948	fec operon regulator FecR
bf_rs_01062	0.90075564	2-oxoacid ferredoxin oxidoreductase
bf_rs_03176	0.89918261	tRNA-Cys(gca)
bf_rs_01586	0.89872304	Enamine/imine deaminase
bf_rs_02895	0.89735416	hypothetical protein
bf_rs_02533	0.89694346	30S ribosomal protein S7
bf_rs_02973	0.88439951	hypothetical protein
bf_rs_01705	0.88331711	hypothetical protein
bf_rs_01329	0.8832437	7%2C8-dihydro-6-hydroxymethylpterin-pyrophosphokinase (HPPK)
bf_rs_00113	0.8811749	Transcriptional regulatory protein CssR
bf_rs_01126	0.87811703	hypothetical protein
bf_rs_02779	0.87476747	tRNA-Ser(tga)
bf_rs_01283	0.85878664	ATP synthase epsilon chain
bf_rs_01904	0.84923802	putative multidrug resistance protein EmrK
bf_rs_00893	0.84761778	hypothetical protein
bf_rs_00753	0.84507226	hypothetical protein
bf_rs_01440	0.83817494	LysM domain/BON superfamily protein
bf_rs_02364	0.83783458	Outer membrane protein TolC precursor
bf_rs_01900	0.83597516	Glutaconyl-CoA decarboxylase subunit beta
bf_rs_02145	0.82745043	multifunctional tRNA nucleotidyl transferase/2'3'-cyclic phosphodiesterase/2'nucleotidase/phosphatase
bf_rs_02960	0.82700303	Initiator Replication protein
bf_rs_00591	0.82217009	tRNA-Tyr(gta)
bf_rs_02781	0.81197346	Type-1 restriction enzyme R protein
bf_rs_02908	0.81175107	putative type I restriction enzymeP M protein
bf_rs_00021	0.80858197	hypothetical protein
bf_rs_02534	0.80579627	30S ribosomal protein S12
bf_rs_02532	0.80016137	Elongation factor G
bf_rs_02086	-0.8081468	Membrane-bound lytic murein transglycosylase D precursor
bf_rs_02659	-0.8224957	Rhomboid family protein

bf_rs_00696	-0.8475926	4-hydroxythreonine-4-phosphate dehydrogenase
bf_rs_01143	-0.8547906	Glycerate dehydrogenase
bf_rs_01631	-0.8768321	hypothetical protein
bf_rs_01737	-0.8771644	hypothetical protein
bf_rs_02111	-0.8832072	Pyridoxine kinase
bf_rs_00381	-0.8951966	Pesticin receptor precursor
bf_rs_01629	-0.9149566	hypothetical protein
bf_rs_01477	-0.9190529	Sirohydrochlorin cobaltochelatase
bf_rs_02293	-0.9222049	Alkaline phosphatase synthesis sensor protein PhoR
bf_rs_01006	-0.9272701	2-oxoisovalerate dehydrogenase subunit beta
bf_rs_00094	-0.9354762	putative oxidoreductase UxuB
bf_rs_00655	-0.9413947	hypothetical protein
bf_rs_01240	-0.9417596	hypothetical protein
bf_rs_02707	-0.9484609	FKBP-type 22 kDa peptidyl-prolyl cis-trans isomerase
bf_rs_01610	-0.9545397	Superoxide dismutase [Mn/Fe]
bf_rs_02976	-0.9691988	hypothetical protein
bf_rs_00859	-0.9742635	hypothetical protein
bf_rs_02536	-0.9883208	hypothetical protein
bf_rs_01771	-0.9915956	ECF RNA polymerase sigma factor SigG
bf_rs_01273	-0.993827	Dihydroorotate dehydrogenase (quinone)
bf_rs_01465	-1.0026354	Outer membrane efflux protein
bf_rs_01800	-1.0056264	Quercetin 2%2C3-dioxygenase
bf_rs_01153	-1.0121551	LemA family protein
bf_rs_00804	-1.030075	5-amino-6-(5-phosphoribosylamino)uracil reductase
bf_rs_02914	-1.0365247	hypothetical protein
bf_rs_01094	-1.0393486	site-specific tyrosine recombinase XerD
bf_rs_00858	-1.0467807	VIT family protein
bf_rs_01920	-1.0537024	Toluene efflux pump periplasmic linker protein TtgD precursor
bf_rs_00656	-1.0622069	Thioredoxin reductase
bf_rs_00273	-1.0721348	Glutaminase 1
bf_rs_02058	-1.0737126	2-oxoglutarate carboxylase small subunit
bf_rs_02803	-1.0996581	NADP-dependent alcohol dehydrogenase C 2
bf_rs_01486	-1.1164628	Multidrug export protein EmrB
bf_rs_00695	-1.1196561	hypothetical protein
bf_rs_00878	-1.1219033	Sodium-dependent dicarboxylate transporter SdcS
bf_rs_02120	-1.1290797	hypothetical protein
bf_rs_01709	-1.1314864	Thioredoxin-1
bf_rs_03013	-1.13866	Iron-binding zinc finger CDGSH type

bf_rs_00996	-1.1438901	metal-dependent hydrolase
bf_rs_00797	-1.1473893	hypothetical protein
bf_rs_01168	-1.1700034	Outer membrane porin F precursor
bf_rs_02276	-1.1734706	Ribonucleoside-diphosphate reductase NrdZ
bf_rs_00311	-1.1769065	Chaperone protein Skp precursor
bf_rs_02308	-1.1872936	Glutathione peroxidase homolog BsaA
bf_rs_00779	-1.187941	H(+)/Cl(-) exchange transporter ClcA
bf_rs_01503	-1.1915586	Ribonucleoside-diphosphate reductase subunit beta
bf_rs_00721	-1.1956832	hypothetical protein
bf_rs_00418	-1.2101859	Efflux pump membrane transporter BepE
bf_rs_01487	-1.2124012	putative multidrug resistance protein EmrK
bf_rs_00557	-1.2310067	Alpha/beta hydrolase family protein
bf_rs_02334	-1.2444157	P-protein
bf_rs_00796	-1.2459206	hypothetical protein
bf_rs_02082	-1.2529842	hypothetical protein
bf_rs_02077	-1.2532428	Beta-lactamase type II precursor
bf_rs_00254	-1.2612446	hypothetical protein
bf_rs_02722	-1.2625819	hypothetical protein
bf_rs_00417	-1.271637	Outer membrane protein TolC precursor
bf_rs_00844	-1.2830586	lipoprotein involved with copper homeostasis and adhesion
bf_rs_00667	-1.2847118	hypothetical protein
bf_rs_02045	-1.2950846	Cupin domain protein
bf_rs_01396	-1.2964615	hypothetical protein
bf_rs_02050	-1.2975506	hypothetical protein
bf_rs_02095	-1.303823	Peptide methionine sulfoxide reductase MsrA/MsrB
bf_rs_02059	-1.3089473	Methylmalonyl-CoA carboxyltransferase 1.3S subunit
bf_rs_02034	-1.3091907	bacterioferritin
bf_rs_02166	-1.314465	Anaerobic ribonucleoside-triphosphate reductase
bf_rs_00198	-1.3231242	ECF RNA polymerase sigma factor SigH
bf_rs_00556	-1.3269467	LemA family protein
bf_rs_01960	-1.3378983	Oxygen-insensitive NAD(P)H nitroreductase
bf_rs_00253	-1.3431219	Cytochrome c-type protein NrfH
bf_rs_02567	-1.3476378	Anaerobic C4-dicarboxylate transporter DcuA
bf_rs_02993	-1.3515175	LexA repressor
bf_rs_00619	-1.3574769	RNA polymerase sigma factor SigM
bf_rs_00356	-1.3640885	hypothetical protein
bf_rs_01397	-1.3712617	hypothetical protein
bf_rs_01989	-1.3715409	Pyruvate dehydrogenase [ubiquinone]

bf_rs_00272	-1.3728099	Glutamate decarboxylase
bf_rs_01395	-1.3775276	hypothetical protein
bf_rs_00238	-1.3800271	hypothetical protein
bf_rs_02219	-1.3809837	4-hydroxy-3-methylbut-2-enyl diphosphate reductase
bf_rs_01684	-1.3927229	Diaminopimelate epimerase
bf_rs_01325	-1.3940762	hypothetical protein
bf_rs_01562	-1.3966586	acid-resistance membrane protein
bf_rs_00355	-1.4124654	hypothetical protein
bf_rs_01357	-1.4179478	putative peroxiredoxin
bf_rs_00930	-1.4186478	Bifunctional aspartate aminotransferase and L-aspartate beta-decarboxylase
bf_rs_00233	-1.4294595	hypothetical protein
bf_rs_00989	-1.4295437	DUF based on B. Theta Gene description
bf_rs_00331	-1.4317878	hypothetical protein
bf_rs_01957	-1.4418027	putative oxidoreductase/MSMEI_2347
bf_rs_00990	-1.4525212	hypothetical protein
bf_rs_00956	-1.4549231	hypothetical protein
bf_rs_02113	-1.4572691	Lactate utilization protein B
bf_rs_02538	-1.4592502	hypothetical protein
bf_rs_00665	-1.460306	ECF RNA polymerase sigma factor SigW
bf_rs_02537	-1.4639961	hypothetical protein
bf_rs_00980	-1.4769224	putative inner membrane protein
bf_rs_00133	-1.4941466	hypothetical protein
bf_rs_01690	-1.5060874	Guanosine-5'-triphosphate%2C3'-diphosphate pyrophosphatase
bf_rs_00332	-1.5129506	Malate dehydrogenase
bf_rs_01266	-1.5325706	Transcriptional activator protein Anr
bf_rs_01167	-1.5501012	Collagen triple helix repeat (20 copies)
bf_rs_02083	-1.5580982	Phosphotransferase RcsD
bf_rs_00452	-1.5665639	hypothetical protein
bf_rs_02114	-1.5826976	Lactate utilization protein A
bf_rs_01711	-1.6312913	5-methyltetrahydropteroyltriglutamate--homocysteine methyltransferase
bf_rs_00234	-1.638754	hypothetical protein
bf_rs_02080	-1.6469501	hypothetical protein
bf_rs_02568	-1.655064	L-asparaginase 2 precursor
bf_rs_02470	-1.6590086	PBP superfamily domain protein
bf_rs_02051	-1.6643223	hypothetical protein

bf_rs_00931	-1.6680404	Aspartate/alanine antiporter
bf_rs_01414	-1.6840453	Efflux pump membrane transporter BepE
bf_rs_00235	-1.6996337	Periplasmic beta-glucosidase precursor
bf_rs_00236	-1.700038	SusD family protein
bf_rs_02197	-1.7017285	Outer membrane efflux protein
bf_rs_00958	-1.7175992	hypothetical protein
bf_rs_01544	-1.7186707	hypothetical protein
bf_rs_01757	-1.7208456	hypothetical protein
bf_rs_01295	-1.7226524	inner membrane protein
bf_rs_00960	-1.7394796	hypothetical protein
bf_rs_00854	-1.7404828	hypothetical protein
bf_rs_02414	-1.7415846	Outer membrane protein 40 precursor
bf_rs_01543	-1.7540328	hypothetical protein
bf_rs_02930	-1.7691478	fermentation/respiration switch protein
bf_rs_02569	-1.790518	hypothetical protein
bf_rs_00329	-1.8197717	Glutamate/gamma-aminobutyrate antiporter
bf_rs_02075	-1.8377218	hypothetical protein
bf_rs_00330	-1.8482564	hypothetical protein
bf_rs_00999	-1.8611781	hypothetical protein
bf_rs_02905	-1.8651553	ISXO2-like transposase domain protein
bf_rs_02802	-1.8757986	Putative NAD(P)H-dependent FMN-containing oxidoreductase YwqN
bf_rs_02244	-1.8863317	Choloylglycine hydrolase
bf_rs_00998	-1.8961329	hypothetical protein
bf_rs_00237	-1.9472779	TonB-dependent Receptor Plug Domain protein
bf_rs_01412	-1.9590933	Outer membrane protein OprM precursor
bf_rs_02906	-2.0236036	hypothetical protein
bf_rs_02469	-2.0237868	tetratricopeptide repeat protein
bf_rs_00891	-2.0238123	Porin subfamily protein
bf_rs_01274	-2.0261186	Acetylxylan esterase precursor
bf_rs_01000	-2.0540976	hypothetical protein
bf_rs_01307	-2.0886013	hypothetical protein
bf_rs_00199	-2.1109472	hypothetical protein
bf_rs_00200	-2.121964	putative TonB-dependent receptor precursor
bf_rs_01092	-2.1261581	hypothetical protein
bf_rs_00961	-2.1752793	hypothetical protein
bf_rs_00908	-2.2150308	Histidine decarboxylase proenzyme precursor
bf_rs_02474	-2.2428322	colicin uptake protein TolQ

bf_rs_02471	-2.2770435	Gram-negative bacterial tonB protein
bf_rs_01363	-2.2862609	Inner membrane protein YhiM
bf_rs_01413	-2.3699461	Efflux pump periplasmic linker BepF
bf_rs_01090	-2.4543795	ECF RNA polymerase sigma factor SigW
bf_rs_01091	-2.4580421	hypothetical protein
bf_rs_02472	-2.7595166	Biopolymer transport protein ExbD/TolR
bf_rs_02473	-2.8077479	Biopolymer transport protein ExbD/TolR
bf_rs_00201	-2.9879808	hypothetical protein

Table S2: All Genes up- and down-regulated in ***B. fragilis***, in C. difficile *LuxS-Bacteroides fragilis* co-cultures relative to *B. fragilis* mono-culture.

Gene identifier	log2FoldChange	Product
bf_rs_03116	1.50249038	hypothetical protein
bf_rs_00412	1.48934005	Tyrosine recombinase XerD
bf_rs_02127	1.29548052	fec operon regulator FecR
bf_rs_02593	1.2806558	tRNA-Leu(caa)
bf_rs_01792	1.2353753	Reverse rubrerythrin-1
bf_rs_02909	1.22084668	hypothetical protein
bf_rs_01427	1.20096345	ATP-dependent Clp protease ATP-binding subunit ClpC
bf_rs_02997	1.18828678	hypothetical protein
bf_rs_01065	1.17672925	tRNA-Thr(cgt)
bf_rs_00574	1.13371334	hypothetical protein
bf_rs_01993	1.1096845	60 kDa chaperonin
bf_rs_01994	1.0940297	10 kDa chaperonin
bf_rs_02911	1.08305958	Tyrosine recombinase XerC
bf_rs_02143	1.06695477	NAD-specific glutamate dehydrogenase
bf_rs_02972	1.06319546	fec operon regulator FecR
bf_rs_00620	1.03149045	fec operon regulator FecR
bf_rs_01491	1.02145126	hypothetical protein

bf_rs_02039	1.01576918	tRNA-Phe(gaa)
bf_rs_03113	0.99029687	hypothetical protein
bf_rs_03172	0.98787019	tRNA-Arg(gcg)
bf_rs_00358	0.98011931	MarR family protein
bf_rs_00832	0.95663866	hypothetical protein
bf_rs_00767	0.95138856	hypothetical protein
bf_rs_01889	0.93817056	Septum formation protein Maf
bf_rs_01282	0.93225515	ATP synthase subunit beta
bf_rs_03056	0.92592987	hypothetical protein
bf_rs_02999	0.92188748	hypothetical protein
bf_rs_00178	0.90537518	30S ribosomal protein S20
bf_rs_02814	0.89716045	hypothetical protein
bf_rs_02866	0.8857347	hypothetical protein
bf_rs_02896	0.8711559	hypothetical protein
bf_rs_00295	0.86561938	50S ribosomal protein L34
bf_rs_03169	0.84394207	tRNA-Asp(gtc)
bf_rs_01072	0.84372681	Cellobiose 2-epimerase
bf_rs_02507	0.83556286	50S ribosomal protein L36
bf_rs_02553	0.81701194	30S ribosomal protein S21
bf_rs_03177	0.80237688	tRNA-Lys(ttt)
bf_rs_01910	0.80050296	50S ribosomal protein L31 type B
bf_rs_01301	-0.8025912	dTDP-4-dehydrorhamnose reductase
bf_rs_02606	-0.8052951	Aminopeptidase YwaD precursor
bf_rs_01852	-0.8152527	Transaldolase
bf_rs_01735	-0.8355356	putative oxidoreductase
bf_rs_02275	-0.8444998	FMN reductase [NAD(P)H]
bf_rs_02683	-0.8621557	Lipoprotein-releasing system transmembrane protein LolE
bf_rs_00953	-0.8710608	putative A/G-specific adenine glycosylase YfhQ
bf_rs_00810	-0.9141991	hypothetical protein
bf_rs_02167	-0.9143676	Pyruvate formate-lyase 1-activating enzyme
bf_rs_02588	-0.9255988	Bifunctional transcriptional activator/DNA repair enzyme Ada
bf_rs_00809	-0.9858948	Cadmium%2C zinc and cobalt-transporting ATPase

bf_rs_01476	-1.017128	Colicin I receptor precursor
bf_rs_01210	-1.0192883	putative metallo-hydrolase
bf_rs_00766	-1.0324571	hypothetical protein
bf_rs_01961	-1.0695528	Molecular chaperone Hsp31 and glyoxalase 3
bf_rs_02112	-1.1114543	Lactate utilization protein C
bf_rs_00727	-1.19678	hypothetical protein
bf_rs_03146	-1.3302347	hypothetical protein
bf_rs_01478	-1.3347272	hypothetical protein
bf_rs_02716	-1.4038976	hypothetical protein
bf_rs_03155	9.49727508	Virus attachment protein p12 family protein
bf_rs_03086	7.42483668	Desulfoferrodoxin
bf_rs_03072	5.99041778	Rubrerythrin
bf_rs_03166	5.22671344	hypothetical protein
bf_rs_00677	2.94941467	hypothetical protein
bf_rs_00222	2.55126285	hypothetical protein
bf_rs_00221	2.16886211	DNA-binding transcriptional repressor MngR
bf_rs_01618	2.07361235	hypothetical protein
bf_rs_02052	1.77272895	NADP-dependent 7-alpha-hydroxysteroid dehydrogenase
bf_rs_02940	1.7284758	fec operon regulator FecR
bf_rs_02743	1.69887539	RNA polymerase sigma factor SigV
bf_rs_00043	1.67587978	tRNA-Gln(ttg)
bf_rs_01338	1.66917587	tRNA-Arg(tct)
bf_rs_03094	1.64631852	hypothetical protein
bf_rs_01987	1.62881003	hypothetical protein
bf_rs_02241	1.6208994	fec operon regulator FecR
bf_rs_01305	1.61776139	Sensor histidine kinase RcsC
bf_rs_02399	1.54668945	hypothetical protein
bf_rs_01379	1.51680269	tRNA-Lys(ctt)
bf_rs_00148	1.47897635	L-fucose isomerase
bf_rs_03031	1.47570767	hypothetical protein
bf_rs_00791	1.4591713	Alkyl hydroperoxide reductase subunit F
bf_rs_03008	1.4538937	mRNA interferase YafQ

bf_rs_01565	1.45036582	hypothetical protein
bf_rs_02411	1.4347406	Carbamoyl-phosphate synthase large chain
bf_rs_02029	1.43244153	2-isopropylmalate synthase
bf_rs_00365	1.42773623	fec operon regulator FecR
bf_rs_01426	1.40284414	Chaperone protein HtpG
bf_rs_01566	1.36719931	transcriptional repressor DicA
bf_rs_02926	1.35419467	hypothetical protein
bf_rs_01061	1.35058075	indolepyruvate oxidoreductase subunit beta
bf_rs_00674	1.31952666	fec operon regulator FecR
bf_rs_00846	1.31111918	hypothetical protein
bf_rs_02028	1.28560337	3-isopropylmalate dehydrogenase
bf_rs_02841	1.2694133	hypothetical protein
bf_rs_03132	1.26257754	hypothetical protein
bf_rs_01568	1.24792281	integration host factor subunit alpha
bf_rs_00591	1.24630888	tRNA-Tyr(gta)
bf_rs_02150	1.24574493	hypothetical protein
bf_rs_00371	1.2423177	tRNA-Met(cat)
bf_rs_02030	1.22383423	3-isopropylmalate dehydratase small subunit
bf_rs_02031	1.22255565	3-isopropylmalate dehydratase large subunit
bf_rs_00864	1.21646959	hypothetical protein
bf_rs_03138	1.21442784	hypothetical protein
bf_rs_02408	1.20626989	Fimbrillin-A associated anchor proteins Mfa1 and Mfa2
bf_rs_03037	1.20593408	hypothetical protein
bf_rs_01253	1.20349607	UDP-glucose 4-epimerase
bf_rs_01783	1.19659048	hypothetical protein
bf_rs_03176	1.19636334	tRNA-Cys(gca)
bf_rs_02433	1.18260592	Transcriptional regulatory protein DegU
bf_rs_02895	1.17406524	hypothetical protein
bf_rs_03009	1.16616354	hypothetical protein
bf_rs_01086	1.16540725	hypothetical protein
bf_rs_01202	1.16407331	hypothetical protein
bf_rs_01284	1.16107249	hypothetical protein

bf_rs_02599	1.13133631	fec operon regulator FecR
bf_rs_01126	1.12127525	hypothetical protein
bf_rs_01705	1.1114447	hypothetical protein
bf_rs_03154	1.106627	tRNA-Leu(taa)
bf_rs_02590	1.09676216	site-specific tyrosine recombinase XerC
bf_rs_02675	1.09630555	Autoinducer 2 sensor kinase/phosphatase LuxQ
bf_rs_01668	1.09579608	ACT domain protein
bf_rs_00577	1.07939668	HTH-type transcriptional activator Btr
bf_rs_01239	1.06702287	Leucine Rich repeats (2 copies)
bf_rs_01784	1.0640091	hypothetical protein
bf_rs_02946	1.0584182	Tyrosine recombinase XerC
bf_rs_02832	1.0498986	23S ribosomal RNA
bf_rs_02252	1.04906334	Methylmalonyl-CoA mutase large subunit
bf_rs_02657	1.03765279	DNA-binding protein HU
bf_rs_00865	1.0352581	tRNA-Cys(gca)
bf_rs_01794	1.0333348	Inner membrane protein YhaI
bf_rs_00863	1.01842316	Ferrous iron transport protein B
bf_rs_02533	1.01465797	30S ribosomal protein S7
bf_rs_01699	1.01265797	hypothetical protein
bf_rs_01283	1.00391663	ATP synthase epsilon chain
bf_rs_02779	1.0020912	tRNA-Ser(tga)
bf_rs_02389	1.00101624	30S ribosomal protein S2
bf_rs_02364	0.99687963	Outer membrane protein TolC precursor
bf_rs_00831	0.99546516	fec operon regulator FecR
bf_rs_00753	0.99535172	hypothetical protein
bf_rs_01277	0.98879852	Undecaprenol kinase
bf_rs_01445	0.98821021	hypothetical protein
bf_rs_00627	0.9850084	Glycosyl hydrolase family 57
bf_rs_01586	0.97286913	Enamine/imine deaminase
bf_rs_00114	0.96362387	Signal-transduction histidine kinase senX3
bf_rs_00811	0.95941118	Outer membrane protein 41 precursor
bf_rs_02959	0.95457172	hypothetical protein

bf_rs_00113	0.95250686	Transcriptional regulatory protein CssR
bf_rs_01029	0.94955754	Galactokinase
bf_rs_03015	0.94822705	hypothetical protein
bf_rs_01704	0.93246371	Oxygen regulatory protein NreC
bf_rs_00793	0.93168683	Alkyl hydroperoxide reductase subunit C
bf_rs_01838	0.92354425	hypothetical protein
bf_rs_01329	0.88731815	7%2C8-dihydro-6-hydroxymethylpterin-pyrophosphokinase (HPPK)
bf_rs_02390	0.88503445	30S ribosomal protein S9
bf_rs_02023	0.87013396	hypothetical protein
bf_rs_02230	0.86405934	Acetolactate synthase isozyme 2 large subunit
bf_rs_00756	0.86104914	50S ribosomal protein L25
bf_rs_00843	0.85771165	Alpha-xylosidase
bf_rs_02908	0.85299383	putative type I restriction enzymeP M protein
bf_rs_02534	0.85194894	30S ribosomal protein S12
bf_rs_01908	0.84560935	Fructose-bisphosphate aldolase
bf_rs_00150	0.84557721	Lactaldehyde reductase
bf_rs_00893	0.82647446	hypothetical protein
bf_rs_00021	0.82219587	hypothetical protein
bf_rs_01900	0.80783599	Glutaconyl-CoA decarboxylase subunit beta
bf_rs_02145	0.80663874	multifunctional tRNA nucleotidyl transferase/2'3'-cyclic phosphodiesterase/2'nucleotidase/phosphatase
bf_rs_02388	0.80475804	Elongation factor Ts
bf_rs_01440	0.80392404	LysM domain/BON superfamily protein
bf_rs_02781	0.80238847	Type-1 restriction enzyme R protein
bf_rs_00676	0.80123476	ECF RNA polymerase sigma factor SigW
bf_rs_01629	-0.8022802	hypothetical protein
bf_rs_02218	-0.8101734	Cytidylate kinase
bf_rs_00915	-0.8115897	Cytidine deaminase
bf_rs_03013	-0.8190102	Iron-binding zinc finger CDGSH type
bf_rs_01610	-0.8238728	Superoxide dismutase [Mn/Fe]
bf_rs_02914	-0.833247	hypothetical protein

bf_rs_01771	-0.8440513	ECF RNA polymerase sigma factor SigG
bf_rs_01465	-0.8542414	Outer membrane efflux protein
bf_rs_00667	-0.8587571	hypothetical protein
bf_rs_01143	-0.8619834	Glycerate dehydrogenase
bf_rs_02718	-0.867328	Miniconductance mechanosensitive channel MscM precursor
bf_rs_00713	-0.8858522	GTPase Obg
bf_rs_02803	-0.8956159	NADP-dependent alcohol dehydrogenase C 2
bf_rs_02234	-0.901416	Serine dehydratase alpha chain
bf_rs_02120	-0.9186621	hypothetical protein
bf_rs_00418	-0.91889	Efflux pump membrane transporter BepE
bf_rs_01800	-0.9265082	Quercetin 2%2C3-dioxygenase
bf_rs_01486	-0.9302885	Multidrug export protein EmrB
bf_rs_02308	-0.9336015	Glutathione peroxidase homolog BsaA
bf_rs_02059	-0.9483879	Methylmalonyl-CoA carboxyltransferase 1.3S subunit
bf_rs_01006	-0.950982	2-oxoisovalerate dehydrogenase subunit beta
bf_rs_00796	-0.9578412	hypothetical protein
bf_rs_00797	-0.9605315	hypothetical protein
bf_rs_01709	-0.9715214	Thioredoxin-1
bf_rs_00804	-0.99059	5-amino-6-(5-phosphoribosylamino)uracil reductase
bf_rs_01397	-0.9999215	hypothetical protein
bf_rs_00094	-1.0009305	putative oxidoreductase UxuB
bf_rs_00417	-1.0044964	Outer membrane protein TolC precursor
bf_rs_02086	-1.0142848	Membrane-bound lytic murein transglycosylase D precursor
bf_rs_02536	-1.0237507	hypothetical protein
bf_rs_01273	-1.0267843	Dihydroorotate dehydrogenase (quinone)
bf_rs_00198	-1.0326919	ECF RNA polymerase sigma factor SigH
bf_rs_00695	-1.0329689	hypothetical protein
bf_rs_00273	-1.0403668	Glutaminase 1
bf_rs_00133	-1.0426138	hypothetical protein
bf_rs_00996	-1.0481186	metal-dependent hydrolase
bf_rs_02722	-1.0489901	hypothetical protein
bf_rs_02976	-1.0509659	hypothetical protein

bf_rs_01153	-1.0556578	LemA family protein
bf_rs_02567	-1.0561453	Anaerobic C4-dicarboxylate transporter DcuA
bf_rs_02050	-1.070767	hypothetical protein
bf_rs_00557	-1.0770803	Alpha/beta hydrolase family protein
bf_rs_00858	-1.0784808	VIT family protein
bf_rs_02077	-1.0831795	Beta-lactamase type II precursor
bf_rs_02111	-1.08887	Pyridoxine kinase
bf_rs_02045	-1.0974955	Cupin domain protein
bf_rs_00665	-1.1051248	ECF RNA polymerase sigma factor SigW
bf_rs_00238	-1.1093411	hypothetical protein
bf_rs_00844	-1.1187241	lipoprotein involved with copper homeostasis and adhesion
bf_rs_00956	-1.1285733	hypothetical protein
bf_rs_00878	-1.1336931	Sodium-dependent dicarboxylate transporter SdcS
bf_rs_01325	-1.1429498	hypothetical protein
bf_rs_02095	-1.1429531	Peptide methionine sulfoxide reductase MsrA/MsrB
bf_rs_01094	-1.1488791	site-specific tyrosine recombinase XerD
bf_rs_01989	-1.150831	Pyruvate dehydrogenase [ubiquinone]
bf_rs_02538	-1.1514013	hypothetical protein
bf_rs_02993	-1.1518235	LexA repressor
bf_rs_01240	-1.154515	hypothetical protein
bf_rs_00656	-1.1580733	Thioredoxin reductase
bf_rs_00779	-1.1636445	H(+)/Cl(-) exchange transporter ClcA
bf_rs_01487	-1.1673847	putative multidrug resistance protein EmrK
bf_rs_01562	-1.1674059	acid-resistance membrane protein
bf_rs_02537	-1.1718679	hypothetical protein
bf_rs_00619	-1.1745272	RNA polymerase sigma factor SigM
bf_rs_02659	-1.181242	Rhomboid family protein
bf_rs_02058	-1.2097667	2-oxoglutarate carboxylase small subunit
bf_rs_00311	-1.2125034	Chaperone protein Skp precursor
bf_rs_02034	-1.2158301	bacterioferritin
bf_rs_01957	-1.2235202	putative oxidoreductase/MSMEI_2347
bf_rs_02470	-1.233513	PBP superfamily domain protein

bf_rs_01920	-1.2428509	Toluene efflux pump periplasmic linker protein TtgD precursor
bf_rs_00331	-1.2440999	hypothetical protein
bf_rs_01266	-1.2581519	Transcriptional activator protein Anr
bf_rs_02114	-1.2751312	Lactate utilization protein A
bf_rs_01396	-1.2754052	hypothetical protein
bf_rs_01167	-1.2786394	Collagen triple helix repeat (20 copies)
bf_rs_00272	-1.2798191	Glutamate decarboxylase
bf_rs_00452	-1.2842719	hypothetical protein
bf_rs_01395	-1.2880023	hypothetical protein
bf_rs_01684	-1.2907739	Diaminopimelate epimerase
bf_rs_00930	-1.2932448	Bifunctional aspartate aminotransferase and L-aspartate beta-decarboxylase
bf_rs_01503	-1.2942115	Ribonucleoside-diphosphate reductase subunit beta
bf_rs_01960	-1.3016038	Oxygen-insensitive NAD(P)H nitroreductase
bf_rs_02334	-1.3016943	P-protein
bf_rs_00356	-1.3021361	hypothetical protein
bf_rs_01295	-1.322733	inner membrane protein
bf_rs_00980	-1.3254225	putative inner membrane protein
bf_rs_01477	-1.3276994	Sirohydrochlorin cobaltochelatase
bf_rs_01757	-1.3547535	hypothetical protein
bf_rs_01357	-1.3565358	putative peroxiredoxin
bf_rs_02906	-1.3577911	hypothetical protein
bf_rs_00721	-1.3607892	hypothetical protein
bf_rs_02083	-1.378718	Phosphotransferase RcsD
bf_rs_02082	-1.3791335	hypothetical protein
bf_rs_00330	-1.3858288	hypothetical protein
bf_rs_01690	-1.3927457	Guanosine-5'-triphosphate%2C3'-diphosphate pyrophosphatase
bf_rs_00958	-1.3980968	hypothetical protein
bf_rs_02276	-1.4009092	Ribonucleoside-diphosphate reductase NrdZ
bf_rs_02802	-1.4168218	Putative NAD(P)H-dependent FMN-containing oxidoreductase YwqN
bf_rs_00960	-1.4225697	hypothetical protein

bf_rs_00999	-1.4252064	hypothetical protein
bf_rs_01543	-1.4322056	hypothetical protein
bf_rs_00854	-1.4373897	hypothetical protein
bf_rs_00355	-1.4376383	hypothetical protein
bf_rs_00931	-1.4384082	Aspartate/alanine antiporter
bf_rs_00254	-1.4394472	hypothetical protein
bf_rs_00236	-1.4453883	SusD family protein
bf_rs_02075	-1.4465711	hypothetical protein
bf_rs_02219	-1.4522683	4-hydroxy-3-methylbut-2-enyl diphosphate reductase
bf_rs_02051	-1.4625414	hypothetical protein
bf_rs_00199	-1.4826842	hypothetical protein
bf_rs_02905	-1.5008279	ISXO2-like transposase domain protein
bf_rs_02707	-1.5012662	FKBP-type 22 kDa peptidyl-prolyl cis-trans isomerase
bf_rs_00989	-1.5084547	DUF based on B. Theta Gene description
bf_rs_02080	-1.518875	hypothetical protein
bf_rs_02930	-1.5235038	fermentation/respiration switch protein
bf_rs_02414	-1.5255661	Outer membrane protein 40 precursor
bf_rs_00556	-1.5284233	LemA family protein
bf_rs_00990	-1.5419876	hypothetical protein
bf_rs_01544	-1.5552672	hypothetical protein
bf_rs_02166	-1.5855451	Anaerobic ribonucleoside-triphosphate reductase
bf_rs_01090	-1.5907614	ECF RNA polymerase sigma factor SigW
bf_rs_00253	-1.5909689	Cytochrome c-type protein NrfH
bf_rs_00233	-1.5950836	hypothetical protein
bf_rs_02113	-1.6011148	Lactate utilization protein B
bf_rs_01092	-1.6308183	hypothetical protein
bf_rs_00332	-1.6386106	Malate dehydrogenase
bf_rs_02244	-1.6620174	Choloylglycine hydrolase
bf_rs_00235	-1.6642256	Periplasmic beta-glucosidase precursor
bf_rs_00200	-1.6720026	putative TonB-dependent receptor precursor
bf_rs_02568	-1.6946538	L-asparaginase 2 precursor
bf_rs_00998	-1.7057636	hypothetical protein

bf_rs_00234	-1.716765	hypothetical protein
bf_rs_00329	-1.7304116	Glutamate/gamma-aminobutyrate antiporter
bf_rs_02569	-1.7390944	hypothetical protein
bf_rs_00237	-1.7550649	TonB-dependent Receptor Plug Domain protein
bf_rs_01414	-1.757573	Efflux pump membrane transporter BepE
bf_rs_01412	-1.7893962	Outer membrane protein OprM precursor
bf_rs_02197	-1.8030906	Outer membrane efflux protein
bf_rs_01363	-1.8438535	Inner membrane protein YhiM
bf_rs_00961	-1.8620409	hypothetical protein
bf_rs_01307	-1.8783795	hypothetical protein
bf_rs_01091	-1.9090812	hypothetical protein
bf_rs_01000	-1.9486584	hypothetical protein
bf_rs_00908	-1.9734855	Histidine decarboxylase proenzyme precursor
bf_rs_00891	-2.0182707	Porin subfamily protein
bf_rs_01711	-2.0210519	5-methyltetrahydropteroyltriglutamate--homocysteine methyltransferase
bf_rs_02469	-2.1202025	tetratricopeptide repeat protein
bf_rs_01274	-2.1584938	Acetylxylan esterase precursor
bf_rs_00201	-2.2886939	hypothetical protein
bf_rs_02471	-2.3649883	Gram-negative bacterial tonB protein
bf_rs_01413	-2.3962242	Efflux pump periplasmic linker BepF
bf_rs_02474	-2.5668838	colicin uptake protein TolQ
bf_rs_02473	-2.8621158	Biopolymer transport protein ExbD/TolR
bf_rs_02472	-2.9218949	Biopolymer transport protein ExbD/TolR

Bibliography

AAS, J., GESSERT, C. E. & BAKKEN, J. S. 2003. Recurrent Clostridium difficile colitis: case series involving 18 patients treated with donor stool administered via a nasogastric tube. *Clin Infect Dis,* 36**,** 580-5.

ABEE, T., KOVACS, A. T., KUIPERS, O. P. & VAN DER VEEN, S. 2011. Biofilm formation and dispersal in Gram-positive bacteria. *Curr Opin Biotechnol,* 22**,** 172-9.

ABT, M. C., MCKENNEY, P. T. & PAMER, E. G. 2016. Clostridium difficile colitis: pathogenesis and host. *Nat Rev Microbiol,* 14**,** 609-20.

ADAMU, B. O. & LAWLEY, T. D. 2013. Bacteriotherapy for the treatment of intestinal dysbiosis caused by Clostridium difficile infection. *Curr Opin Microbiol*.

AHMED, N. A., PETERSEN, F. C. & SCHEIE, A. A. 2009. AI-2/LuxS is involved in increased biofilm formation by Streptococcus intermedius in the presence of antibiotics. *Antimicrob Agents Chemother,* 53**,** 4258-63.

ALLSOPP, L. P., TOTSIKA, M., TREE, J. J., ULETT, G. C., MABBETT, A. N., WELLS, T. J., KOBE, B., BEATSON, S. A. & SCHEMBRI, M. A. 2010. UpaH is a newly identified autotransporter protein that contributes to biofilm formation and bladder colonization by uropathogenic Escherichia coli CFT073. *Infect Immun,* 78**,** 1659-69.

ANANTHAKRISHNAN, A. N. 2011. Clostridium difficile infection: epidemiology, risk factors and management. *Nat Rev Gastroenterol Hepatol,* 8**,** 17-26.

ANDREWS, S. C., ROBINSON, A. K. & RODRIGUEZ-QUINONES, F. 2003. Bacterial iron homeostasis. *FEMS Microbiol Rev,* 27**,** 215-37.

ANTUNES, L. C., FERREIRA, L. Q., FERREIRA, E. O., MIRANDA, K. R., AVELAR, K. E., DOMINGUES, R. M. & FERREIRA, M. C. 2005. Bacteroides species produce Vibrio harveyi autoinducer 2-related molecules. *Anaerobe,* 11**,** 295-301.

ANTUNES, L. C., FERREIRA, R. B., BUCKNER, M. M. & FINLAY, B. B. 2010. Quorum sensing in bacterial virulence. *Microbiology,* 156**,** 2271-82.

ARNDT, D., GRANT, J. R., MARCU, A., SAJED, T., PON, A., LIANG, Y. & WISHART, D. S. 2016. PHASTER: a better, faster version of the PHAST phage search tool. *Nucleic Acids Res,* 44**,** W16-21.

ASLAM, S., HAMILL, R. J. & MUSHER, D. M. 2005. Treatment of Clostridium difficile-associated disease: old therapies and new strategies. *Lancet Infect Dis,* 5**,** 549-57.

AUGER, S., KRIN, E., AYMERICH, S. & GOHAR, M. 2006. Autoinducer 2 affects biofilm formation by Bacillus cereus. *Appl Environ Microbiol,* 72**,** 937-41.

BANKEVICH, A., NURK, S., ANTIPOV, D., GUREVICH, A. A., DVORKIN, M., KULIKOV, A. S., LESIN, V. M., NIKOLENKO, S. I., PHAM, S., PRJIBELSKI, A. D., PYSHKIN, A. V., SIROTKIN, A. V., VYAHHI, N.,

TESLER, G., ALEKSEYEV, M. A. & PEVZNER, P. A. 2012. SPAdes: a new genome assembly algorithm and its applications to single-cell sequencing. *J Comput Biol,* 19**,** 455-77.
BARBUT, F., RICHARD, A., HAMADI, K., CHOMETTE, V., BURGHOFFER, B. & PETIT, J. C. 2000. Epidemiology of recurrences or reinfections of Clostridium difficile-associated diarrhea. *J Clin Microbiol,* 38**,** 2386-8.
BARTLETT, J. G. 1994. Clostridium difficile: history of its role as an enteric pathogen and the current state of knowledge about the organism. *Clin Infect Dis,* 18 Suppl 4**,** S265-72.
BASSLER, B. L., GREENBERG, E. P. & STEVENS, A. M. 1997. Cross-species induction of luminescence in the quorum-sensing bacterium Vibrio harveyi. *J Bacteriol,* 179**,** 4043-5.
BASSLER, B. L. & LOSICK, R. 2006. Bacterially speaking. *Cell,* 125**,** 237-46.
BELOIN, C., ROUX, A. & GHIGO, J. M. 2008. Escherichia coli biofilms. *Curr Top Microbiol Immunol,* 322**,** 249-89.
BORRIELLO, S. P., DAVIES, H. A., KAMIYA, S., REED, P. J. & SEDDON, S. 1990. Virulence factors of Clostridium difficile. *Rev Infect Dis,* 12 Suppl 2**,** S185-91.
BRITTON, R. A. & YOUNG, V. B. 2012. Interaction between the intestinal microbiota and host in Clostridium difficile colonization resistance. *Trends Microbiol,* 20**,** 313-9.
BRUCKNER, R. & TITGEMEYER, F. 2002. Carbon catabolite repression in bacteria: choice of the carbon source and autoregulatory limitation of sugar utilization. *FEMS Microbiol Lett,* 209**,** 141-8.
BUFFIE, C. G., BUCCI, V., STEIN, R. R., MCKENNEY, P. T., LING, L., GOBOURNE, A., NO, D., LIU, H., KINNEBREW, M., VIALE, A., LITTMANN, E., VAN DEN BRINK, M. R. M., JENQ, R. R., TAUR, Y., SANDER, C., CROSS, J., TOUSSAINT, N. C., XAVIER, J. B. & PAMER, E. G. 2014. Precision microbiome restoration of bile acid-mediated resistance to Clostridium difficile. *Nature,* 517**,** 205-8.
CALABI, E., WARD, S., WREN, B., PAXTON, T., PANICO, M., MORRIS, H., DELL, A., DOUGAN, G. & FAIRWEATHER, N. 2001. Molecular characterization of the surface layer proteins from Clostridium difficile. *Mol Microbiol,* 40**,** 1187-99.
CAO, M., FENG, Y., WANG, C., ZHENG, F., LI, M., LIAO, H., MAO, Y., PAN, X., WANG, J., HU, D., HU, F. & TANG, J. 2011. Functional definition of LuxS, an autoinducer-2 (AI-2) synthase and its role in full virulence of Streptococcus suis serotype 2. *J Microbiol,* 49**,** 1000-11.
CARTER, G. P. 2005. Quorum sensing in Clostridium difficile: analysis of a luxS-type signalling system. *Journal of Medical Microbiology,* 54**,** 119-127.
CARTER, G. P., LYRAS, D., ALLEN, D. L., MACKIN, K. E., HOWARTH, P. M., O'CONNOR, J. R. & ROOD, J. I. 2007. Binary toxin production in Clostridium difficile is regulated by CdtR, a LytTR family response regulator. *J Bacteriol,* 189**,** 7290-301.

CARTER, G. P., PURDY, D., WILLIAMS, P. & MINTON, N. P. 2005. Quorum sensing in Clostridium difficile: analysis of a luxS-type signalling system. *J Med Microbiol,* 54**,** 119-27.
CARTER, G. P., ROOD, J. I. & LYRAS, D. 2012. The role of toxin A and toxin B in the virulence of Clostridium difficile. *Trends Microbiol,* 20**,** 21-9.
CARTMAN, S. T., HEAP, J. T., KUEHNE, S. A., COCKAYNE, A. & MINTON, N. P. 2010. The emergence of 'hypervirulence' in Clostridium difficile. *Int J Med Microbiol,* 300**,** 387-95.
CERQUETTI, M., MOLINARI, A., SEBASTIANELLI, A., DIOCIAIUTI, M., PETRUZZELLI, R., CAPO, C. & MASTRANTONIO, P. 2000. Characterization of surface layer proteins from different Clostridium difficile clinical isolates. *Microb Pathog,* 28**,** 363-72.
CHATZIDAKI-LIVANIS, M., GEVA-ZATORSKY, N. & COMSTOCK, L. E. 2016. Bacteroides fragilis type VI secretion systems use novel effector and immunity proteins to antagonize human gut Bacteroidales species. *Proc Natl Acad Sci U S A,* 113**,** 3627-32.
CHEN, X., SCHAUDER, S., POTIER, N., VAN DORSSELAER, A., PELCZER, I., BASSLER, B. L. & HUGHSON, F. M. 2002. Structural identification of a bacterial quorum-sensing signal containing boron. *Nature,* 415**,** 545-9.
CHOI, S. C. 2016. On the study of microbial transcriptomes using second- and third-generation sequencing technologies. *J Microbiol,* 54**,** 527-36.
COHEN, S. H., TANG, Y. J. & SILVA, J., JR. 2000. Analysis of the pathogenicity locus in Clostridium difficile strains. *J Infect Dis,* 181**,** 659-63.
COLLINS, J., ROBINSON, C., DANHOF, H., KNETSCH, C. W., VAN LEEUWEN, H. C., LAWLEY, T. D., AUCHTUNG, J. M. & BRITTON, R. A. 2018a. Dietary trehalose enhances virulence of epidemic Clostridium difficile. *Nature,* 553**,** 291-294.
COLLINS, J., ROBINSON, C., DANHOF, H., KNETSCH, C. W., VAN LEEUWEN, H. C., LAWLEY, T. D., AUCHTUNG, J. M. & BRITTON, R. A. 2018b. Dietary trehalose enhances virulence of epidemic Clostridium difficile. *Nature,* 553**,** 291.
CORNELY, O. A., CROOK, D. W., ESPOSITO, R., POIRIER, A., SOMERO, M. S., WEISS, K., SEARS, P. & GORBACH, S. 2012. Fidaxomicin versus vancomycin for infection with Clostridium difficile in Europe, Canada, and the USA: a double-blind, non-inferiority, randomised controlled trial. *Lancet Infect Dis,* 12**,** 281-9.
COSTERTON, J. W., STEWART, P. S. & GREENBERG, E. P. 1999. Bacterial biofilms: a common cause of persistent infections. *Science,* 284**,** 1318-22.
COULTHURST, S. J., KURZ, C. L. & SALMOND, G. P. 2004. luxS mutants of Serratia defective in autoinducer-2-dependent 'quorum sensing' show strain-dependent impacts on virulence and production of carbapenem and prodigiosin. *Microbiology,* 150**,** 1901-10.
COYNE, M. J., ROELOFS, K. G. & COMSTOCK, L. E. 2016. Type VI secretion systems of human gut Bacteroidales segregate into three genetic

architectures, two of which are contained on mobile genetic elements. *BMC Genomics,* 17, 58.
CROWTHER, G. S., CHILTON, C. H., TODHUNTER, S. L., NICHOLSON, S., FREEMAN, J., BAINES, S. D. & WILCOX, M. H. 2014. Development and validation of a chemostat gut model to study both planktonic and biofilm modes of growth of Clostridium difficile and human microbiota. *PLoS One,* 9, e88396.
CUBITT, A. B., HEIM, R., ADAMS, S. R., BOYD, A. E., GROSS, L. A. & TSIEN, R. Y. 1995. Understanding, improving and using green fluorescent proteins. *Trends in Biochemical Sciences,* 20, 448-455.
CURRY, S. R., MARSH, J. W., MUTO, C. A., O'LEARY, M. M., PASCULLE, A. W. & HARRISON, L. H. 2007. tcdC genotypes associated with severe TcdC truncation in an epidemic clone and other strains of Clostridium difficile. *J Clin Microbiol,* 45, 215-21.
DANG, T. H., DE LA RIVA, L., FAGAN, R. P., STORCK, E. M., HEAL, W. P., JANOIR, C., FAIRWEATHER, N. F. & TATE, E. W. 2010. Chemical probes of surface layer biogenesis in Clostridium difficile. *ACS Chem Biol,* 5, 279-85.
DAPA, T., LEUZZI, R., NG, Y. K., BABAN, S. T., ADAMO, R., KUEHNE, S. A., SCARSELLI, M., MINTON, N. P., SERRUTO, D. & UNNIKRISHNAN, M. 2013. Multiple Factors Modulate Biofilm Formation by the Anaerobic Pathogen Clostridium difficile. *Journal of Bacteriology,* 195, 545 - 555.
ĐAPA, T., LEUZZI, R., NG, Y. K., BABAN, S. T., ADAMO, R., KUEHNE, S. A., SCARSELLI, M., MINTON, N. P., SERRUTO, D. & UNNIKRISHNAN, M. 2013. Multiple Factors Modulate Biofilm Formation by the Anaerobic Pathogen Clostridium difficile. *J Bacteriol,* 195, 545-55.
DAPA, T. & UNNIKRISHNAN, M. 2013. Biofilm formation by Clostridium difficile. *Gut Microbes,* 4.
DAVEY, M. E. & O'TOOLE G, A. 2000. Microbial biofilms: from ecology to molecular genetics. *Microbiol Mol Biol Rev,* 64, 847-67.
DAVIES, D. G., PARSEK, M. R., PEARSON, J. P., IGLEWSKI, B. H., COSTERTON, J. W. & GREENBERG, E. P. 1998. The involvement of cell-to-cell signals in the development of a bacterial biofilm. *Science,* 280, 295-8.
DAWSON, L. F., VALIENTE, E., FAULDS-PAIN, A., DONAHUE, E. H. & WREN, B. W. 2012. Characterisation of Clostridium difficile biofilm formation, a role for Spo0A. *PLoS One,* 7, e50527.
DE ARAUJO, C., BALESTRINO, D., ROTH, L., CHARBONNEL, N. & FORESTIER, C. 2010. Quorum sensing affects biofilm formation through lipopolysaccharide synthesis in Klebsiella pneumoniae. *Res Microbiol,* 161, 595-603.
DE KEERSMAECKER, S. C., VARSZEGI, C., VAN BOXEL, N., HABEL, L. W., METZGER, K., DANIELS, R., MARCHAL, K., DE VOS, D. & VANDERLEYDEN, J. 2005. Chemical synthesis of (S)-4,5-dihydroxy-2,3-

pentanedione, a bacterial signal molecule precursor, and validation of its activity in Salmonella typhimurium. *J Biol Chem,* 280**,** 19563-8.
DEAKIN, L. J., CLARE, S., FAGAN, R. P., DAWSON, L. F., PICKARD, D. J., WEST, M. R., WREN, B. W., FAIRWEATHER, N. F., DOUGAN, G. & LAWLEY, T. D. 2012. Clostridium difficile spo0A gene is a persistence and transmission factor. *Infect Immun*.
DEATHERAGE, D. E. & BARRICK, J. E. 2014. Identification of mutations in laboratory-evolved microbes from next-generation sequencing data using breseq. *Methods Mol Biol,* 1151**,** 165-88.
DEMBEK, M., BARQUIST, L., BOINETT, C. J., CAIN, A. K., MAYHO, M., LAWLEY, T. D., FAIRWEATHER, N. F. & FAGAN, R. P. 2015. High-throughput analysis of gene essentiality and sporulation in Clostridium difficile. *MBio,* 6**,** e02383.
DERIU, E., LIU, J. Z., PEZESHKI, M., EDWARDS, R. A., OCHOA, R. J., CONTRERAS, H., LIBBY, S. J., FANG, F. C. & RAFFATELLU, M. 2013. Probiotic Bacteria Reduce Salmonella Typhimurium Intestinal Colonization by Competing for Iron. *Cell Host Microbe,* 14**,** 26-37.
DIGGLE, S. P., GRIFFIN, A. S., CAMPBELL, G. S. & WEST, S. A. 2007. Cooperation and conflict in quorum-sensing bacterial populations. *Nature,* 450**,** 411-4.
DINEEN, S. S., VILLAPAKKAM, A. C., NORDMAN, J. T. & SONENSHEIN, A. L. 2007. Repression of Clostridium difficile toxin gene expression by CodY. *Mol Microbiol,* 66**,** 206-19.
DINGLE, T. C., MULVEY, G. L. & ARMSTRONG, G. D. 2011. Mutagenic analysis of the Clostridium difficile flagellar proteins, FliC and FliD, and their contribution to virulence in hamsters. *Infect Immun,* 79**,** 4061-7.
DIXIT, S., DUBEY, R. C., MAHESHWARI, D. K., SETH, P. K. & BAJPAI, V. K. 2017. Roles of quorum sensing molecules from Rhizobium etli RT1 in bacterial motility and biofilm formation. *Braz J Microbiol,* 48**,** 815-21.
DOHERTY, N., HOLDEN, M. T., QAZI, S. N., WILLIAMS, P. & WINZER, K. 2006. Functional analysis of luxS in Staphylococcus aureus reveals a role in metabolism but not quorum sensing. *J Bacteriol,* 188**,** 2885-97.
DUAN, Q., ZHOU, M., ZHU, L. & ZHU, G. 2013. Flagella and bacterial pathogenicity. *J Basic Microbiol,* 53**,** 1-8.
DUBBERKE, E. R. & OLSEN, M. A. 2012. Burden of Clostridium difficile on the healthcare system. *Clin Infect Dis,* 55 Suppl 2**,** S88-92.
DUBBERKE, E. R., RESKE, K. A., NOBLE-WANG, J., THOMPSON, A., KILLGORE, G., MAYFIELD, J., CAMINS, B., WOELTJE, K., MCDONALD, J. R., MCDONALD, L. C. & FRASER, V. J. 2007. Prevalence of Clostridium difficile environmental contamination and strain variability in multiple health care facilities. *American Journal of Infection Control,* 35**,** 315-318.
DUBOIS, T., DANCER-THIBONNIER, M., MONOT, M., HAMIOT, A., BOUILLAUT, L., SOUTOURINA, O., MARTIN-VERSTRAETE, I. &

DUPUY, B. 2016. Control of Clostridium difficile Physiopathology in Response to Cysteine Availability. *Infect Immun,* 84**,** 2389-405.
DUTTON, L. C., PASZKIEWICZ, K. H., SILVERMAN, R. J., SPLATT, P. R., SHAW, S., NOBBS, A. H., LAMONT, R. J., JENKINSON, H. F. & RAMSDALE, M. 2016. Transcriptional landscape of trans-kingdom communication between Candida albicans and Streptococcus gordonii. *Molecular Oral Microbiology,* 31**,** 136-161.
EDMISTON, C. E., JR., AVANT, G. R. & WILSON, F. A. 1982. Anaerobic bacterial populations on normal and diseased human biopsy tissue obtained at colonoscopy. *Appl Environ Microbiol,* 43**,** 1173-81.
EMERSON, J. E., REYNOLDS, C. B., FAGAN, R. P., SHAW, H. A., GOULDING, D. & FAIRWEATHER, N. F. 2009. A novel genetic switch controls phase variable expression of CwpV, a Clostridium difficile cell wall protein. *Mol Microbiol,* 74**,** 541-56.
ENGEBRECHT, J. & SILVERMAN, M. 1984. Identification of genes and gene products necessary for bacterial bioluminescence. *Proc Natl Acad Sci U S A,* 81**,** 4154-8.
EYRE, D. W., CULE, M. L., WILSON, D. J., GRIFFITHS, D., VAUGHAN, A., O'CONNOR, L., IP, C. L. C., GOLUBCHIK, T., BATTY, E. M., FINNEY, J. M., WYLLIE, D. H., DIDELOT, X., PIAZZA, P., BOWDEN, R., DINGLE, K. E., HARDING, R. M., CROOK, D. W., WILCOX, M. H., PETO, T. E. A. & WALKER, A. S. 2013. Diverse sources of C. difficile infection identified on whole-genome sequencing. *N Engl J Med,* 369**,** 1195-205.
FAGAN, R. P., ALBESA-JOVE, D., QAZI, O., SVERGUN, D. I., BROWN, K. A. & FAIRWEATHER, N. F. 2009. Structural insights into the molecular organization of the S-layer from Clostridium difficile. *Mol Microbiol,* 71**,** 1308-22.
FEDERLE, M. J. & BASSLER, B. L. 2003. Interspecies communication in bacteria. *Journal of Clinical Investigation,* 112**,** 1291-1299.
FERREYRA, J. A., WU, K. J., HRYCKOWIAN, A. J., BOULEY, D. M., WEIMER, B. C. & SONNENBURG, J. L. 2014. Gut microbiota-produced succinate promotes C. difficile infection after antibiotic treatment or motility disturbance. *Cell Host Microbe,* 16**,** 770-7.
FIEGNA, F. & VELICER, G. J. 2003. Competitive fates of bacterial social parasites: persistence and self-induced extinction of Myxococcus xanthus cheaters. *Proc Biol Sci,* 270**,** 1527-34.
FINNEY, J. M. T. 1893. Gastroenterostomy for cicatrizing ulcer of the pylorus. *Johns Hopkins Medical journal,* 4**,** 53-55.
FRANKS, A. H., HARMSEN, H. J., RAANGS, G. C., JANSEN, G. J., SCHUT, F. & WELLING, G. W. 1998. Variations of bacterial populations in human feces measured by fluorescent in situ hybridization with group-specific 16S rRNA-targeted oligonucleotide probes. *Appl Environ Microbiol,* 64**,** 3336-45.

FUENTES, S., VAN NOOD, E., TIMS, S., HEIKAMP-DE JONG, I., TER BRAAK, C. J., KELLER, J. J., ZOETENDAL, E. G. & DE VOS, W. M. 2014. Reset of a critically disturbed microbial ecosystem: faecal transplant in recurrent Clostridium difficile infection. *Isme j,* 8**,** 1621-33.
FUJITA, Y., MATSUOKA, H. & HIROOKA, K. 2007. Regulation of fatty acid metabolism in bacteria. *Mol Microbiol,* 66**,** 829-39.
FUQUA, C., PARSEK, M. R. & GREENBERG, E. P. 2001. Regulation of gene expression by cell-to-cell communication: acyl-homoserine lactone quorum sensing. *Annu Rev Genet,* 35**,** 439-68.
FUX, C. A., WILSON, S. & STOODLEY, P. 2004. Detachment characteristics and oxacillin resistance of Staphyloccocus aureus biofilm emboli in an in vitro catheter infection model. *J Bacteriol,* 186**,** 4486-91.
GEORGE, E. A. & MUIR, T. W. 2007. Molecular mechanisms of agr quorum sensing in virulent staphylococci. *Chembiochem,* 8**,** 847-55.
GERRITSEN, J., SMIDT, H., RIJKERS, G. T. & DE VOS, W. M. 2011. Intestinal microbiota in human health and disease: the impact of probiotics. *Genes Nutr,* 6**,** 209-40.
GONZALEZ BARRIOS, A. F., ZUO, R., HASHIMOTO, Y., YANG, L., BENTLEY, W. E. & WOOD, T. K. 2006. Autoinducer 2 controls biofilm formation in Escherichia coli through a novel motility quorum-sensing regulator (MqsR, B3022). *J Bacteriol,* 188**,** 305-16.
GOORHUIS, A., BAKKER, D., CORVER, J., DEBAST, S. B., HARMANUS, C., NOTERMANS, D. W., BERGWERFF, A. A., DEKKER, F. W. & KUIJPER, E. J. 2008. Emergence of Clostridium difficile infection due to a new hypervirulent strain, polymerase chain reaction ribotype 078. *Clin Infect Dis,* 47**,** 1162-70.
GOVIND, R. & DUPUY, B. 2012. Secretion of Clostridium difficile Toxins A and B Requires the Holin-like Protein TcdE. *PLOS Pathogens,* 8**,** e1002727.
GOVIND, R., FITZWATER, L. & NICHOLS, R. 2015. Observations on the Role of TcdE Isoforms in Clostridium difficile Toxin Secretion. *J Bacteriol,* 197**,** 2600-9.
GOY, S. D., OLLING, A., NEUMANN, D., PICH, A. & GERHARD, R. 2015. Human neutrophils are activated by a peptide fragment of Clostridium difficile toxin B presumably via formyl peptide receptor. *Cell Microbiol,* 17**,** 893-909.
GRIFFIN, A. S., WEST, S. A. & BUCKLING, A. 2004. Cooperation and competition in pathogenic bacteria. *Nature,* 430**,** 1024-7.
HALL-STOODLEY, L., COSTERTON, J. W. & STOODLEY, P. 2004. Bacterial biofilms: from the natural environment to infectious diseases. *Nat Rev Microbiol,* 2**,** 95-108.
HALL-STOODLEY, L. & STOODLEY, P. 2005. Biofilm formation and dispersal and the transmission of human pathogens. *Trends Microbiol,* 13**,** 7-10.
HALL-STOODLEY, L. & STOODLEY, P. 2009. Evolving concepts in biofilm infections. *Cell Microbiol,* 11**,** 1034-43.

HALL, I. C. & O'TOOLE, E. 1935. Intestinal flora in new-born infants: With a description of a new pathogenic anaerobe, bacillus difficilis. *American Journal of Diseases of Children,* 49**,** 390-402.
HAMBRE M, R. G., MCKEE M, MACPHILLAMY H, 1943. The toxicity of penicillin as prepared for clinical use. *American Journal of Medical Science,* 206**,** 642–652.
HAMILTON, M. J., WEINGARDEN, A. R., UNNO, T., KHORUTS, A. & SADOWSKY, M. J. 2013. High-throughput DNA sequence analysis reveals stable engraftment of gut microbiota following transplantation of previously frozen fecal bacteria. *Gut Microbes,* 4**,** 125-35.
HAMMER, B. K. & BASSLER, B. L. 2003. Quorum sensing controls biofilm formation in Vibrio cholerae. *Mol Microbiol,* 50**,** 101-4.
HARDIE, K. R. & HEURLIER, K. 2008. Establishing bacterial communities by 'word of mouth': LuxS and autoinducer 2 in biofilm development. *Nat Rev Microbiol,* 6**,** 635-43.
HARGREAVES, K. R., COLVIN, H. V., PATEL, K. V., CLOKIE, J. J. & CLOKIE, M. R. 2013. Genetically diverse Clostridium difficile strains harboring abundant prophages in an estuarine environment. *Appl Environ Microbiol,* 79**,** 6236-43.
HARSHEY, R. M. 2003. Bacterial motility on a surface: many ways to a common goal. *Annu Rev Microbiol,* 57**,** 249-73.
HENSGENS, M. P., DEKKERS, O. M., DEMEULEMEESTER, A., BUITING, A. G., BLOEMBERGEN, P., VAN BENTHEM, B. H., LE CESSIE, S. & KUIJPER, E. J. 2014. Diarrhoea in general practice: when should a Clostridium difficile infection be considered? Results of a nested case-control study. *Clin Microbiol Infect,* 20**,** O1067-74.
HENSGENS, M. P., GOORHUIS, A., VAN KINSCHOT, C. M., CROBACH, M. J., HARMANUS, C. & KUIJPER, E. J. 2011. Clostridium difficile infection in an endemic setting in the Netherlands. *Eur J Clin Microbiol Infect Dis,* 30**,** 587-93.
HILGERS, M. T. & LUDWIG, M. L. 2001. Crystal structure of the quorum-sensing protein LuxS reveals a catalytic metal site. *Proc Natl Acad Sci U S A,* 98**,** 11169-74.
HOPKINS, M. J. & MACFARLANE, G. T. 2002. Changes in predominant bacterial populations in human faeces with age and with Clostridium difficile infection. *J Med Microbiol,* 51**,** 448-54.
HOPKINS, M. J. & MACFARLANE, G. T. 2003. Nondigestible oligosaccharides enhance bacterial colonization resistance against Clostridium difficile in vitro. *Appl Environ Microbiol,* 69**,** 1920-7.
HUANG, Z., MERIC, G., LIU, Z., MA, R., TANG, Z. & LEJEUNE, P. 2009. luxS-based quorum-sensing signaling affects Biofilm formation in Streptococcus mutans. *J Mol Microbiol Biotechnol,* 17**,** 12-9.

JANARTHANAN, S., DITAH, I., ADLER, D. G. & EHRINPREIS, M. N. 2012. Clostridium difficile-associated diarrhea and proton pump inhibitor therapy: a meta-analysis. *Am J Gastroenterol,* 107**,** 1001-10.
JANOIR, C., PECHINE, S., GROSDIDIER, C. & COLLIGNON, A. 2007. Cwp84, a surface-associated protein of Clostridium difficile, is a cysteine protease with degrading activity on extracellular matrix proteins. *J Bacteriol,* 189**,** 7174-80.
JI, G., BEAVIS, R. C. & NOVICK, R. P. 1995. Cell density control of staphylococcal virulence mediated by an octapeptide pheromone. *Proc Natl Acad Sci U S A,* 92**,** 12055-9.
JIRICNY, N., DIGGLE, S. P., WEST, S. A., EVANS, B. A., BALLANTYNE, G., ROSS-GILLESPIE, A. & GRIFFIN, A. S. 2010. Fitness correlates with the extent of cheating in a bacterium. *J Evol Biol,* 23**,** 738-47.
JUST, I., SELZER, J., WILM, M., VON EICHEL-STREIBER, C., MANN, M. & AKTORIES, K. 1995. Glucosylation of Rho proteins by Clostridium difficile toxin B. *Nature,* 375**,** 500-3.
KAISER, J. C., KING, A. N., GRIGG, J. C., SHELDON, J. R., EDGELL, D. R., MURPHY, M. E. P., BRINSMADE, S. R. & HEINRICHS, D. E. 2018. Repression of branched-chain amino acid synthesis in Staphylococcus aureus is mediated by isoleucine via CodY, and by a leucine-rich attenuator peptide. *PLoS Genet,* 14**,** e1007159.
KANEHISA, M. & GOTO, S. 2000. KEGG: kyoto encyclopedia of genes and genomes. *Nucleic Acids Res,* 28**,** 27-30.
KANEHISA, M., SATO, Y. & MORISHIMA, K. 2016. BlastKOALA and GhostKOALA: KEGG Tools for Functional Characterization of Genome and Metagenome Sequences. *J Mol Biol,* 428**,** 726-731.
KARIM, M. M., HISAMOTO, T., MATSUNAGA, T., ASAHI, Y., NOIRI, Y., EBISU, S., KATO, A. & AZAKAMI, H. 2013. LuxS affects biofilm maturation and detachment of the periodontopathogenic bacterium Eikenella corrodens. *J Biosci Bioeng,* 116**,** 313-8.
KARJALAINEN, T., WALIGORA-DUPRIET, A. J., CERQUETTI, M., SPIGAGLIA, P., MAGGIONI, A., MAURI, P. & MASTRANTONIO, P. 2001. Molecular and genomic analysis of genes encoding surface-anchored proteins from Clostridium difficile. *Infect Immun,* 69**,** 3442-6.
KEREN, I., KALDALU, N., SPOERING, A., WANG, Y. & LEWIS, K. 2004a. Persister cells and tolerance to antimicrobials. *FEMS Microbiol Lett,* 230**,** 13-8.
KEREN, I., SHAH, D., SPOERING, A., KALDALU, N. & LEWIS, K. 2004b. Specialized persister cells and the mechanism of multidrug tolerance in Escherichia coli. *J Bacteriol,* 186**,** 8172-80.
KHANNA, S., PARDI, D. S., KELLY, C. R., KRAFT, C. S., DHERE, T., HENN, M. R., LOMBARDO, M. J., VULIC, M., OHSUMI, T., WINKLER, J., PINDAR, C., MCGOVERN, B. H., POMERANTZ, R. J., AUNINS, J. G., COOK, D. N. & HOHMANN, E. L. 2016. A Novel Microbiome

Therapeutic Increases Gut Microbial Diversity and Prevents Recurrent Clostridium difficile Infection. *J Infect Dis,* 214**,** 173-81.
KHORUTS, A., DICKSVED, J., JANSSON, J. K. & SADOWSKY, M. J. 2010. Changes in the composition of the human fecal microbiome after bacteriotherapy for recurrent Clostridium difficile-associated diarrhea. *J Clin Gastroenterol,* 44**,** 354-60.
KIM, Y. G., GRAHAM, D. Y. & JANG, B. I. 2012. Proton pump inhibitor use and recurrent Clostridium difficile-associated disease: a case-control analysis matched by propensity score. *J Clin Gastroenterol,* 46**,** 397-400.
KIRBY, J. M., AHERN, H., ROBERTS, A. K., KUMAR, V., FREEMAN, Z., ACHARYA, K. R. & SHONE, C. C. 2009. Cwp84, a surface-associated cysteine protease, plays a role in the maturation of the surface layer of Clostridium difficile. *J Biol Chem,* 284**,** 34666-73.
KIRK, J. A., GEBHART, D., BUCKLEY, A. M., LOK, S., SCHOLL, D., DOUCE, G. R., GOVONI, G. R. & FAGAN, R. P. 2017. New class of precision antimicrobials redefines role of Clostridium difficile S-layer in virulence and viability. *Science Translational Medicine,* 9.
KOLTER, R. 2010. Biofilms in lab and nature: a molecular geneticist's voyage to microbial ecology. *Int Microbiol,* 13**,** 1-7.
KORTMAN, G. A., RAFFATELLU, M., SWINKELS, D. W. & TJALSMA, H. 2014. Nutritional iron turned inside out: intestinal stress from a gut microbial perspective. *FEMS Microbiol Rev,* 38**,** 1202-34.
KUEHNE, S. A., CARTMAN, S. T., HEAP, J. T., KELLY, M. L., COCKAYNE, A. & MINTON, N. P. 2010. The role of toxin A and toxin B in Clostridium difficile infection. *Nature,* 467**,** 711-3.
KUEHNE, S. A., CARTMAN, S. T. & MINTON, N. P. 2011. Both, toxin A and toxin B, are important in Clostridium difficile infection. *Gut Microbes,* 2**,** 252-5.
KURAMITSU, H. K., HE, X., LUX, R., ANDERSON, M. H. & SHI, W. 2007. Interspecies Interactions within Oral Microbial Communities. *Microbiol Mol Biol Rev,* 71**,** 653-70.
LAMONTAGNE, F., LABBÉ, A. C., HAECK, O., LESUR, O., LALANCETTE, M., PATINO, C., LEBLANC, M., LAVERDIÈRE, M. & PÉPIN, J. 2007. Impact of Emergency Colectomy on Survival of Patients With Fulminant Clostridium difficile Colitis During an Epidemic Caused by a Hypervirulent Strain. *Ann Surg,* 245**,** 267-72.
LANDETE, J. M., LANGA, S., REVILLA, C., MARGOLLES, A., MEDINA, M. & ARQUES, J. L. 2015. Use of anaerobic green fluorescent protein versus green fluorescent protein as reporter in lactic acid bacteria. *Appl Microbiol Biotechnol,* 99**,** 6865-77.
LAWLEY, T. D., CLARE, S., WALKER, A. W., GOULDING, D., STABLER, R. A., CROUCHER, N., MASTROENI, P., SCOTT, P., RAISEN, C., MOTTRAM, L., FAIRWEATHER, N. F., WREN, B. W., PARKHILL, J. & DOUGAN, G. 2009. Antibiotic treatment of clostridium difficile carrier mice triggers

a supershedder state, spore-mediated transmission, and severe disease in immunocompromised hosts. *Infect Immun,* 77**,** 3661-9.
LAWLEY, T. D., CLARE, S., WALKER, A. W., STARES, M. D., CONNOR, T. R., RAISEN, C., GOULDING, D., RAD, R., SCHREIBER, F., BRANDT, C., DEAKIN, L. J., PICKARD, D. J., DUNCAN, S. H., FLINT, H. J., CLARK, T. G., PARKHILL, J. & DOUGAN, G. 2012. Targeted restoration of the intestinal microbiota with a simple, defined bacteriotherapy resolves relapsing Clostridium difficile disease in mice. *PLoS Pathog,* 8**,** e1002995.
LAWSON, P. A., CITRON, D. M., TYRRELL, K. L. & FINEGOLD, S. M. 2016. Reclassification of Clostridium difficile as Clostridioides difficile (Hall and O'Toole 1935) Prevot 1938. *Anaerobe,* 40**,** 95-9.
LEE, A. S. & SONG, K. P. 2005. LuxS/autoinducer-2 quorum sensing molecule regulates transcriptional virulence gene expression in Clostridium difficile. *Biochem Biophys Res Commun,* 335**,** 659-66.
LEONG, C. & ZELENITSKY, S. 2013. Treatment Strategies for Recurrent Clostridium difficile Infection. *Can J Hosp Pharm,* 66**,** 361-8.
LESSA, F. C., WINSTON, L. G. & MCDONALD, L. C. 2015. Burden of Clostridium difficile infection in the United States. *N Engl J Med,* 372**,** 2369-70.
LEWIS, K. 2005. Persister cells and the riddle of biofilm survival. *Biochemistry (Mosc),* 70**,** 267-74.
LEWIS, K. 2008. Multidrug tolerance of biofilms and persister cells. *Curr Top Microbiol Immunol,* 322**,** 107-31.
LI, H. & DURBIN, R. 2009. Fast and accurate short read alignment with Burrows-Wheeler transform. *Bioinformatics,* 25**,** 1754-60.
LI, H. & DURBIN, R. 2010. Fast and accurate long-read alignment with Burrows-Wheeler transform. *Bioinformatics,* 26**,** 589-95.
LI, H., HANDSAKER, B., WYSOKER, A., FENNELL, T., RUAN, J., HOMER, N., MARTH, G., ABECASIS, G. & DURBIN, R. 2009. The Sequence Alignment/Map format and SAMtools. *Bioinformatics,* 25**,** 2078-9.
LI, H., LI, X., WANG, Z., FU, Y., AI, Q., DONG, Y. & YU, J. 2015. Autoinducer-2 regulates Pseudomonas aeruginosa PAO1 biofilm formation and virulence production in a dose-dependent manner. *BMC Microbiol,* 15.
LI, Y. H. & TIAN, X. 2012. Quorum Sensing and Bacterial Social Interactions in Biofilms. *Sensors (Basel),* 12**,** 2519-38.
LOUIE, T. J., MILLER, M. A., MULLANE, K. M., WEISS, K., LENTNEK, A., GOLAN, Y., GORBACH, S., SEARS, P. & SHUE, Y. K. 2011. Fidaxomicin versus vancomycin for Clostridium difficile infection. *N Engl J Med,* 364**,** 422-31.
LOVE, M. I., HUBER, W. & ANDERS, S. 2014. Moderated estimation of fold change and dispersion for RNA-seq data with DESeq2. *Genome Biology,* 15**,** 550.

LUND, B. M. & PECK, M. W. 2015. A Possible Route for Foodborne Transmission of Clostridium difficile? *Foodborne Pathogens and Disease,* 12, 177-182.
LYRAS, D., O'CONNOR, J. R., HOWARTH, P. M., SAMBOL, S. P., CARTER, G. P., PHUMOONNA, T., POON, R., ADAMS, V., VEDANTAM, G., JOHNSON, S., GERDING, D. N. & ROOD, J. I. 2009. Toxin B is essential for virulence of Clostridium difficile. *Nature,* 458, 1176-9.
MACY, J. M., LJUNGDAHL, L. G. & GOTTSCHALK, G. 1978. Pathway of succinate and propionate formation in Bacteroides fragilis. *J Bacteriol,* 134, 84-91.
MAH, T. F. & O'TOOLE, G. A. 2001. Mechanisms of biofilm resistance to antimicrobial agents. *Trends Microbiol,* 9, 34-9.
MAJEED, H., LAMPERT, A., GHAZARYAN, L. & GILLOR, O. 2013. The Weak Shall Inherit: Bacteriocin-Mediated Interactions in Bacterial Populations. *PLOS ONE,* 8, e63837.
MALDARELLI, G. A., PIEPENBRINK, K. H., SCOTT, A. J., FREIBERG, J. A., SONG, Y., ACHERMANN, Y., ERNST, R. K., SHIRTLIFF, M. E., SUNDBERG, E. J., DONNENBERG, M. S. & VON ROSENVINGE, E. C. 2016. Type IV pili promote early biofilm formation by Clostridium difficile. *Pathog Dis,* 74.
MANGES, A. R., LABBE, A., LOO, V. G., ATHERTON, J. K., BEHR, M. A., MASSON, L., TELLIS, P. A. & BROUSSEAU, R. 2010. Comparative metagenomic study of alterations to the intestinal microbiota and risk of nosocomial Clostridum difficile-associated disease. *J Infect Dis,* 202, 1877-84.
MANSE, J. S. & BALDWIN, M. R. 2015. Binding and entry of Clostridium difficile toxin B is mediated by multiple domains. *FEBS Lett,* 589, 3945-51.
MARSH, J. W., ARORA, R., SCHLACKMAN, J. L., SHUTT, K. A., CURRY, S. R. & HARRISON, L. H. 2012. Association of relapse of Clostridium difficile disease with BI/NAP1/027. *J Clin Microbiol,* 50, 4078-82.
MARTIN, M. J., CLARE, S., GOULDING, D., FAULDS-PAIN, A., BARQUIST, L., BROWNE, H. P., PETTIT, L., DOUGAN, G., LAWLEY, T. D. & WREN, B. W. 2013. The agr locus regulates virulence and colonization genes in Clostridium difficile 027. *J Bacteriol,* 195, 3672-81.
MCDONALD, L. C., KILLGORE, G. E., THOMPSON, A., OWENS, R. C., JR., KAZAKOVA, S. V., SAMBOL, S. P., JOHNSON, S. & GERDING, D. N. 2005. An epidemic, toxin gene-variant strain of Clostridium difficile. *N Engl J Med,* 353, 2433-41.
MELNICK, J., LIS, E., PARK, J. H., KINSLAND, C., MORI, H., BABA, T., PERKINS, J., SCHYNS, G., VASSIEVA, O., OSTERMAN, A. & BEGLEY, T. P. 2004. Identification of the two missing bacterial genes involved in thiamine salvage: thiamine pyrophosphokinase and thiamine kinase. *J Bacteriol,* 186, 3660-2.

MOLLE, V., FUJITA, M., JENSEN, S. T., EICHENBERGER, P., GONZALEZ-PASTOR, J. E., LIU, J. S. & LOSICK, R. 2003. The SpooA regulon of Bacillus subtilis. *Mol Microbiol,* 50**,** 1683-701.

MORE, M. I., FINGER, L. D., STRYKER, J. L., FUQUA, C., EBERHARD, A. & WINANS, S. C. 1996. Enzymatic synthesis of a quorum-sensing autoinducer through use of defined substrates. *Science,* 272**,** 1655-8.

MORFELDT, E., TAYLOR, D., VON GABAIN, A. & ARVIDSON, S. 1995. Activation of alpha-toxin translation in Staphylococcus aureus by the trans-encoded antisense RNA, RNAIII. *Embo j,* 14**,** 4569-77.

NEALSON, K. H. & HASTINGS, J. W. 1979. Bacterial bioluminescence: its control and ecological significance. *Microbiol Rev,* 43**,** 496-518.

NEALSON, K. H., PLATT, T. & HASTINGS, J. W. 1970. Cellular control of the synthesis and activity of the bacterial luminescent system. *J Bacteriol,* 104**,** 313-22.

NETT, M., IKEDA, H. & MOORE, B. S. 2009. Genomic basis for natural product biosynthetic diversity in the actinomycetes. *Nat Prod Rep,* 26**,** 1362-84.

NG, J., HIROTA, S. A., GROSS, O., LI, Y., ULKE-LEMEE, A., POTENTIER, M. S., SCHENCK, L. P., VILAYSANE, A., SEAMONE, M. E., FENG, H., ARMSTRONG, G. D., TSCHOPP, J., MACDONALD, J. A., MURUVE, D. A. & BECK, P. L. 2010. Clostridium difficile toxin-induced inflammation and intestinal injury are mediated by the inflammasome. *Gastroenterology,* 139**,** 542-52, 552.e1-3.

NG, K. M., FERREYRA, J. A., HIGGINBOTTOM, S. K., LYNCH, J. B., KASHYAP, P. C., GOPINATH, S., NAIDU, N., CHOUDHURY, B., WEIMER, B. C., MONACK, D. M. & SONNENBURG, J. L. 2013. Microbiota-liberated host sugars facilitate post-antibiotic expansion of enteric pathogens. *Nature,* 502**,** 96-9.

NG, W. L. & BASSLER, B. L. 2009. Bacterial quorum-sensing network architectures. *Annu Rev Genet,* 43**,** 197-222.

NICOLAS, P., MADER, U., DERVYN, E., ROCHAT, T., LEDUC, A., PIGEONNEAU, N., BIDNENKO, E., MARCHADIER, E., HOEBEKE, M., AYMERICH, S., BECHER, D., BISICCHIA, P., BOTELLA, E., DELUMEAU, O., DOHERTY, G., DENHAM, E. L., FOGG, M. J., FROMION, V., GOELZER, A., HANSEN, A., HARTIG, E., HARWOOD, C. R., HOMUTH, G., JARMER, H., JULES, M., KLIPP, E., LE CHAT, L., LECOINTE, F., LEWIS, P., LIEBERMEISTER, W., MARCH, A., MARS, R. A., NANNAPANENI, P., NOONE, D., POHL, S., RINN, B., RUGHEIMER, F., SAPPA, P. K., SAMSON, F., SCHAFFER, M., SCHWIKOWSKI, B., STEIL, L., STULKE, J., WIEGERT, T., DEVINE, K. M., WILKINSON, A. J., VAN DIJL, J. M., HECKER, M., VOLKER, U., BESSIERES, P. & NOIROT, P. 2012. Condition-dependent transcriptome reveals high-level regulatory architecture in Bacillus subtilis. *Science,* 335**,** 1103-6.

NOBBS, A. H., LAMONT, R. J. & JENKINSON, H. F. 2009. Streptococcus adherence and colonization. *Microbiol Mol Biol Rev,* 73**,** 407-50, Table of Contents.
NOVICK, R. P. & GEISINGER, E. 2008. Quorum sensing in staphylococci. *Annu Rev Genet,* 42**,** 541-64.
NUSS, A. M., BECKSTETTE, M., PIMENOVA, M., SCHMUHL, C., OPITZ, W., PISANO, F., HEROVEN, A. K. & DERSCH, P. 2017. Tissue dual RNA-seq allows fast discovery of infection-specific functions and riboregulators shaping host-pathogen transcriptomes. *Proc Natl Acad Sci U S A,* 114**,** E791-e800.
OLLING, A., GOY, S., HOFFMANN, F., TATGE, H., JUST, I. & GERHARD, R. 2011. The repetitive oligopeptide sequences modulate cytopathic potency but are not crucial for cellular uptake of Clostridium difficile toxin A. *PLoS One,* 6**,** e17623.
OLLING, A., SEEHASE, S., MINTON, N. P., TATGE, H., SCHROTER, S., KOHLSCHEEN, S., PICH, A., JUST, I. & GERHARD, R. 2012. Release of TcdA and TcdB from Clostridium difficile cdi 630 is not affected by functional inactivation of the tcdE gene. *Microb Pathog,* 52**,** 92-100.
OLSEN, I. 2015. Biofilm-specific antibiotic tolerance and resistance. *Eur J Clin Microbiol Infect Dis,* 34**,** 877-86.
OTTER, J. A., YEZLI, S. & FRENCH, G. L. 2015. The Role Played by Contaminated Surfaces in the Transmission of Nosocomial Pathogens. *Infection Control & Hospital Epidemiology,* 32**,** 687-699.
OWENS, R. C., JR., DONSKEY, C. J., GAYNES, R. P., LOO, V. G. & MUTO, C. A. 2008. Antimicrobial-associated risk factors for Clostridium difficile infection. *Clin Infect Dis,* 46 Suppl 1**,** S19-31.
PANTALEON, V., SOAVELOMANDROSO, A. P., BOUTTIER, S., BRIANDET, R., ROXAS, B., CHU, M., COLLIGNON, A., JANOIR, C., VEDANTAM, G. & CANDELA, T. 2015. The Clostridium difficile Protease Cwp84 Modulates both Biofilm Formation and Cell-Surface Properties. *PLoS One,* 10**,** e0124971.
PASQUALE, V., ROMANO, V. J., RUPNIK, M., DUMONTET, S., CIZNAR, I., ALIBERTI, F., MAURI, F., SAGGIOMO, V. & KROVACEK, K. 2011. Isolation and characterization of Clostridium difficile from shellfish and marine environments. *Folia Microbiol (Praha),* 56**,** 431-7.
PEIXOTO, R. J., MIRANDA, K. R., FERREIRA, E. O., DE PAULA, G. R., ROCHA, E. R., LOBO, L. A. & DOMINGUES, R. M. 2014. Production of AI-2 is mediated by the S-ribosylhomocystein lyase gene luxS in Bacteroides fragilis and Bacteroides vulgatus. *J Basic Microbiol,* 54**,** 644-9.
PEPIN, J., SAHEB, N., COULOMBE, M. A., ALARY, M. E., CORRIVEAU, M. P., AUTHIER, S., LEBLANC, M., RIVARD, G., BETTEZ, M., PRIMEAU, V., NGUYEN, M., JACOB, C. E. & LANTHIER, L. 2005. Emergence of fluoroquinolones as the predominant risk factor for Clostridium

difficile-associated diarrhea: a cohort study during an epidemic in Quebec. *Clin Infect Dis,* 41**,** 1254-60.
PEREIRA, F. C., SAUJET, L., TOME, A. R., SERRANO, M., MONOT, M., COUTURE-TOSI, E., MARTIN-VERSTRAETE, I., DUPUY, B. & HENRIQUES, A. O. 2013. The spore differentiation pathway in the enteric pathogen Clostridium difficile. *PLoS Genet,* 9**,** e1003782.
PEREZ-ARELLANO, I. & PEREZ-MARTINEZ, G. 2003. Optimization of the green fluorescent protein (GFP) expression from a lactose-inducible promoter in Lactobacillus casei. *FEMS Microbiol Lett,* 222**,** 123-7.
PETROF, E. O., GLOOR, G. B., VANNER, S. J., WEESE, S. J., CARTER, D., DAIGNEAULT, M. C., BROWN, E. M., SCHROETER, K. & ALLEN-VERCOE, E. 2013. Stool substitute transplant therapy for the eradication of Clostridium difficile infection: 'RePOOPulating' the gut. *Microbiome,* 1**,** 3.
PIGGOT, P. J. & HILBERT, D. W. 2004. Sporulation of Bacillus subtilis. *Curr Opin Microbiol,* 7**,** 579-86.
POPAT, R., CRUSZ, S. A., MESSINA, M., WILLIAMS, P., WEST, S. A. & DIGGLE, S. P. 2012. Quorum-sensing and cheating in bacterial biofilms. *Proc Biol Sci,* 279**,** 4765-71.
PRESSLER, U., STAUDENMAIER, H., ZIMMERMANN, L. & BRAUN, V. 1988. Genetics of the iron dicitrate transport system of Escherichia coli. *J Bacteriol,* 170**,** 2716-24.
QUINLAN, A. R. 2014. BEDTools: The Swiss-Army Tool for Genome Feature Analysis. *Curr Protoc Bioinformatics,* 47**,** 11.12.1-34.
QUINLAN, A. R. & HALL, I. M. 2010. BEDTools: a flexible suite of utilities for comparing genomic features. *Bioinformatics,* 26**,** 841-842.
RAINEY, P. B. & RAINEY, K. 2003. Evolution of cooperation and conflict in experimental bacterial populations. *Nature,* 425**,** 72-4.
RASMUSSEN, B. 2000. Filamentous microfossils in a 3,235-million-year-old volcanogenic massive sulphide deposit. *Nature,* 405**,** 676-9.
REZZONICO, F. & DUFFY, B. 2008. Lack of genomic evidence of AI-2 receptors suggests a non-quorum sensing role for luxS in most bacteria. *BMC Microbiol,* 8**,** 154.
RICKARD, A. H., PALMER, R. J., JR., BLEHERT, D. S., CAMPAGNA, S. R., SEMMELHACK, M. F., EGLAND, P. G., BASSLER, B. L. & KOLENBRANDER, P. E. 2006. Autoinducer 2: a concentration-dependent signal for mutualistic bacterial biofilm growth. *Mol Microbiol,* 60**,** 1446-56.
RIMMELE, M. & BOOS, W. 1994. Trehalose-6-phosphate hydrolase of Escherichia coli. *J Bacteriol,* 176**,** 5654-64.
RISSMAN, A. I., MAU, B., BIEHL, B. S., DARLING, A. E., GLASNER, J. D. & PERNA, N. T. 2009. Reordering contigs of draft genomes using the Mauve aligner. *Bioinformatics,* 25**,** 2071-3.

ROBINSON, C. D., AUCHTUNG, J. M., COLLINS, J. & BRITTON, R. A. 2014. Epidemic Clostridium difficile strains demonstrate increased competitive fitness compared to nonepidemic isolates. *Infect Immun,* 82, 2815-25.

ROHLKE, F. & STOLLMAN, N. 2012. Fecal microbiota transplantation in relapsing Clostridium difficile infection. *Therap Adv Gastroenterol,* 5, 403-20.

ROMLING, U. & BALSALOBRE, C. 2012. Biofilm infections, their resilience to therapy and innovative treatment strategies. *J Intern Med,* 272, 541-61.

ROSS-GILLESPIE, A., GARDNER, A., WEST, S. A. & GRIFFIN, A. S. 2007. Frequency dependence and cooperation: theory and a test with bacteria. *Am Nat,* 170, 331-42.

ROSSMANN, F. S., RACEK, T., WOBSER, D., PUCHALKA, J., RABENER, E. M., REIGER, M., HENDRICKX, A. P., DIEDERICH, A. K., JUNG, K., KLEIN, C. & HUEBNER, J. 2015. Phage-mediated dispersal of biofilm and distribution of bacterial virulence genes is induced by quorum sensing. *PLoS Pathog,* 11, e1004653.

ROUX, A., PAYNE, S. M. & GILMORE, M. S. 2009. Microbial Telesensing: Probing the environment for friends, foes and food. *Cell Host Microbe,* 6, 115-24.

RUPNIK, M., WILCOX, M. H. & GERDING, D. N. 2009. Clostridium difficile infection: new developments in epidemiology and pathogenesis. *Nat Rev Microbiol,* 7, 526-36.

RUSSELL, A., WEXLER, A., HARDING, B., WHITNEY, J., BOHN, A., GOO, Y., TRAN, B., BARRY, N., ZHENG, H., PETERSON, S., CHOU, S., GONEN, T., GOODLETT, D., GOODMAN, A. & MOUGOUS, J. 2014. A type VI secretion-related pathway in Bacteroidetes mediates interbacterial antagonism. *Cell Host Microbe,* 16, 227-36.

RUTHERFORD, K., PARKHILL, J., CROOK, J., HORSNELL, T., RICE, P., RAJANDREAM, M. A. & BARRELL, B. 2000. Artemis: sequence visualization and annotation. *Bioinformatics (Oxford, England),* 16, 944-945.

RUTHERFORD, S. T. & BASSLER, B. L. 2012. Bacterial quorum sensing: its role in virulence and possibilities for its control. *Cold Spring Harb Perspect Med,* 2.

SAENZ, H. L., AUGSBURGER, V., VUONG, C., JACK, R. W., GOTZ, F. & OTTO, M. 2000. Inducible expression and cellular location of AgrB, a protein involved in the maturation of the staphylococcal quorum-sensing pheromone. *Arch Microbiol,* 174, 452-5.

SAKURAGI, Y. & KOLTER, R. 2007. Quorum-sensing regulation of the biofilm matrix genes (pel) of Pseudomonas aeruginosa. *J Bacteriol,* 189, 5383-6.

SALYERS, A. A. 1984. Bacteroides of the human lower intestinal tract. *Annu Rev Microbiol,* 38, 293-313.

SANDOZ, K. M., MITZIMBERG, S. M. & SCHUSTER, M. 2007. Social cheating in Pseudomonas aeruginosa quorum sensing. *Proc Natl Acad Sci U S A,* 104, 15876-81.
SARA, M. & SLEYTR, U. B. 2000. S-Layer proteins. *J Bacteriol,* 182, 859-68.
SARKER, M. R. & PAREDES-SABJA, D. 2012. Molecular basis of early stages of Clostridium difficile infection: germination and colonization. *Future Microbiol,* 7, 933-43.
SCHAEFER, A. L., HANZELKA, B. L., EBERHARD, A. & GREENBERG, E. P. 1996. Quorum sensing in Vibrio fischeri: probing autoinducer-LuxR interactions with autoinducer analogs. *J Bacteriol,* 178, 2897-901.
SCHAUDER, S., SHOKAT, K., SURETTE, M. G. & BASSLER, B. L. 2001. The LuxS family of bacterial autoinducers: biosynthesis of a novel quorum-sensing signal molecule. *Mol Microbiol,* 41, 463-76.
SCHINDELIN, J., ARGANDA-CARRERAS, I., FRISE, E., KAYNIG, V., LONGAIR, M., PIETZSCH, T., PREIBISCH, S., RUEDEN, C., SAALFELD, S., SCHMID, B., TINEVEZ, J. Y., WHITE, D. J., HARTENSTEIN, V., ELICEIRI, K., TOMANCAK, P. & CARDONA, A. 2012. Fiji: an open-source platform for biological-image analysis. *Nat Methods,* 9, 676-82.
SCHUBERT, A. M., ROGERS, M. A., RING, C., MOGLE, J., PETROSINO, J. P., YOUNG, V. B., ARONOFF, D. M. & SCHLOSS, P. D. 2014. Microbiome data distinguish patients with Clostridium difficile infection and non-C. difficile-associated diarrhea from healthy controls. *MBio,* 5, e01021-14.
SCHWAN, C., KRUPPKE, A. S., NOLKE, T., SCHUMACHER, L., KOCH-NOLTE, F., KUDRYASHEV, M., STAHLBERG, H. & AKTORIES, K. 2014. Clostridium difficile toxin CDT hijacks microtubule organization and reroutes vesicle traffic to increase pathogen adherence. *Proc Natl Acad Sci U S A,* 111, 2313-8.
SEBAIHIA, M., WREN, B. W., MULLANY, P., FAIRWEATHER, N. F., MINTON, N., STABLER, R., THOMSON, N. R., ROBERTS, A. P., CERDENO-TARRAGA, A. M., WANG, H., HOLDEN, M. T., WRIGHT, A., CHURCHER, C., QUAIL, M. A., BAKER, S., BASON, N., BROOKS, K., CHILLINGWORTH, T., CRONIN, A., DAVIS, P., DOWD, L., FRASER, A., FELTWELL, T., HANCE, Z., HOLROYD, S., JAGELS, K., MOULE, S., MUNGALL, K., PRICE, C., RABBINOWITSCH, E., SHARP, S., SIMMONDS, M., STEVENS, K., UNWIN, L., WHITHEAD, S., DUPUY, B., DOUGAN, G., BARRELL, B. & PARKHILL, J. 2006. The multidrug-resistant human pathogen Clostridium difficile has a highly mobile, mosaic genome. *Nat Genet,* 38, 779-86.
SECOR, P. R. E. A. 2016. Biofilm assembly becomes crystal clear – filamentous bacteriophage. 3, 49-52.
SEEKATZ, A. M. & YOUNG, V. B. 2014. Clostridium difficile and the microbiota. *J Clin Invest,* 124, 4182-9.

SEEMANN, T. 2014. Prokka: rapid prokaryotic genome annotation. *Bioinformatics,* 30**,** 2068-9.
SEKULOVIC, O., OSPINA BEDOYA, M., FIVIAN-HUGHES, A. S., FAIRWEATHER, N. F. & FORTIER, L. C. 2015. The Clostridium difficile cell wall protein CwpV confers phase-variable phage resistance. *Mol Microbiol,* 98**,** 329-42.
SEMENYUK, E. G., LANING, M. L., FOLEY, J., JOHNSTON, P. F., KNIGHT, K. L., GERDING, D. N. & DRIKS, A. 2014. Spore formation and toxin production in Clostridium difficile biofilms. *PLoS One,* 9**,** e87757.
SEMENYUK, E. G., POROYKO, V. A., JOHNSTON, P. F., JONES, S. E., KNIGHT, K. L., GERDING, D. N. & DRIKS, A. 2015. Analysis of Bacterial Communities during Clostridium difficile Infection in the Mouse. *Infect Immun,* 83**,** 4383-91.
SETLOW, P. 2007. I will survive: DNA protection in bacterial spores. *Trends Microbiol,* 15**,** 172-80.
SHAO, H., LAMONT, R. J. & DEMUTH, D. R. 2007. Autoinducer 2 Is Required for Biofilm Growth of Aggregatibacter (Actinobacillus) actinomycetemcomitans. *Infect Immun,* 75**,** 4211-8.
SIRCILI, M. P., WALTERS, M., TRABULSI, L. R. & SPERANDIO, V. 2004. Modulation of enteropathogenic Escherichia coli virulence by quorum sensing. *Infect Immun,* 72**,** 2329-37.
SMITS, W. K., LYRAS, D., LACY, D. B., WILCOX, M. H. & KUIJPER, E. J. 2016. Clostridium difficile infection. *Nat Rev Dis Primers,* 2**,** 16020.
SOAVELOMANDROSO, A. P., GAUDIN, F., HOYS, S., NICOLAS, V., VEDANTAM, G., JANOIR, C. & BOUTTIER, S. 2017. Biofilm Structures in a Mono-Associated Mouse Model of Clostridium difficile Infection. *Frontiers in Microbiology,* 8**,** 2086.
SOLANO, C., ECHEVERZ, M. & LASA, I. 2014. Biofilm dispersion and quorum sensing. *Current Opinion in Microbiology,* 18**,** 96-104.
SORG, J. A. & SONENSHEIN, A. L. 2008. Bile salts and glycine as cogerminants for Clostridium difficile spores. *J Bacteriol,* 190**,** 2505-12.
STAUDENMAIER, H., VAN HOVE, B., YARAGHI, Z. & BRAUN, V. 1989. Nucleotide sequences of the fecBCDE genes and locations of the proteins suggest a periplasmic-binding-protein-dependent transport mechanism for iron(III) dicitrate in Escherichia coli. *J Bacteriol,* 171**,** 2626-33.
STEVENSON, E., MINTON, N. P. & KUEHNE, S. A. 2015. The role of flagella in Clostridium difficile pathogenicity. *Trends Microbiol,* 23**,** 275-82.
STROEHER, U. H., PATON, A. W., OGUNNIYI, A. D. & PATON, J. C. 2003. Mutation of luxS of Streptococcus pneumoniae affects virulence in a mouse model. *Infect Immun,* 71**,** 3206-12.
SUGIMURA, Y. & SAITO, K. 2017. Comparative transcriptome analysis between Solanum lycopersicum L. and Lotus japonicus L. during

arbuscular mycorrhizal development. *Soil Science and Plant Nutrition,* 63, 127-136.
SZTAJER, H., LEMME, A., VILCHEZ, R., SCHULZ, S., GEFFERS, R., YIP, C. Y., LEVESQUE, C. M., CVITKOVITCH, D. G. & WAGNER-DOBLER, I. 2008. Autoinducer-2-regulated genes in Streptococcus mutans UA159 and global metabolic effect of the luxS mutation. *J Bacteriol,* 190, 401-15.
TAKEOKA, A., TAKUMI, K., KOGA, T. & KAWATA, T. 1991. Purification and characterization of S layer proteins from Clostridium difficile GAI 0714. *J Gen Microbiol,* 137, 261-7.
TANGHE, A., VAN DIJCK, P. & THEVELEIN, J. M. 2003. Determinants of Freeze Tolerance in Microorganisms, Physiological Importance, and Biotechnological Applications. *Advances in Applied Microbiology*. Academic Press.
TASTEYRE, A., BARC, M. C., COLLIGNON, A., BOUREAU, H. & KARJALAINEN, T. 2001. Role of FliC and FliD flagellar proteins of Clostridium difficile in adherence and gut colonization. *Infect Immun,* 69, 7937-40.
TER BEEK, A., KEIJSER, B. J., BOORSMA, A., ZAKRZEWSKA, A., ORIJ, R., SMITS, G. J. & BRUL, S. 2008. Transcriptome analysis of sorbic acid-stressed Bacillus subtilis reveals a nutrient limitation response and indicates plasma membrane remodeling. *J Bacteriol,* 190, 1751-61.
THERIOT, C. M., BOWMAN, A. A. & YOUNG, V. B. 2016. Antibiotic-Induced Alterations of the Gut Microbiota Alter Secondary Bile Acid Production and Allow for Clostridium difficile Spore Germination and Outgrowth in the Large Intestine. *mSphere,* 1.
THERIOT, C. M. & YOUNG, V. B. 2015. Interactions Between the Gastrointestinal Microbiome and Clostridium difficile. *Annu Rev Microbiol,* 69, 445-61.
TVEDE, M. & RASK-MADSEN, J. 1989. Bacteriotherapy for chronic relapsing Clostridium difficile diarrhoea in six patients. *Lancet,* 1, 1156-60.
VAISHNAVI, C. 2015. Fidaxomicin - the new drug for Clostridium difficile infection. *Indian J Med Res,* 141, 398-407.
VAN DER WAAIJ, L. A., HARMSEN, H. J., MADJIPOUR, M., KROESE, F. G., ZWIERS, M., VAN DULLEMEN, H. M., DE BOER, N. K., WELLING, G. W. & JANSEN, P. L. 2005. Bacterial population analysis of human colon and terminal ileum biopsies with 16S rRNA-based fluorescent probes: commensal bacteria live in suspension and have no direct contact with epithelial cells. *Inflamm Bowel Dis,* 11, 865-71.
VAN NOOD, E., VRIEZE, A., NIEUWDORP, M., FUENTES, S., ZOETENDAL, E. G., DE VOS, W. M., VISSER, C. E., KUIJPER, E. J., BARTELSMAN, J. F., TIJSSEN, J. G., SPEELMAN, P., DIJKGRAAF, M. G. & KELLER, J. J. 2013. Duodenal infusion of donor feces for recurrent Clostridium difficile. *N Engl J Med,* 368, 407-15.

VARDAKAS, K. Z., POLYZOS, K. A., PATOUNI, K., RAFAILIDIS, P. I., SAMONIS, G. & FALAGAS, M. E. 2012. Treatment failure and recurrence of Clostridium difficile infection following treatment with vancomycin or metronidazole: a systematic review of the evidence. *Int J Antimicrob Agents,* 40**,** 1-8.

VARGA, J. J., THERIT, B. & MELVILLE, S. B. 2008. Type IV pili and the CcpA protein are needed for maximal biofilm formation by the gram-positive anaerobic pathogen Clostridium perfringens. *Infect Immun,* 76**,** 4944-51.

VEDANTAM, G., CLARK, A., CHU, M., MCQUADE, R., MALLOZZI, M. & VISWANATHAN, V. K. 2012. Clostridium difficile infection: toxins and non-toxin virulence factors, and their contributions to disease establishment and host response. *Gut Microbes,* 3**,** 121-34.

VENDEVILLE, A., WINZER, K., HEURLIER, K., TANG, C. M. & HARDIE, K. R. 2005. Making 'sense' of metabolism: autoinducer-2, LuxS and pathogenic bacteria. *Nat Rev Microbiol,* 3**,** 383-96.

VLAMAKIS, H., AGUILAR, C., LOSICK, R. & KOLTER, R. 2008. Control of cell fate by the formation of an architecturally complex bacterial community. *Genes Dev,* 22**,** 945-53.

VLAMAKIS, H., CHAI, Y., BEAUREGARD, P., LOSICK, R. & KOLTER, R. 2013. Sticking together: building a biofilm the Bacillus subtilis way. *Nat Rev Microbiol,* 11**,** 157-68.

VOLLAARD, E. J. & CLASENER, H. A. 1994. Colonization resistance. *Antimicrob Agents Chemother,* 38**,** 409-14.

VOTH, D. E. & BALLARD, J. D. 2005. Clostridium difficile toxins: mechanism of action and role in disease. *Clin Microbiol Rev,* 18**,** 247-63.

WAGEGG, W. & BRAUN, V. 1981. Ferric citrate transport in Escherichia coli requires outer membrane receptor protein fecA. *J Bacteriol,* 145**,** 156-63.

WALIGORA, A. J., HENNEQUIN, C., MULLANY, P., BOURLIOUX, P., COLLIGNON, A. & KARJALAINEN, T. 2001. Characterization of a cell surface protein of Clostridium difficile with adhesive properties. *Infect Immun,* 69**,** 2144-53.

WALTER, B. M., CARTMAN, S. T., MINTON, N. P., BUTALA, M. & RUPNIK, M. 2015. The SOS Response Master Regulator LexA Is Associated with Sporulation, Motility and Biofilm Formation in Clostridium difficile. *PLoS One,* 10**,** e0144763.

WANG, B. Y. & KURAMITSU, H. K. 2005. Interactions between oral bacteria: inhibition of Streptococcus mutans bacteriocin production by Streptococcus gordonii. *Appl Environ Microbiol,* 71**,** 354-62.

WARNY, M., PEPIN, J., FANG, A., KILLGORE, G., THOMPSON, A., BRAZIER, J., FROST, E. & MCDONALD, L. C. 2005. Toxin production by an emerging strain of Clostridium difficile associated with outbreaks of severe disease in North America and Europe. *Lancet,* 366**,** 1079-84.

WEINGARDEN, A. R., CHEN, C., BOBR, A., YAO, D., LU, Y., NELSON, V. M., SADOWSKY, M. J. & KHORUTS, A. 2014. Microbiota transplantation restores normal fecal bile acid composition in recurrent Clostridium difficile infection. *Am J Physiol Gastrointest Liver Physiol,* 306**,** G310-9.

WESTALL, F., DE WIT, M. J., DANN, J., VAN DER GAAST, S., DE RONDE, C. E. J. & GERNEKE, D. 2001. Early Archean fossil bacteria and biofilms in hydrothermally-influenced sediments from the Barberton greenstone belt, South Africa. *Precambrian Research,* 106**,** 93-116.

WILCOX, M. H., MOONEY, L., BENDALL, R., SETTLE, C. D. & FAWLEY, W. N. 2008. A case-control study of community-associated Clostridium difficile infection. *J Antimicrob Chemother,* 62**,** 388-96.

WILSON, C. M., AGGIO, R. B., O'TOOLE, P. W., VILLAS-BOAS, S. & TANNOCK, G. W. 2012. Transcriptional and metabolomic consequences of LuxS inactivation reveal a metabolic rather than quorum-sensing role for LuxS in Lactobacillus reuteri 100-23. *J Bacteriol,* 194**,** 1743-6.

WINSTON, J. A. & THERIOT, C. M. 2016. Impact of microbial derived secondary bile acids on colonization resistance against Clostridium difficile in the gastrointestinal tract. *Anaerobe,* 41**,** 44-50.

WINZER, K., HARDIE, K. R. & WILLIAMS, P. 2003. LuxS and autoinducer-2: their contribution to quorum sensing and metabolism in bacteria. *Adv Appl Microbiol,* 53**,** 291-396.

WOLF, T., KÄMMER, P., BRUNKE, S. & LINDE, J. 2018. Two's company: studying interspecies relationships with dual RNA-seq. *Current Opinion in Microbiology,* 42**,** 7-12.

XAVIER, K. B. & BASSLER, B. L. 2003. LuxS quorum sensing: more than just a numbers game. *Curr Opin Microbiol,* 6**,** 191-7.

YOON, S., YU, J., MCDOWELL, A., KIM, S. H., YOU, H. J. & KO, G. 2017. Bile salt hydrolase-mediated inhibitory effect of Bacteroides ovatus on growth of Clostridium difficile. *J Microbiol,* 55**,** 892-899.

YOSHIDA, A., ANSAI, T., TAKEHARA, T. & KURAMITSU, H. K. 2005. LuxS-based signaling affects Streptococcus mutans biofilm formation. *Appl Environ Microbiol,* 71**,** 2372-80.

YOUNG, R. 1992. Bacteriophage lysis: mechanism and regulation. *Microbiol Rev,* 56**,** 430-81.

ZACKULAR, J. P., BAXTER, N. T., IVERSON, K. D., SADLER, W. D., PETROSINO, J. F., CHEN, G. Y. & SCHLOSS, P. D. 2013. The gut microbiome modulates colon tumorigenesis. *MBio,* 4**,** e00692-13.

ZAR, F. A., BAKKANAGARI, S. R., MOORTHI, K. M. & DAVIS, M. B. 2007. A comparison of vancomycin and metronidazole for the treatment of Clostridium difficile-associated diarrhea, stratified by disease severity. *Clin Infect Dis,* 45**,** 302-7.

ZHANG, L.-H. & DONG, Y.-H. 2004. Quorum sensing and signal interference: diverse implications. *Molecular Microbiology,* 53**,** 1563-1571.

ZHOU, Y., LIANG, Y., LYNCH, K. H., DENNIS, J. J. & WISHART, D. S. 2011. PHAST: a fast phage search tool. *Nucleic Acids Res,* 39**,** W347-52.
ZHU, J. & MEKALANOS, J. J. 2003. Quorum sensing-dependent biofilms enhance colonization in Vibrio cholerae. *Dev Cell,* 5**,** 647-56.
ZOETENDAL, E. G., VON WRIGHT, A., VILPPONEN-SALMELA, T., BEN-AMOR, K., AKKERMANS, A. D. & DE VOS, W. M. 2002. Mucosa-associated bacteria in the human gastrointestinal tract are uniformly distributed along the colon and differ from the community recovered from feces. *Appl Environ Microbiol,* 68**,** 3401-7.